

DPVT C/255
October 1993

HEAVY VEHICLE SIMULATOR TESTING OF TRIAL SECTIONS FOR CALTRANS

AUTHORS: F C RUST
J L DU PLESSIS
B M J A VERHAEGHE
J E GROBLER

PREPARED FOR:
California Department of Transportation (CALTRANS)
Sacramento
California

PREPARED BY:
Division of Roads and
Transport Technology, CSIR
South Africa

EXECUTIVE SUMMARY

Internationally, interest in accelerated pavement testing (APT) is increasing, in particular testing with mobile machines which allow the performance of in-service roads to be assessed. The Californian Department of Transportation (CALTRANS) commissioned the University of California at Berkeley (UCB), Dynatest Consulting and the Council for Scientific and Industrial Research (CSIR) in South Africa to conduct a pilot study to evaluate the potential of the South African Heavy Vehicle Simulator (HVS) for conducting pavement studies for CALTRANS.

The main objectives of the work were to :

- evaluate the rutting behaviour of a dense-graded Asphalt Concrete (AC) overlay subjected to channelized traffic at 25 °C and 40 °C compared with its behaviour under wandering traffic with a normal distribution
- compare the cracking behaviour of a 75 mm thick AC overlay at 10 °C with that of a 38 mm thick Asphalt Rubber Hot Mix gap-graded (ARHM) overlay.

In addition to a comprehensive laboratory evaluation of the materials conducted by UCB, five HVS tests were conducted on AC and ARHM overlays designed according to CALTRANS procedures. To control the test temperature a special temperature control chamber was developed for the HVS. The main findings were that :

- channelized traffic may result in a 50% reduction in the expected life of an AC overlay (in terms of rutting) relative to that of an identical mix subjected to normal wandering traffic
- a reduction of 50% in layer thickness is justified to obtain similar performance in fatigue mode if conventional AC is replaced by ARHM. However, cognisance should be taken of the reduction in structural capacity (in terms of protection of the sublayers) by using an ARHM of half thickness.

The scope of work for this pilot project was limited and a number of suggestions are made for both enhancing the value obtained by analysing the data from these tests as well as conducting further HVS testing.

TABLE OF CONTENTS

1	INTRODUCTION	1
2	OBJECTIVES AND SCOPE OF THE STUDY	2
3	DESIGN AND CONSTRUCTION OF TRIAL SECTIONS	3
3.1	Objectives and pavement selection	3
3.2	Selection of test sections	4
3.3	Mix designs	4
3.4	Construction monitoring	6
3.5	Tests on cores taken from the sections	6
4	HVS EVALUATION OF THE RUTTING PERFORMANCE OF THE AC OVERLAY	8
4.1	Work procedure	8
4.2	Temperatures measured	9
4.3	Surface rutting	10
4.4	In-depth deflections and moduli	11
4.5	Surface deflections	13
4.6	Comparison of results with other HVS testing	13
5	HVS EVALUATION OF THE CRACKING PERFORMANCE OF THE AC OVERLAY COMPARED WITH THE ARHM OVERLAYS	15
5.1	Trial sections	15
5.2	Predicted life to cracking	15
5.3	Work procedure	16
5.4	Temperature control chamber	16
5.5	Cracking performance of the sections	18
5.6	Surface rutting	19
5.7	In-depth permanent deformation	19
5.8	Surface deflection	19
5.9	In-depth deflections and moduli	19
6	SUGGESTIONS FOR ENHANCING THE RESULTS OF THE PILOT PROJECT	22
7	CONCLUSIONS	23
7.1	Channelized vs wandering traffic	23
7.2	Cracking of the AC layer compared with the ARHM layers	23
8	ACKNOWLEDGEMENTS	24
9	REFERENCES	24
	APPENDIX A: BRIEF DESCRIPTION OF THE HVS	A.1
A.1	The Heavy Vehicle Simulator	A.1
A.2	HVS Instrumentation	A.2

LIST OF TABLES

Table 3.1:	Summary of HVS tests conducted for CALTRANS	4
Table 3.2:	Target gradings, operating ranges and target binder contents	5
Table 3.3:	Grading of aggregate fractions and batching information	5
Table 3.4:	Average results of dynamic tests	6
Table 3.5:	As-built data on gradings and binder contents	7
Table 3.6:	Specific gravity of cores removed from the overlay sections	7
Table 3.7:	Resilient modulus values of cores from the overlay sections	7
Table 4.1:	Data collection schedule for both the wandering and channelized traffic sections	9
Table 4.2:	Average temperatures measured on channelized and wandering traffic sections (°C)	10
Table 4.3:	Maximum surface rut depth : channelized versus wandering traffic	10
Table 4.4:	Rut rates per 100 000 repetitions and total rutting per phase	12
Table 4.5:	Backcalculated moduli (initial stage) for the channelized traffic section (379A3) (Laboratory resilient modulus used for AC layer) in MPa	12
Table 4.6:	Backcalculated moduli (initial stage) for the wandering traffic section (380A3) (laboratory resilient modulus used for AC layer) in MPa	13
Table 4.7:	Increases in surface deflection after the settling in phase (mm)	13
Table 4.8:	Typical (Phase II) surface rutting rates in asphalt base pavements tested under the HVS	14
Table 5.1:	Data collection schedule for the 75 mm AC overlay and ARHM sections	17
Table 5.2:	Temperatures measured during the testing of the 75 mm AC overlay and the ARHM overlays	17
Table 5.3:	Cracking life of the 75 mm AC overlay and the ARHM overlays	18
Table 5.4:	Initial stiffness moduli (MPa) backcalculated for the 75 mm AC overlay section	20
Table 5.5:	Initial stiffness moduli (MPa) backcalculated for the 38 mm ARHM overlay section	20
Table 5.6:	Initial stiffness moduli (MPa) backcalculated for the 25 mm ARHM overlay section	21

LIST OF FIGURES

- Figure 3.1: Deflectograph measurements on P6/1, Bapsfontein to Bronkhorstspuit
Figure 3.2: RSD deflection measurements on (P6/1), Bapsfontein to Bronkhorstspuit
Figure 3.3: Target and actual average gradings for AC mix
Figure 3.4: Target and actual average gradings for ARHM mix
- Figure 4.1: RSD deflection measurements on wandering and channelized traffic sections
Figure 4.2: Pavement profile with MDD Module depths
Figure 4.3: Rut profile after 164 000 repetitions on the channelized traffic section
Figure 4.4: Rut profile after 164 000 repetitions on the wandering traffic section
Figure 4.5: Maximum surface rutting on the channelized traffic section
Figure 4.6: Maximum surface rutting on the wandering traffic section
Figure 4.7: Maximum rut depth on the channelized and wandering traffic sections
Figure 4.8: Multi-depth deflections - channelized traffic (Section 379A3 - MDD4, temperature = 25°C)
Figure 4.9: Multi-depth deflections - channelized traffic (Section 379A3 - MDD12, temperature = 40°C)
Figure 4.10: Multi-depth deflections - wandering traffic (Section 380A3 - MDD4, temperature = 25°C)
Figure 4.11: Multi-depth deflections - wandering traffic (Section 380A3 - MDD12, temperature = 40°C)
Figure 4.12: Multi-depth deformation - channelized traffic (Section 379A3 - MDD4, temperature = 25°C)
Figure 4.13: Multi-depth deformation - channelized traffic (Section 379A3 - MDD12, temperature = 40°C)
Figure 4.14: Multi-depth deformation - wandering traffic (Section 380A3 - MDD4, temperature = 25°C)
Figure 4.15: Multi-depth deformation - wandering traffic (Section 380A3 - MDD12, temperature = 40°C)
Figure 4.16: Surface deflection - channelized traffic section (Section 379A3 - 40 kN Test wheel load)
Figure 4.17: Surface deflection - channelized traffic section (Section 379A3 - 70kN Test wheel load)
Figure 4.18: Surface deflection - wandering traffic section (Section 380A3 - 40kN Test wheel load)
Figure 4.19: Surface deflection - wandering traffic section (Section 380A3 - 70kN Test wheel load)
- Figure 5.1: RSD deflection measurements of the cold temperature sections
Figure 5.2: Reduction in deflection resulting from pavement overlays
Figure 5.3: Tolerable Deflection Chart
Figure 5.4: Maximum surface rutting on section 381A3 (75 mm AC overlay)
Figure 5.5: Maximum surface rutting on section 382A3 (38 mm ARHM overlay)
Figure 5.6: Maximum surface rutting on section 383A3 (25 mm ARHM overlay)
Figure 5.7: Multi-depth permanent deformation, MDD4 (Section 381A3, 75 mm AC overlay)
Figure 5.8: Multi-depth permanent deformation, MDD12 (Section 381A3, 75 mm AC overlay)
Figure 5.9: Multi-depth permanent deformation, MDD4 (Section 382A3, 38 mm ARHM overlay)

- Figure 5.10: Multi-depth permanent deformation, MDD12, (Section 382A3, 38 mm ARHM overlay)
- Figure 5.11: Multi-depth permanent deformation, MDD4 (Section 383A3, 25 mm ARHM overlay)
- Figure 5.12: Multi-depth permanent deformation, MDD12 (Section 383A3, 25 mm ARHM overlay)
- Figure 5.13: Surface deflection on section 381A3 (75 mm AC overlay)
- Figure 5.14: Surface deflection on section 382A3 (38 mm ARHM overlay)
- Figure 5.15: Surface deflection on section 383A3 (25 mm ARHM overlay)
- Figure 5.16: Multi-depth deflections, MDD4 (Section 381A3, 75 mm AC overlay)
- Figure 5.17: Multi-depth deflections, MDD12 (Section 381A3, 75 mm AC overlay)
- Figure 5.18: Multi-depth deflections, MDD4 (Section 382A3, 38 mm ARHM overlay)
- Figure 5.19: Multi-depth deflections, MDD12 (Section 382A3, 38 mm ARHM overlay)
- Figure 5.20: Multi-depth deflections, MDD4 (Section 383A3, 25 mm ARHM overlay)
- Figure 5.21: Multi-depth Deflections, MDD12 (section 383A3, 25mm ARHM overlay)

Figure A.1: Line diagram of the Heavy Vehicle Simulator (HVS)

Figure A.2: Layout of a typical HVS test section

LIST OF PHOTOGRAPHS

- Photograph 1: The surface of P6/1, Bapsfontein to Bronkhorspruit, showing extensive cracking
- Photograph 2: Surface distress observed during HVS testing of P6/1 in 1979 HVS test section 43A4 (after Maree ref.)
- Photograph 3: Construction of the CALTRANS trials
- Photograph 4: Heaters used to elevate the temperature in the asphalt mix
- Photograph 5: Rutting after channelized traffic
- Photograph 6: Rutting after wandering traffic
- Photograph 7: The HVS with the temperature control chamber fitted
- Photograph 8: The inside of the temperature control chamber showing the air conditioning units
- Photograph 9: Final stage of cracking on section 381A3 - 75 mm AC overlay
- Photograph 10: Close up view of cracking on section 381A3 - 75 mm AC overlay
- Photograph 11: Final stage of cracking on section 382A3 - 38 mm ARHM overlay
- Photograph 12: Final stage of cracking on section 383A3 - 25 mm ARHM overlay
-
- Photograph A.1: Prototype HVS commissioned in October 1970
- Photograph A.2: One of the three, currently used, production type HVSs
- Photograph A.3: Long distance hauling of the HVS using a tractor
- Photograph A.4: The test carriage fitted with a dual truck wheel
- Photograph A.5: Electronic Profilometer
- Photograph A.6: The Road Surface Deflectometer (RSD)
- Photograph A.7: The Multi-Depth Deflectometer (MDD)
- Photograph A.8: The Crack-Activity Meter (CAM)

1 INTRODUCTION

Accelerated pavement testing (APT) is conducted in a number of countries either by using stationary test equipment for the testing of trial sections or mobile units that can be used on in-service roads. The stationary equipment includes circular tracks (e.g. the LCPC facility at Nantes) or linear tracking equipment (e.g. University of Delft). Mobile equipment currently available includes the Australian Accelerated Loading Facility (ALF), the Texas Mobile Load Simulator (MLS) and the South African Heavy Vehicle Simulator (HVS).

The CSIR's fleet of three Heavy Vehicle Simulators (HVSs) has been used to investigate pavement behaviour and performance over the last 20 years¹. A brief description of the HVS system including the pavement response measurement technologies is given in Appendix A. This work provided the foundation for the current state-of-the-art of new pavement design and pavement rehabilitation design in South Africa. The HVS has also been used to evaluate new technologies such as the "inverted" pavement designs, modified binders, asphalt rubber, emulsion treated bases and large stone asphalt mixes prior to their use on South African roads. The work over the last 20 years has resulted in a significant database which can be used to assess the results of any new test.

In April 1993, CALTRANS commissioned the University of California at Berkeley (UCB), Dynatest Consulting and the CSIR to conduct a pilot study to evaluate the potential of the HVS for conducting pavement studies for CALTRANS. The project included both HVS testing of field trials (conducted in South Africa) as well as a laboratory evaluation of field samples of the materials (conducted at UCB). The HVS work programme called for the evaluation of both a dense-graded asphalt concrete (AC) with a conventional binder and a gap-graded asphalt-rubber hot mix (ARHM). In the first two HVS tests, the AC mix was evaluated at elevated and ambient temperatures for rutting under both normal wandering traffic as well as channelized traffic. In the second series of tests, the fatigue performance of the AC mix was compared with that of the ARHM at controlled temperatures. For this purpose a special temperature control chamber was developed for the HVS. This device was used to control the road surface temperature of the test sections at 10 °C. In one instance, at the end of a test, the road surface temperature was reduced to -5 °C.

In this document, the results of the HVS testing are discussed and due to the fact that the scope of the work for this pilot project was limited, suggestions are made regarding enhanced analysis of the data obtained from this work. Suggestions regarding further HVS testing to address the topics investigated more comprehensively are also made.

2 OBJECTIVES AND SCOPE OF THE STUDY

The overall objective of this project is to evaluate the HVS developed by the Council of Scientific and Industrial Research (CSIR) of South Africa and the potential to provide CALTRANS with complete operational Accelerated Pavement Testing (APT) capabilities using the HVS system technology on high priority issues, such as the evaluation of polymer and rubber modified asphalts, large stone mixes and IVHS technology effects on pavement structures. This APT capability includes the HVS equipment, associated measuring and monitoring systems, and the expertise developed in South Africa since 1968 related to APT, the latter including access to the HVS data base plus associated analyses as well as the staff support to train the University of California at Berkeley (UCB) and CALTRANS staff to effectively use the system.

Current topics of interest to CALTRANS include the effect of Intelligent Vehicle Highway System (IVHS) implementation on pavement structures and the use of asphalt rubber hot-mix (ARHM) overlays as an alternative to conventional AC overlays. This pilot study addressed these two issues through the following specific objectives :

Objective I : Comparison of the rutting of a dense-graded asphalt mix under wandering traffic with its behaviour under channelized traffic

One of the pavement-related concerns for IVHS implementation is that traffic loading will be more channelized on IVHS roadways than is currently the case under normal traffic. This will affect the rate of rut development, which may affect IVHS vehicle pavement sensor interaction. A preliminary evaluation of the effect of traffic channelization on rut development was carried out with the HVS system on a typical CALTRANS pavement section. To simulate channelized traffic, the loading beam of the HVS was fixed in one position, thus preventing any sideways movement during trafficking. During wandering traffic, the HVS is used in its usual mode resulting in a traffic pattern with a normal distribution. Data from similar rutting tests was retrieved from the HVS database and compared with the generated results.

Objective II : Comparison of the fatigue performance of a 38 mm ARHM under accelerated traffic with that of a 75 mm conventional dense-graded asphalt mix

CALTRANS has published a guideline allowing the use of reduced thickness of ARHM overlays in lieu of AC overlays, based primarily on the Ravendale² field test results. HVS testing in which the fatigue performance of a 38 mm ARHM overlay was compared with that of a 75 mm conventional overlay was conducted to verify the Ravendale results. In this case the traffic pattern followed a normal distribution.

The CSIR addressed the above objectives by using HVS system technology which enables the rapid evaluation of pavement field performance. A brief description of the HVS system is given in Appendix A. In addition to the above, laboratory evaluations of the mixes used in the HVS test sections were conducted both at the University of California at Berkeley and by the CALTRANS staff in Sacramento, the results of which are not integrated in this document.

3 DESIGN AND CONSTRUCTION OF TRIAL SECTIONS

3.1 Objectives and pavement selection

To address the stated objectives I and II above, six trial overlays were constructed on the P6/1 from Bapsfontein to Bronkhorstspruit near Pretoria. The overlays were constructed using materials and mix design procedures conforming to CALTRANS specifications. The following sections were constructed :

- **Channelized vs wandering traffic**
A 100 mm overlay was constructed on two adjacent 40 m long sections on an existing pavement with a granular base. These were used for evaluating the effect of wandering vs channelized traffic on the rutting behaviour of the AC overlay.
- **Fatigue performance on the ARHM compared with the AC overlay**
The target surface deflection (80th percentile) for this experiment was 1,25 mm under a 40 kN wheel load on the existing pavement prior to overlaying. Based on the CALTRANS TM356 overlay design procedure, and for a TI equal to 7, this would call for a 75 mm overlay of asphaltic concrete. The "equivalent" ARHM overlay would be 38 mm thick. Two other ARHM overlays of 25 mm and 50 mm respectively, were constructed for additional testing, should the 38 mm layer last for either a longer or shorter period than anticipated.

A prerequisite was that the pavement should contain no cemented materials. Using both the Pavement Management System of the Transvaal Provincial Administration and Deflectograph surveys, road P6/1 was selected.

The pavement structure prior to overlaying consist of:

- 40 mm of old asphaltic seals
- 215 mm of natural sandstone gravel
- 90 mm of weathered laterite (ferricrete)
- 280 mm of weathered shale
- the subgrade consisting of weathered shale the quality of which improves with depth

The condition of the pavement prior to overlaying can be seen in Photograph 1. It is clear that the pavement was severely cracked and showed significant rutting. The P6/1 was one of the first roads tested with the HVS in 1979. Photograph 2 shows the distress simulated by the HVS 14 years ago³. The similarity in distress compared with that in Photograph 1 is remarkable. Photograph 3 shows a general view of the construction of the trial sections.

3.2 Selection of test sections

The surface deflections as measured with both the CSIR Deflectograph and the RSD are shown in Figures 3.1 and 3.2. The RSD measurements, which are more accurate, were used to select the specific 8 m sections for HVS testing. The overlays, each 40 m in length, were constructed based on the principle that the deflections on the first two sections should be similar and that the support should be as sound as possible seeing that rutting in the AC layer was to be the dominant distress factor. On the remaining four sections the deflections were in the order of 1,2 mm prior to overlaying, which is within the range found on the Ravendale² project.

The HVS tests conducted are summarized in Table 3.1 below:

Table 3.1: Summary of HVS tests conducted for CALTRANS

Section number	Overlay type	Type of traffic	Wheel load (kN)	Test temperature (°C)
379A3	100mm AC	Channelized	70/100	25/40
380A3	100mm AC	Wandering	70/100	25/40
381A3	75mm AC	Wandering	40/80	10
382A3	38mm ARHM	Wandering	40/80	10/-5
383A3	25mm ARHM	Wandering	40/80	10

3.3 Mix designs

The CALTRANS laboratories prepared the mix designs for the AC and ARHM mixes, based on the Hveem method for determination of the optimum binder content. The aggregates and binders actually used in the project were used in the mix design. The target gradings, operating ranges and design binder contents specified for the project are given in Table 3.2.

An asphalt rubber binder (Arm-R-ShieldTM) was used to construct the ARHM mixes. The asphalt rubber blend consisted of approximately 78% 80/100 penetration grade asphalt binder, 20% recycled rubber (of which 30% was natural rubber) and 2% extender oil. The AC mix was manufactured with unmodified 60/70 penetration grade asphalt binder.

The batching information and the gradings of the aggregate fractions used to constitute the AC and ARHM mixes are given in Table 3.3. The coarse aggregate and crusher sand fractions consisted of Reef Quartzite. Small amounts of natural sand and mine sand were required to increase the fines and filler contents of the AC mixes. Figures 3.3 and 3.4 show the target and actual gradings achieved for the two mixes.

TABLE 3.2: Target gradings, operating ranges and target binder contents

Sieve Size (mm)	ARHM			AC		
	Target	Lower Limit	Upper Limit	Target	Lower Limit	Upper Limit
19,0	100	100	100	100	95	100
13,2	100	90	100	83		
9,5	83	78	88	72	65	80
4,75	36	31	41	52	47	57
2,36	21	17	25	38	33	43
0,600	10	6	14	20	15	25
0,075	3	2	7	4	3	8
% binder/aggregate	6,0	5,8	6,1	4,9	4,7	5,0
% binder/total mass	5,6	5,5	5,8	4,6	4,5	4,8
% voids	2,65	2,70	2,60	-	-	-

TABLE 3.3: Grading of aggregate fractions and batching information

Sieve Size (mm)	Percentage passing sieve size					
	19,0 mm	13,2 mm	9,5 mm	Crusher sand	Natural sand	Mine sand
26,5	100					
19,0	83	100				
13,2	6	94	100			
9,5		20	96	100	100	
4,75		1	7	99	93	
2,36			3	74	77	
1,18			2	50	50	
0,600			2	34	27	100
0,300			2	21	14	95
0,150			1	12	7	54
0,075			1	7	4	17
Batching information						
AC	26 %	24 %	-	32 %	12 %	6 %
ARHM	-	16 %	55 %	29 %	-	-

The AC and ARHM mixes were blended in the CSIR laboratory at optimum binder contents. They were then conditioned by short term oven ageing (STOA) for a period of 4 hours at mixing temperature and compacted by means of the Hugo hammer⁴ (impact-kneading compaction), after which they were subjected to dynamic testing. The following properties were determined on 100 mm asphalt briquettes :

- resilient modulus (10 Hz haversine loading frequency, 0,9 seconds rest period, 25°C);
- indirect tensile strength (50 mm/minute, 25°C), and
- dynamic creep modulus (0,5 Hz square wave, 100 kPa, 40°C, 3,600 load repetitions).

The average results are given in Table 3.4. It should be noted that ARHM mixes are frequently used in South Africa but that they are generally manufactured at higher binder contents (up to 7 per cent by mass of total mix).

TABLE 3.4: Average results of dynamic tests

Property	ARHM	AC
Resilient Modulus (MPa)	1 509	2 747
Indirect tensile strength (kPa)	727	1 508
Dynamic creep modulus (MPa)	11,5	13,1

3.4 Construction monitoring

During construction of the trial mixes, the following were monitored:

- paving thickness;
- the number of roller passes and types of roller used;
- in situ densities, and
- temperature of the mix prior to paving, during paving and during compaction.

In addition, gradings and binder contents were monitored by testing uncompacted material from each truck load as well as cores taken from the sections after construction. The average gradings and binder contents for the AC and ARHM mixes are given in Table 3.5. The average mixing and compaction temperatures were as follows :

AC :	Mixing temperature:	146°C
	Compaction temperature:	137°C
ARHM :	Mixing temperature:	155°C
	Compaction temperature:	140°C

3.5 Tests on cores taken from the sections

Cores were taken from all the sections to determine specific gravities as well as resilient moduli, using the indirect tensile test (ITT). The values are given in Tables 3.6 and 3.7 below. The reduction in resilient modulus of the AC mix as temperature increases should be noted.

Table 3.5 : As-built data on gradings and binder contents

Sieve Size (mm)	AC (75 and 100 mm)		ARHM (37 and 25 mm)	
	Average	Range	Average	Range
26,5	100	100	100	100
19,0	94	92-98	100	100
13,2	88	85-93	99	98-100
9,5	84	79-88	85	77-89
4,75	55	52-56	37	31-42
2,36	42	39-44	25	23-26
0,600	23	21-24	12	9-13
0,075	7	6-8	4	3-5
% binder / total mass	4,4 %	4,2-4,7	5,7 %	5,6-5,9

Table 3.6 : Specific gravity of cores removed from the overlay sections

	Test section					
	100 mm AC wandering	100 mm AC channelized	75 mm AC	50 mm ARHM	37 mm ARHM	25 mm ARHM
Ave.	2,251	2,256	2,303	2,214	2,190	2,214
Std dev.	0,009	0,010	0,014	0,037	0,037	0,037

Table 3.7 : Resilient modulus values of cores from the overlay sections

Test section	Test temperature	Resilient modulus
Channelized (100mm AC)	25 °C	2 018 MPa
Channelized (100mm AC)	40 °C	705 MPa
Wandering (100mm AC)	25 °C	1 960 MPa
Wandering (100mm AC)	40 °C	808 MPa
75 mm AC	10 °C	3 515 MPa
37,5 mm ARHM	10 °C	2 065 MPa
25 mm ARHM	10 °C	2 065 MPa

4 HVS EVALUATION OF THE RUTTING PERFORMANCE OF THE AC OVERLAY

Within the 80 m length of the 100 mm thick AC overlay section, two 8 m sections were selected based on the RSD deflection data (see Figure 4.1). The surface deflections at these two locations were relatively uniform and comparable. The average deflection on the channelized traffic section was 0,920 mm with a standard deviation of 0,037. In the case of the wandering traffic section, the average deflection was 0,885 mm with a standard deviation of 0,027.

4.1 Work procedure

Both the sections were trafficked with a 70 kN dual wheel load for 116 000 repetitions after which the wheel load was increased to 100 kN. The following information was collected during the test :

- **Temperature measurements**
Thermocouples were installed at six positions on both sides of the test section. Sensors were placed on and below the surface, at 0 m, 30 mm, 60 mm and 100 mm depths. Readings were taken every 2 hours for the duration of the test.
- **Rut measurements**
Rut data was collected with both the Electronic Profilometer and a simple straight edge. Data was collected at points 2, 3, 4 and 5 (for the ambient temperature section), and at points 11, 12, 13 and 14 (for the heated temperature section). Figure A.2 (Appendix A) shows the layout of a typical HVS test section.
- **Pavement in-depth deflections**
MDDs were installed at points 4 and 12. Five modules were installed at the following depths : 85 mm (to determine the deformation within the overlay itself), 350 mm, 500 mm, 720 mm and 1000 mm (see Figure 4.2). Although the ferricrete layer was only 90 mm thick, the third module had to be installed 150 mm below the second one. This limitation is due to the size of the LVDTs currently used.
- **Surface deflections**
RSD (Road Surface Deflection) measurements were taken along the centre line of the test section at the following points: 2, 3, 4 and 5 (for the ambient temperature part of the section) and point 11, 12, 13 and 14 (for the heated part of the section).

To determine the exact conditions prior to HVS trafficking, a complete set of readings was taken after 10 repetitions of HVS traffic to "settle the section in". All measurements after trafficking are related to this set of initial measurements.

Table 4.1 shows the data collection schedule which was identical for both tests.

Table 4.1 : Data collection schedule for both the wandering and channelized traffic sections

Repetitions	Trafficking Wheel Load	Rut	Deflection measurements			
			MDD		RSD	
			40 kN test wheel load	70 kN test wheel load	40 kN Test Wheel Load	70 kN Test Wheel Load
10	70 kN	X	X	X	X	X
5 000	70 kN	X		X		X
10 000	70 kN	X		X		X
20 000	70 kN	X		X		X
30 000	70 kN	X		X		X
50 000	70 kN	X	X	X	X	X
75 000	70 kN	X		X		X
100 000	70 kN	X		X		X
116 000	100 kN	X	X	X	X	X
164 000	100 kN	X	X	X	X	X
200 000	100 kN	X		X		X
250 000	100 kN	X		X		X
275 000	100 kN	X	X	X	X	X

4.2 Temperatures measured

During trafficking, the target surface temperatures were 40 °C for one half of the section and 25 °C for the other half. The temperatures were kept relatively constant by heating the surface with heavy duty heaters (see Photograph 4). Table 4.2 shows the average temperatures at various depths during the test.

Table 4.2 : Average temperatures measured on channelized and wandering traffic sections (°C)

Depth	Channelized traffic section		Wandering traffic section	
	Ambient Temp Portion	Heated Portion	Ambient Temp Portion	Heated Portion
Target Temperature	25	40	25	40
Surface	22,7	38,2	24,1	39,9
30 mm	19,1	33,9	20,7	35,6
60 mm	16,8	30,6	18,5	32,4
100 mm	15,4	28,4	16,9	29,9

4.3 Surface rutting

Both the sections rutted at a slower rate than was expected (based on results from limited laboratory tests), possibly owing to the flexibility of the support layers. The final maximum rut depths for the two sections are summarised in Table 4.3.

Table 4.3 : Maximum surface rut depth : Channelized vs Wandering traffic

Repetitions	Trafficking wheel load (kN)	Maximum rut depth (mm)	
		Channelized traffic	Wandering traffic
116 000	70	13	6
164 000	100	15, test stopped	8
275 000	100		13

Transverse profiles of the surface rutting of the two sections in their respective end states are shown in Figures 4.3 and 4.4. The effect of the channelization of the traffic is clear. This can also be seen in Photographs 5 and 6.

The rut measurements recorded on the **channelized traffic** section are shown in Figure 4.5. It is clear that temperature had a significant effect on rutting. In the case of both the ambient temperature and heated portions of the section, the increase to 100 kN caused a minor secondary settling in after which the rutting remained relatively constant.

The rut measurements recorded on the **wandering traffic** section can be seen in Figure 4.6. Once again temperature had a significant effect on the rut rate. In the portion of the section that was kept at ambient temperature, the increase in wheel load from 70 kN to 100 kN had no significant influence on the rut rate. In the case of the heated section, the rut rate, after settling in, increased with the increase in wheel load from 70 kN to 100 kN.

The effect of channelization of traffic on rutting is shown in Figure 4.7. The maximum rut depth on the channelized section after 150 000 repetitions was approximately double that of the wandering traffic section at the same stage. The rutting behaviour observed on both sections can be divided into three phases :

- Phase I : A "settling in" phase at the 70 kN wheel load during which significant rutting takes place over a relatively short period of time.
- Phase II : A phase during which the rutting takes place at a more constant rate under the 70 kN wheel load.
- Phase III : The final phase where the wheel load was increased to 100 kN.

The rut rates per 100 000 repetitions as well as the total rut per phase, calculated from these results, are shown in Table 4.4. These rut rates and the graphs in Figures 4.5 and 4.6 clearly indicate that the rutting took place mainly during the "settling in" phase after which the rut rate decreased. This behaviour is often observed with HVS tests. Usually a secondary "settling in" phase will be observed when the temperature or the wheel load is increased during a test. This is then usually followed by another "flattening off" of the rut curve.

In the AASHTO road test, the load equivalency exponent or damage factor (n) in the equation $F = (P/40\text{kN})^n$ was defined as 4.2. However, results of HVS testing indicated that the damage factor may range between 2 and 6, depending on the sensitivity of the pavement to overloading. Results of further HVS tests at different wheel loads could be used to determine damage factors for cracking and deformation for these trial mixes.

4.4 In-depth deflections and moduli

The MDDs installed in each section were used to calculate the elastic deformations in each layer at various stages during the tests. The changes in in-depth elastic deflections for the channelized and wandering traffic sections are shown in Figures 4.8 to 4.11. The initial stiffness values for the layers at the start of the test were backcalculated from this data using the ELSYM5 program. The values are given in Tables 4.5 and 4.6 below. This work is additional to the original scope of the project and is included for information purposes only.

The MDDs were also used to measure the permanent deformation within each layer. Figures 4.12 to 4.15 show the permanent deformation measurements for the two tests. This information can be used to determine deformation rates **within the AC layer**. This can then be compared with the results of previous HVS testing, taking cognisance of material properties

and the pavement structural response. Further data analysis can also provide the changes in moduli in the pavement structure as testing progresses.

Table 4.4 : Rut rates per 100 000 repetitions and total rutting per phase

		Rut rate (mm per 100 000 repetitions) and total rut (mm) per phase			
		Channelized traffic		Wandering traffic	
		Phase of trafficking	Rut rate	Total rut	Rut rate
Ambient temperature	Phase I : settling in (70 kN)	20,0	3,0	9,86	2,0
	Phase II : 70 kN wheel load	1,02	1,0	1,05	1,0
	Phase I and II combined	3,43	4,0	2,58	3,0
	Phase III : 100 kN wheel load	4,06	2,0	2,5	4,0
Elevated temperature	Phase I : settling in	59,56	6,7	20,42	6,0
	Phase II : 70 kN wheel load	6,27	6,2	1,17	1,0
	Phases I and II combined	11,14	13,0	6,03	7,0
	Phase III : 100 kN Wheel Load	4,1	2,0	3,76	6,0

Table 4.5 : Backcalculated Moduli (initial stage) for the channelized traffic section (379A3) (laboratory resilient modulus used for AC layer) in MPa

Wheel load	70 kN		40 kN	
	25°C	40°C	25°C	40°C
AC (85 mm)	2 018	705	2 018	705
Base (265 mm)	119	97	63	73
Subbase (150 mm)	51	28	49	21
Subbase (220 mm)	49	44	55	35
Subgrade	191	131	153	113

Table 4.6 : Backcalculated moduli (initial stage) for the wandering traffic section (380A3) (laboratory resilient modulus used for AC layer) in MPa

Wheel load	70 kN		40 kN	
Temperature	25°C	40°C	25°C	40°C
AC (85 mm)	1 960	808	1 960	808
Base (265 mm)	364	100	135	79
Subbase (150 mm)	10	32	28	27
Subbase (220 mm)	31	26	56	23
Subgrade	216	143	236	123

4.5 Surface deflections

The surface deflections measured at various stages during the tests are shown in Figures 4.16 to 4.19. The differential increases in surface deflection between the end of the "settling in" phase and the end of Phase II are given in Table 4.7. This table indicates that temperature and wheel load did not have a major effect on the relative increase in surface deflection after the settling in phase. On the other hand the type of loading (channelized versus wandering traffic) had a noticeable effect - the average increase on the channelized section being 0,34 mm compared with the 0,23 mm on the wandering traffic section.

Table 4.7 : Increases in surface deflection after the settling in phase (mm)

Temperature	Ambient		Heated		Average increase
	40	70	40	70	
Channelized traffic	0,35	0,38	0,28	0,35	0,34
Wandering traffic	0,2	0,26	0,2	0,27	0,23

4.6 Comparison of results with other HVS tests in the HVS database

To place the work conducted in this project in perspective, the results were compared with some information from the HVS database. As part of a recent project on large-aggregate mixes, conducted for the Southern African Bitumen and Tar Association, trial sections of three different mixes using large maximum aggregate sizes (37,5 mm) were tested with the HVS near Dundee in Natal⁵. The pavement structure consisted of a fairly stiff lime-treated subbase (150 mm), large-stone asphalt base (150 mm) and a conventional semi-gap-graded surfacing (40 mm). The rutting behaviour of a semi-gap graded, a continuously graded and a semi-open-graded mix was evaluated. In the event of advanced analysis of the data, the surface rut rates as well as the deformation within the AC layer could be compared with the results obtained during the testing of the Dundee trials.

Table 4.8 contains a summary of the **surface rutting rate** in pavements consisting of asphalt bases with cemented subbases obtained from a number of HVS tests. The previous tests conducted at 70 kN or 80 kN at ambient and elevated temperatures (marked * in Table 4.8) showed rut rates between 0,74 and 1,15 mm per 100 000 repetitions. This compares well with the results obtained from the wandering traffic section (1,05 to 1,17 mm per 100 000 repetitions). However, the combination of channelized traffic and elevated temperature resulted in a rut rate of 6,27 mm per 100 000 repetitions (see Table 4.4), which is significantly higher than the above. This is indicative of the damaging effect of channelized traffic compared with normal wandering traffic.

Table 4.8 : Typical (phase II) surface rutting rates in asphalt base pavements tested under the HVS

Test	Temperature Conditions	Load (kN)	Repetitions (x 1000)	Grading	Rut rate (mm/100 000 reps)
201A3	ambient	80	0-900	semi-gap	1,23
162A3	ambient	80	0-900	semi-gap	0,66
343A3	ambient 40°C	40	1136-1214	semi-gap	0,33
	ambient 40°C	100	1214-1292		0,96 2,97 14,55
223A3	ambient	100	0-522	cont.	2,29
	ambient	100	522-679		2,71
	ambient	100			0,85
	ambient	100			2,38
224A3	ambient	40	0-280	cont.	0,63
	ambient	40	280-298		0,65
	ambient	150			82,44
	ambient	150			108,84
215A3	ambient	100	0-520	cont.	2,23
	ambient	100			2,26
217A3	ambient	100	0-92	cont.	2,16
	ambient	100	92-532		2,82
	ambient	100			1,60
	ambient	100			0,66
	ambient	100	532-800		2,06
	ambient	100			3,12
218A3	30-40°C	40	0-96	cont.	11,9
	ambient	40			2,01
233A3	ambient	70	0-315	cont.	0,74 *
	ambient	70	315-370		1,15 *
	40-50°C	100			25,50
	40-50°C	100			32,69
234A3	ambient	70	0-100	cont.	1,04 *
	ambient	70			0,98 *
235A3	ambient	40	0-802	cont.	0,22
	ambient	40			0,22
183A3	40-50°C	40	0-200	cont.	1,91
	40-50°C	80	200-320		1,11 *
193A3	ambient	40	0-200	semi-gap	2,29
140A3	40-50°C	40	0-200	semi-gap	3,48
367A3	20 °C	100	150	semi-gap	3,75
368A3	20 °C	100	150	semi-open	0,754
369A3	20 °C	100	150	continuous	0,868
370A3	30 °C	40	700	continuous	0,1
370A3	50 °C	40	900	continuous	0,4
379A3	25 °C	70, CH	100	continuous	1,02
379A3	40 °C	70, CH	100	continuous	6,27
380A3	25 °C	70, WAN	90	continuous	1,05
380A3	40 °C	70, WAN	90	continuous	1,17

5 HVS EVALUATION OF THE CRACKING PERFORMANCE OF THE AC OVERLAY COMPARED WITH THE ARHM OVERLAYS

5.1 Trial sections

The main objective of the second part of the project was to verify the current CALTRANS policy which states that for a road with a specific deflection, an ARHM overlay of half thickness can be used instead of a full thickness conventional AC overlay for similar overlay performance. For this purpose, four trial sections were constructed: a 75 mm AC overlay section and three ARHM overlay sections of thickness 50 mm, 38 mm and 25 mm. The testing was scheduled to allow the AC overlay and the 38 mm ARHM overlay to be tested first and then, depending on whether the 38 mm ARHM overlay cracked before or after the AC overlay, the subsequent testing of either the 50 mm or the 25 mm ARHM overlay.

A section of road with an 80th percentile deflection of around 1,2 mm was selected on the P6/1 Bapsfontein to Bronkhorstspuit. Figure 5.1 shows the surface deflections measured as well as the location of the test sections.

5.2 Predicted life to cracking

Using the CALTRANS TM356 overlay design procedure, the life of the sections to cracking was predicted. The average RSD deflection measured over the 40 m, 75mm AC overlay section was 1,208 mm (0,0476 in) with a standard deviation of 0,146 mm (0,0057 in).

$$\begin{aligned} \text{i) GE (ft)} &= 1,89 \times \text{AC thickness (ft)} \\ &= 1,89 \times 0,246 \\ &= 0,47 \end{aligned}$$

From the graph in Figure 5.2 the percentage reduction in deflection is then determined as 42 per cent.

$$\begin{aligned} \text{ii) Surface deflection average} &= 1,208 \text{ mm} \\ \text{Standard deviation} &= 0,146 \text{ mm} \\ \text{DELTA (mean)} &= 1,208 + 0,84 \times 0,146 \\ &= 1,3306 \text{ mm} \\ &= (1,3306 / 25,4) \times 10^3 \\ &= 52,39 \text{ mils} \end{aligned}$$

$$\text{ii) } [\text{DELTA(mean)} - \text{DELTA(tol)}] \div \text{DELTA(mean)} = \% \text{ Reduction}$$

$$\begin{aligned} \text{DELTA(tol)} &= - [(0,42 \times 52,39) - 52,39] \\ &= 32,3 \end{aligned}$$

- iii) Thickness of existing surfacing = 40mm = 0,131 ft
From graph 11 (see Figure 5.3) this results in a TI value of 7,3

$$7,3 = 9,0 \times [\text{ESALS} / 10^6]^{0,119}$$

Thus number of ESALS to failure = 172 000

A 40 kN wheel load was therefore used for all three sections up to 175 000 repetitions after which the wheel load was increased to induce cracking.

5.3 Work procedure

All three sections were trafficked in exactly the same way. A 40 kN dual wheel load was used up to the predicted life of the overlay (175 000 repetitions) after which it was increased to 80 kN. The temperature was initially controlled at 10 °C, but lowered to -5°C at the end of the testing of the 38 mm ARHM overlay in order to induce cracking. As in the case of the tests discussed in section 4, the following information was collected during the test:

- temperature;
- rut measurements;
- pavement in-depth deflections, and
- surface deflections.

In addition, the sections were carefully scrutinised for cracking on a daily basis. Table 5.1 gives a summary of the data collection schedule.

5.4 Temperature control chamber

To control the temperature during HVS testing, a temperature control chamber was specially designed and constructed for this project. The chamber is shown in Photograph 7. The roof is fixed to the frame of the HVS and two air conditioning units are suspended from it (see Photograph 8). The sides and ends of the chamber (consisting of the same insulation material as the roof) are fitted so that they can be easily removed. With the sides and ends of the chamber removed, the HVS can be moved for short distances without having to remove the remaining equipment. At each end, a special sliding panel is fixed to the moving beam of the HVS allowing effective temperature control while the HVS is used in the wandering traffic mode (see Photograph 7).

During the experiments it was found that the temperature could be controlled at 10 °C with ease. At the end of the testing of the 38 mm ARHM overlay, the temperature was lowered to -5°C. During this stage, the air temperature reached a minimum of -26 °C. A summary of the temperatures as recorded by means of thermocouples during each of the tests is given in Table 5.2.

Table 5.1 : Data collection schedule for the 75 mm AC overlay and ARHM sections

Repetitions	Trafficking wheel load	Rut	Deflection measurements 40 kN Test Wheel Load	
			MDD	RSD *
10	40 kN	X	X	X
5 000	40 kN	X	X	X
10 000	40 kN	X	X	X
25 000	40 kN	X	X	X
50 000	40 kN	X	X	X
75 000	40 kN	X	X	X
100 000	40 kN	X	X	X
125 000	40 kN	X	X	X
150 000	40 kN	X	X	X
175 000	80 kN	X	X	X
200 000	80 kN	X	X	X
250 000	80 kN	X	X	X

* - The RSD deflections were measured every 0,5 m on the centre line for the whole length (8 m) of each test section.

Table 5.2 : Temperatures measured during the testing of the 75mm AC overlay and the ARHM overlays

Depth and target temp	75 mm AC 10 °C	38 mm ARHM 10 °C	25 mm ARHM 10 °C	38 mm ARHM -5 °C
Surface	9,6	11,3	12,2	-5.7
30 mm	6,2	8,4	10,4	-9.3
60 mm	3,6	6,8	9,4	-9.2
100 mm	1,2	5,8	8,6	-9.3

5.5 Cracking performance of the sections

The 75 mm AC overlay started to show hairline cracking after 100 000 repetitions. After 175 000 repetitions it showed substantial cracking. The wheel load was then increased to 80 kN for a short period of time. The final state of the cracking on the test section is shown in Photograph 9. Photograph 10 shows a close up view of the cracking on the 75 mm AC overlay.

The same pattern of loading was followed in the case of the 38 mm ARHM overlay. However, after 175 000 repetitions no cracking could be observed. The wheel load was then increased from 40 kN to 80 kN up to 237 000 repetitions. Still no cracking occurred. At this point the temperature control of the chamber was set at its minimum. At the end of the test one half of the test section was cracked as can be seen in Photograph 11. The road surface temperature at the end of the test was -5 °C.

Owing to the fact that the 38 mm ARHM overlay lasted longer than predicted, the 25 mm ARHM overlay section was subsequently tested. Once again no cracking was observed after 175 000 repetitions. The wheel load was then increased to 80 kN. After 237 000 repetitions, the test section had cracked without the temperature having been reduced. The end state of cracking on the 25 mm ARHM overlay is shown in Photograph 12.

This result indicates that a reduction of at least 50 per cent in layer thickness to obtain similar performance in fatigue mode is justified if conventional AC is replaced with ARHM. However, the reduction in structural capacity due to the reduction in layer thickness should be taken cognisance of. The results obtained are given in Table 5.3 below.

Table 5.3 : Cracking life of the 75 mm AC overlay and the ARHM overlays

Repetitions	Wheel Load	AC overlay section (75mm)	38 mm ARHM section	25 mm ARHM section
0 to 100 000	40 kN	Fine cracks at 100 000	-	-
100 000 to 175 000	40 kN	Block cracks at 175 000	-	-
Wheel load changed to 80 kN				
175 000 to 200 000	80 kN	Completely cracked	-	Fine cracks
200 000 to 237 000	80 kN	Test stopped	-	Completely cracked
Surface temperature reduced to -5 °C				
237 000 to 250 000	80 kN	Test stopped	One half of section cracked	test stopped

- indicates no visible cracking

5.6 Surface rutting

As the tests were conducted at low temperatures, surface rutting was not expected to be of major importance. Nevertheless, the surface rutting behaviour of the three sections is shown in Figures 5.4 to 5.6. The AC overlay section showed virtually no surface rutting. This is to be expected as the AC layer was relatively stiff at 10 °C, thus providing a higher resistance to deformation and also, on account of its thickness, improved protection to the underlying layers. Rutting occurred in both the 38 mm and the 25 mm ARHM overlays, owing to the lower protection provided by the less stiff and thinner ARHM overlays. In both these cases, the increase in wheel load to 80 kN resulted in an increase in the rate of rutting.

5.7 In-depth permanent deformation

The in-depth deformations recorded with the MDDs on the three sections are shown in Figures 5.7 to 5.12. In the case of the AC overlay, very little permanent deformation was observed as expected. In the case of both the 38 mm and the 25 mm ARHM overlay sections, some deformation took place in both subbase layers and the ARHM layer. The increase in wheel load to 80 kN had a noticeable effect on the permanent deformation of the subbase layers. This behaviour was not observed in the case of the AC layer - once again indicating that the higher stiffness of the AC layer and its thickness provided protection to the underlying layers.

5.8 Surface deflection

The surface deflections recorded with the RSD are shown in Figures 5.13 to 5.15. In the case of the AC overlay, the surface deflection increased gradually from 0,75 mm to 1,30 mm. The change in wheel load from 40 kN to 80 kN had no significant effect on the rate of increase in surface deflection.

In the case of the 38 mm ARHM overlay, the surface deflection increased from 1,4 mm to 1,7 mm during trafficking with the 40 kN wheel load. The change in wheel load from 40 kN to 80 kN had a significant effect on the rate of change of surface deflection and at the end, the surface deflection recorded was 2,6 mm.

On the 25 mm ARHM overlay section, the increase in surface deflection was less marked. The initial surface deflection was 1,25 mm which increased to 1,47 mm.

5.9 In-depth deflections and moduli

The in-depth deflections measured with the MDD are shown in Figures 5.16 to 5.21. Both the MDDs installed in the 75 mm AC overlay section indicated that, after the initial settling in phase, the in-depth deflections remained relatively constant. After the increase in wheel load from 40 kN to 80 kN, the largest increase in elastic deflection occurred in the second subbase layer.

In the case of the 38 mm ARHM overlay section, the in-depth deflections also remained relatively constant. The deflections measured at MDD 4 showed a slight increase owing to the change in wheel load. A significant decrease was caused by the lowering of the temperature at the end of the test. At MDD12 a more significant increase in deflections was observed after the increase in wheel load. The main increase in deflection occurred in the base and second subbase layers. This implies that the strains induced in the ARHM overlay at point 12 would have been significantly higher than at point 4. It is important to note that this section cracked only in the portion where MDD12 was installed (see Photograph 11).

The deflections on the 25 mm ARHM overlay remained relatively constant throughout the test with only a slight increase in deflection at the change in wheel load.

The in-depth deflections were once again used to backcalculate the initial resilient moduli (using ELSYM5) for the layers. The values are shown in Tables 5.4 to 5.6.

In these calculations the stiffness of the asphalt mix was taken as the resilient modulus determined with the Indirect Tensile Test at the relevant temperature (10 °C).

Table 5.4 : Initial stiffness moduli (MPa) backcalculated for the 75 mm AC overlay section

MDD position	MDD 4	MDD 12
AC (75 mm)	3 515	3 515
Base (250 mm)	168	79
Subbase (150 mm)	33	24
Subbase (225 mm)	24	29
Subgrade	115	134

Table 5.5 : Initial stiffness moduli (MPa) backcalculated for the 38 mm ARHM overlay section

MDD position	MDD 4	MDD 12
ARHM (60 mm)	2 065	2 065
Base (235 mm)	83	81
Subbase (150 mm)	21	15
Subbase (220 mm)	21	22
Subgrade	55	61

Table 5.6 : Initial stiffness moduli (MPa) backcalculated for the 25 mm ARHM overlay section

MDD position	MDD 4	MDD 12
ARHM (60 mm)	2 065	2 065
Base (220 mm)	70	73
Subbase (150 mm)	23	19
Subbase (220 mm)	24	22
Subgrade	117	122

6 SUGGESTIONS FOR ENHANCING THE RESULTS OF THE PILOT PROJECT

The scope of work for this pilot project was limited and focused mainly on the rutting and cracking behaviour. Usually analysis of the data acquired during HVS testing is done in more detail. Some suggestions are therefore made for enhancing the analysis of the data obtained in this project. The limited investigation also left some questions which could be addressed with future HVS testing.

Enhanced data analysis could include *inter alia* the following :

- an evaluation of the rutting within the AC overlay compared with historical HVS test results as well as the material properties measured in the laboratory
- an investigation into the changes in stiffness moduli as the pavement deteriorated under traffic
- comparison of the results obtained in this project with other channelized HVS tests conducted in the past
- an evaluation of the additional protection provided to the underlying layers (additional structural capacity) resulting from the use of the 75 mm AC overlay compared with the ARHM overlays
- mechanistic analysis of the test sections at various stages during the HVS testing to determine the changes in stiffness of the layers during the test and hence the changes in the stresses and strains induced in the layers (in order to improve the understanding of both the rutting and cracking behaviour of the layers)

Additional HVS testing could include :

- accelerated ageing of the AC layer followed by additional HVS testing to assess reduction in rut rates owing to the stiffening of this layer after ageing
- HVS testing of the 100 mm AC overlay on stiff support to assess the rutting behaviour at increased vertical stress conditions in the layer
- the determination of a damage factor for rutting to convert actual traffic to equivalent traffic (from rutting tests at various HVS wheel loads) accurately
- accelerated ageing of the AC and ARHM layers followed by HVS testing to evaluate the effect of ageing on the cracking behaviour of the materials
- HVS testing at lower temperatures to evaluate the effect of temperature cracking
- the determination of a damage factor for cracking at low temperatures in order to convert actual traffic into equivalent traffic (from HVS testing at various wheel loads) accurately

7 CONCLUSIONS

The work conducted in this pilot project was limited and suggestions were made in Section 6 for advanced processing of the data obtained as well as for additional HVS testing. The work reported here should be read in conjunction with the laboratory evaluation of the materials as conducted by the University of California at Berkeley. In general, the HVS testing was successful in all respects and provided some useful indicatory results addressing the two main objectives described in Section 2. The initial information obtained from this pilot project is also indicative of the value of accelerated testing of pavements.

7.1 Channelized vs wandering traffic

The HVS testing has shown that the channelization of traffic caused an approximate doubling of the rate of surface rutting compared with a traffic pattern with a normal distribution. The surface rutting was caused by deformation in both the AC overlay and the underlying layers. In the case of both the channelized and wandering traffic, the surface rutting was significantly affected by the increase in temperature from 25 °C to 40 °C. Most of the rutting occurred during a "settling in" phase. This behaviour is often observed during HVS testing and often a second "settling in" occurs when either the wheel load or the testing temperature is increased.

The surface rut rates indicated that the pavement structure tested would rut at a rate of up to 60 mm per 100 000 repetitions (during the settling in phase) in the case of channelized traffic and of a surface temperature of 40 °C. However, this generally takes place over a short period of time. After the initial settling in phase, the wandering traffic (70 kN) applied at a surface temperature of 40 °C resulted in a rut rate of 1,17 mm per 100 000 repetitions. Previous HVS testing at 70 kN or 80 kN and at elevated temperatures showed rut rates between 0,74 and 1,15 mm per 100 000 repetitions which compares well with the results obtained in this project. However, in the same phase (phase II), the channelized traffic at 40 °C resulted in a rut rate of 6,27 mm per 100 000 repetitions. This is a clear indication that channelization of traffic can significantly affect the rate of surface rutting on this type of pavement.

7.2 Cracking of the AC layer compared with the ARHM layers

The CALTRANS TM356 overlay design procedure predicted that the AC layer will crack at 172 000 repetitions. The first hairline cracks were observed after the application of 100 000 repetitions of a 40 kN dual wheel load at a constant surface temperature of 10 °C. At 175 000 repetitions the AC layer cracked into blocks.

The 38 mm ARHM layer did not show any cracking after 175 000 repetitions of the 40 kN wheel load followed by an additional 62 000 repetitions of an 80 kN wheel load (all at 10 °C). After the surface temperature had been reduced to -5 °C, and an additional 13 000 repetitions applied, one half of the test section showed cracking similar to that observed in the AC overlay

albeit at a much later stage. It is important to note that the in-depth deflections during the end phase of the test were significantly higher (2,6 mm vs 1,7 mm at 60 mm depth) on the cracked half of the section than on the other half.

The 25 mm ARHM overlay section also showed no cracking after 175 000 repetitions. However, in this case the layer cracked after a subsequent application of 60 000 repetitions of an 80 kN dual wheel load.

It can therefore be concluded that the half thickness of ARHM overlay will last at least as long as the full thickness of AC overlay on this pavement structure. However, the reduction in structural capacity due to the reduction in layer thickness should be taken cognisance of. Furthermore, it must be stressed that this work was conducted on fresh asphalt materials and that some accelerated ageing work should be conducted before a final conclusion is drawn.

8 ACKNOWLEDGEMENTS

The following organisations are recognised for their contribution to the funding of the research work :

The California Department of Transportation (CALTRANS)
The Transvaal Provincial Administration
TOSAS (Pty) Ltd

This document is published with the permission of the Director of the Division for Roads and Transport Technology of the CSIR, South Africa.

9 REFERENCES

- 1 Horak, E. Kleyn, E.G. Du Plessis, J. De Villiers, E.M. Thomson, A.J. The impact and Management of the Heavy Vehicle Simulator (HVS) fleet in South Africa. *Proceedings of the 7th International Conference on Asphalt Pavements*. Volume 2, Nottingham, UK, 1992.
- 2 Doty, R.N. Flexible Pavement rehabilitation using asphalt rubber combinations - a progress report. *Proceedings of the 67th Annual Meeting of the Transportation Research Board*. Washington DC, January 1988.
- 3 Maree, J.H. 1982. *Aspects on the Design and Performance of Pavements incorporating Crushed Stone Bases*. PhD Thesis, University of Pretoria.
- 4 Hugo, F. A. Critical review of asphalt paving mixes in current use with proposals for a new mix. *Proceedings of the Conference on Asphalt Pavements for South Africa*. Durban, CSIR, 1969.
- 5 Rust, F.C., Grobler, J.E., Myburgh, P.A., Hugo, F. Towards analytical mix design for large-stone asphalt mixes. *Proceedings of the 7th International Conference on Asphalt Pavements*. Nottingham, 1992.

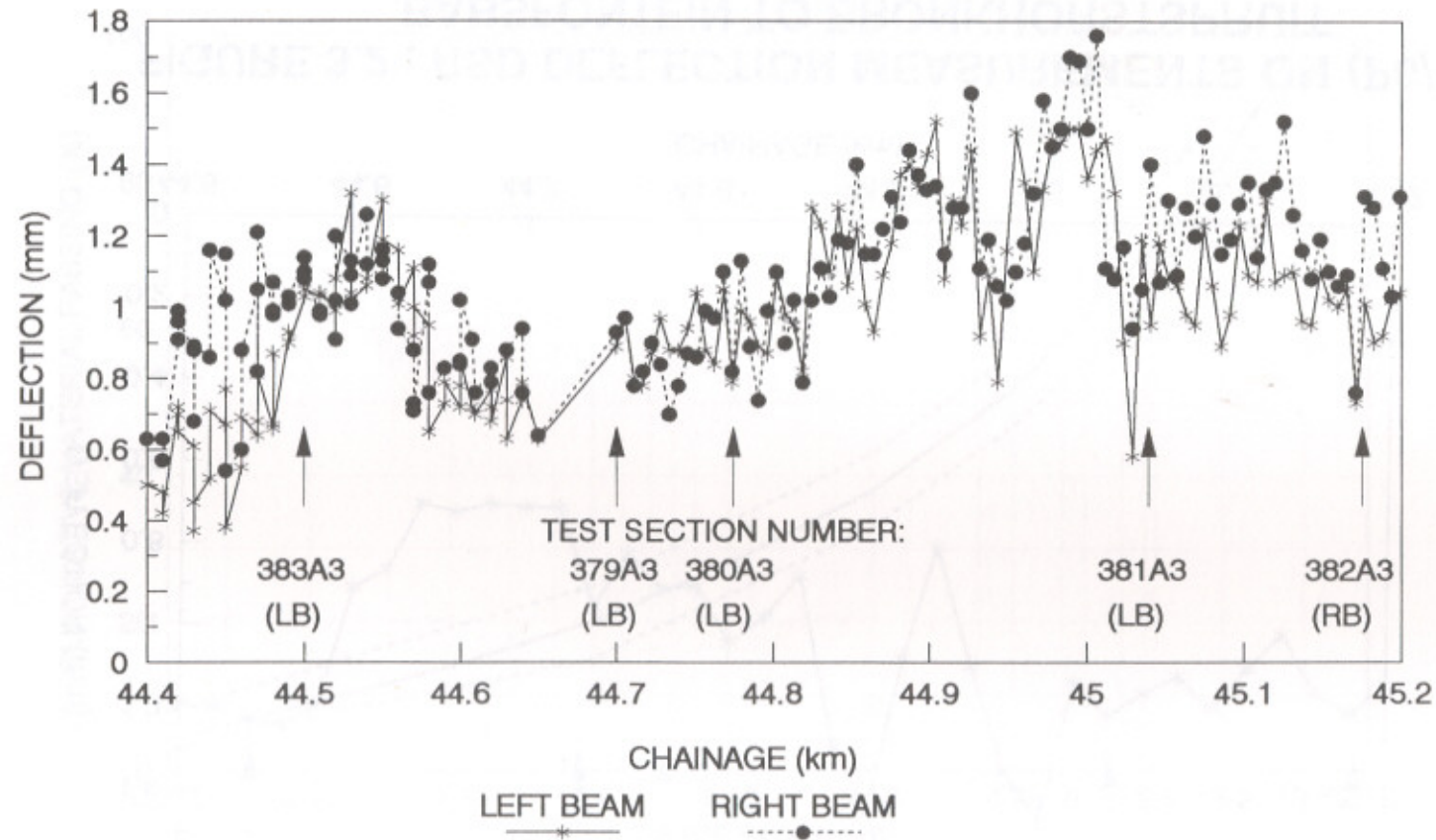


**FIGURE 3.1 : DEFLECTOGRAPH MEASUREMENTS ON P6/1,
 BAPSFONTEIN TO BRONKHORSTSPRUIT**

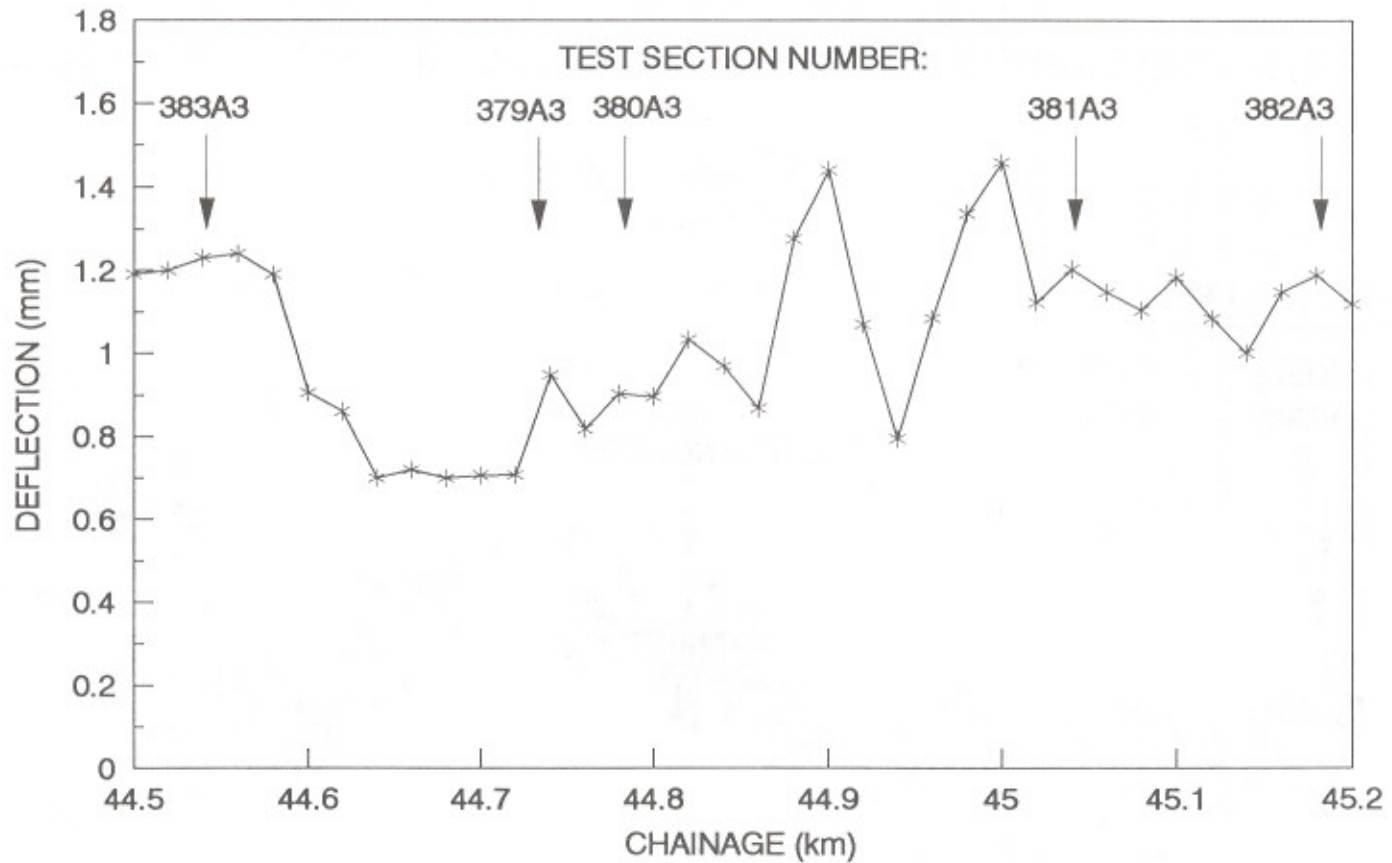


**FIGURE 3.2 : RSD DEFLECTION MEASUREMENTS ON (P6/1),
BABSFontein TO BRONKHORSTSPRUIT**

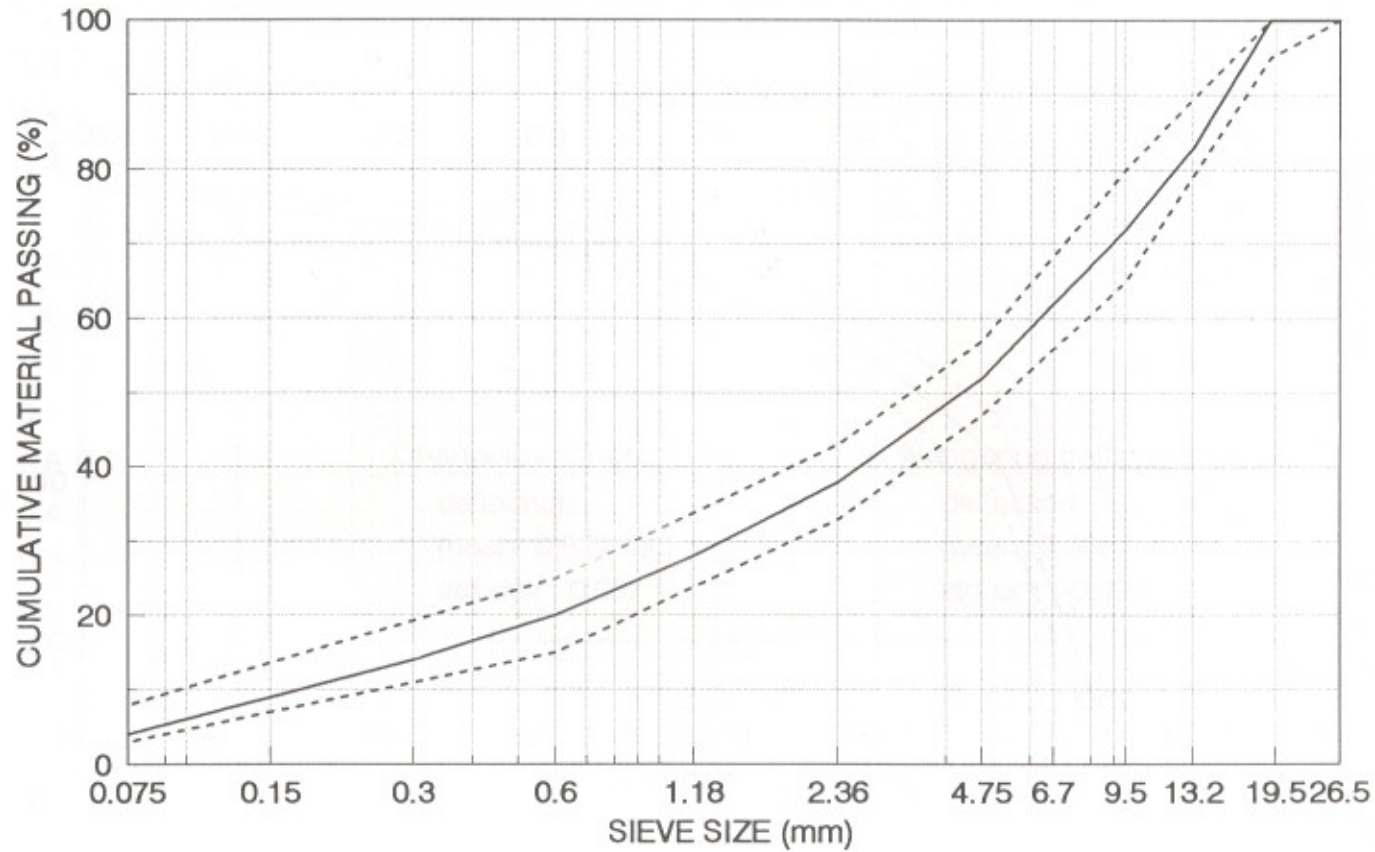


FIGURE 3.3 : TARGET AND ACTUAL AVERAGE GRADINGS FOR AC MIX

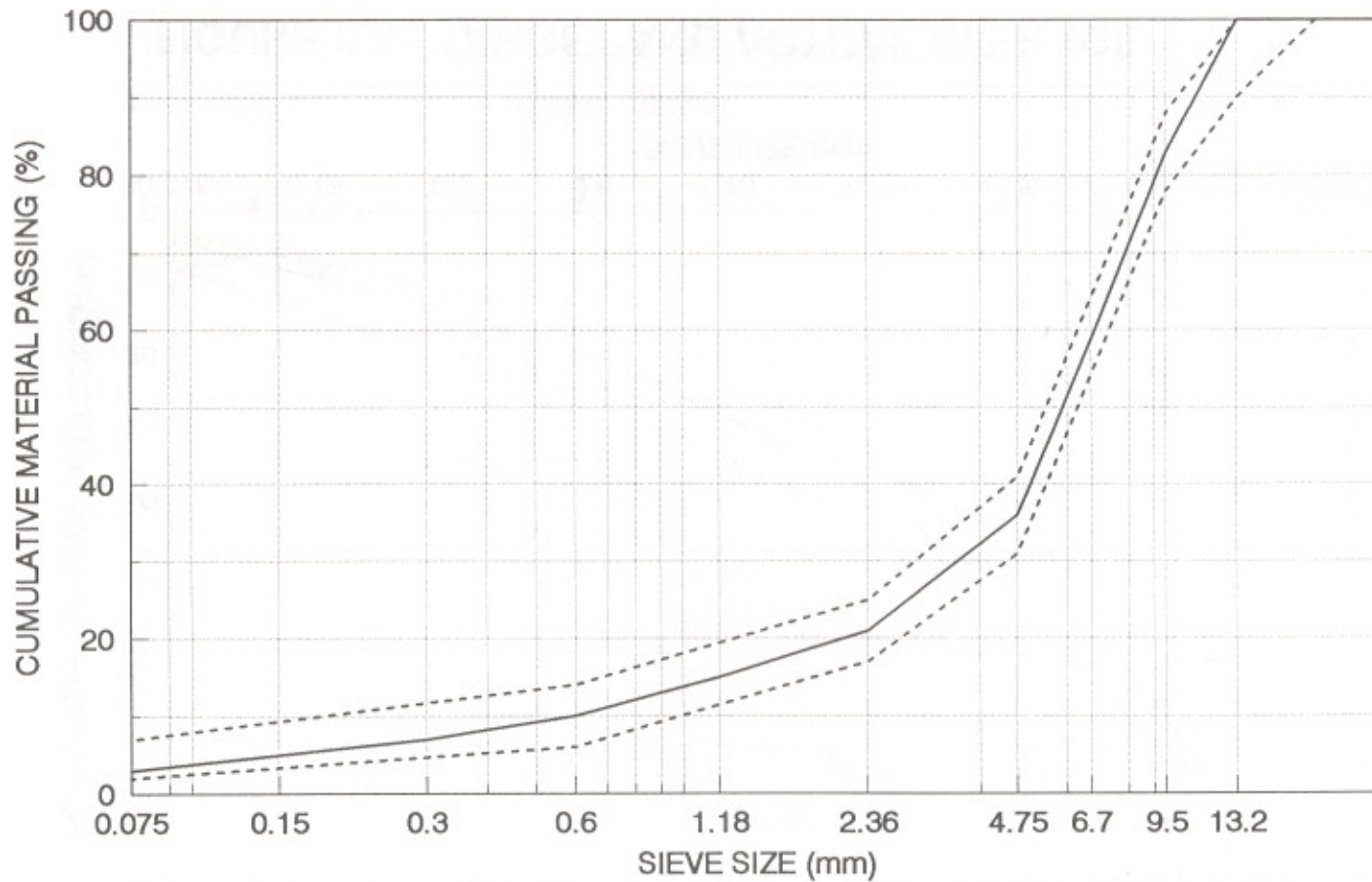


FIGURE 3.4 : TARGET AND ACTUAL AVERAGE GRADINGS FOR ARHM MIX

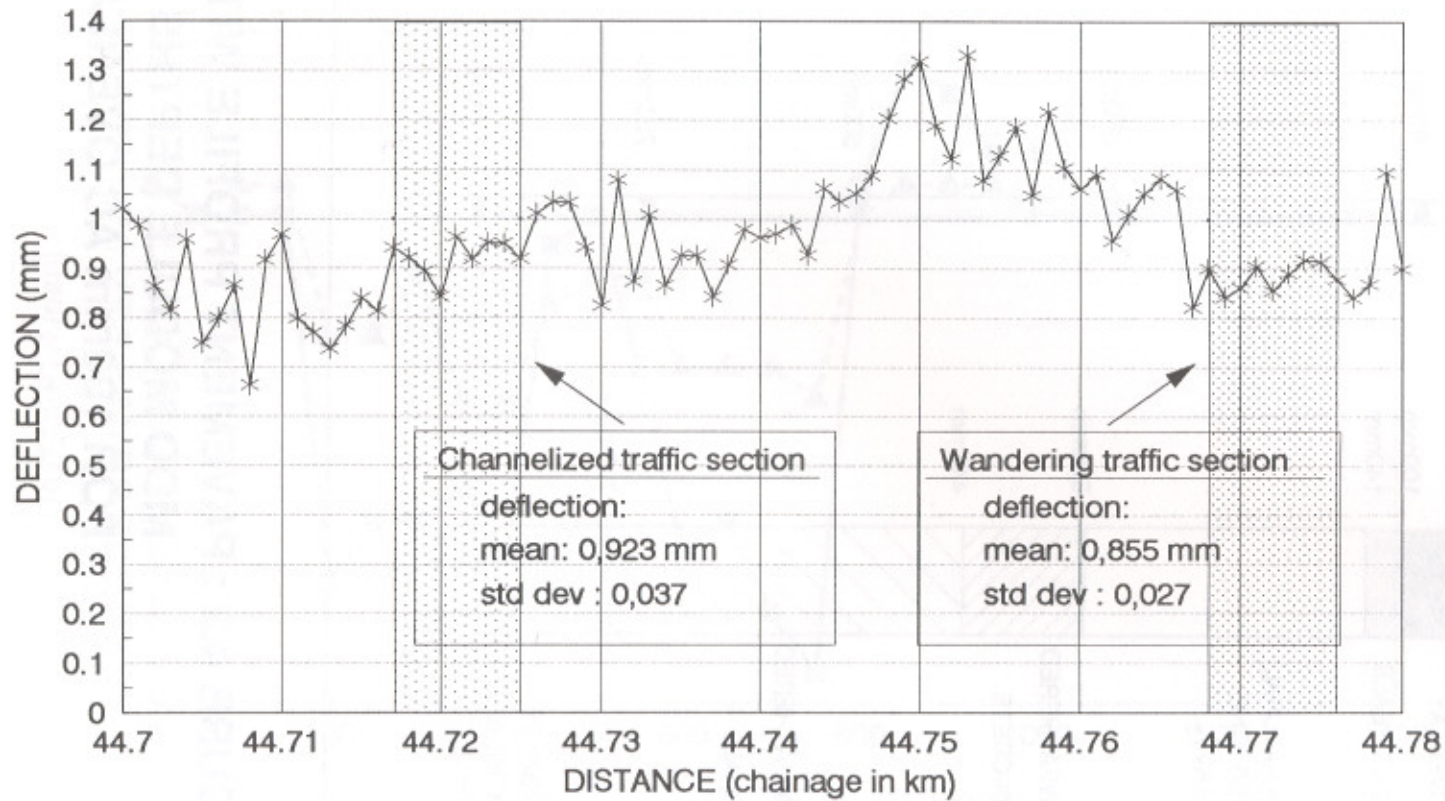


FIGURE 4.1 : RSD DEFLECTION MEASUREMENTS ON WANDERING AND CHANNELIZED TRAFFIC SECTIONS

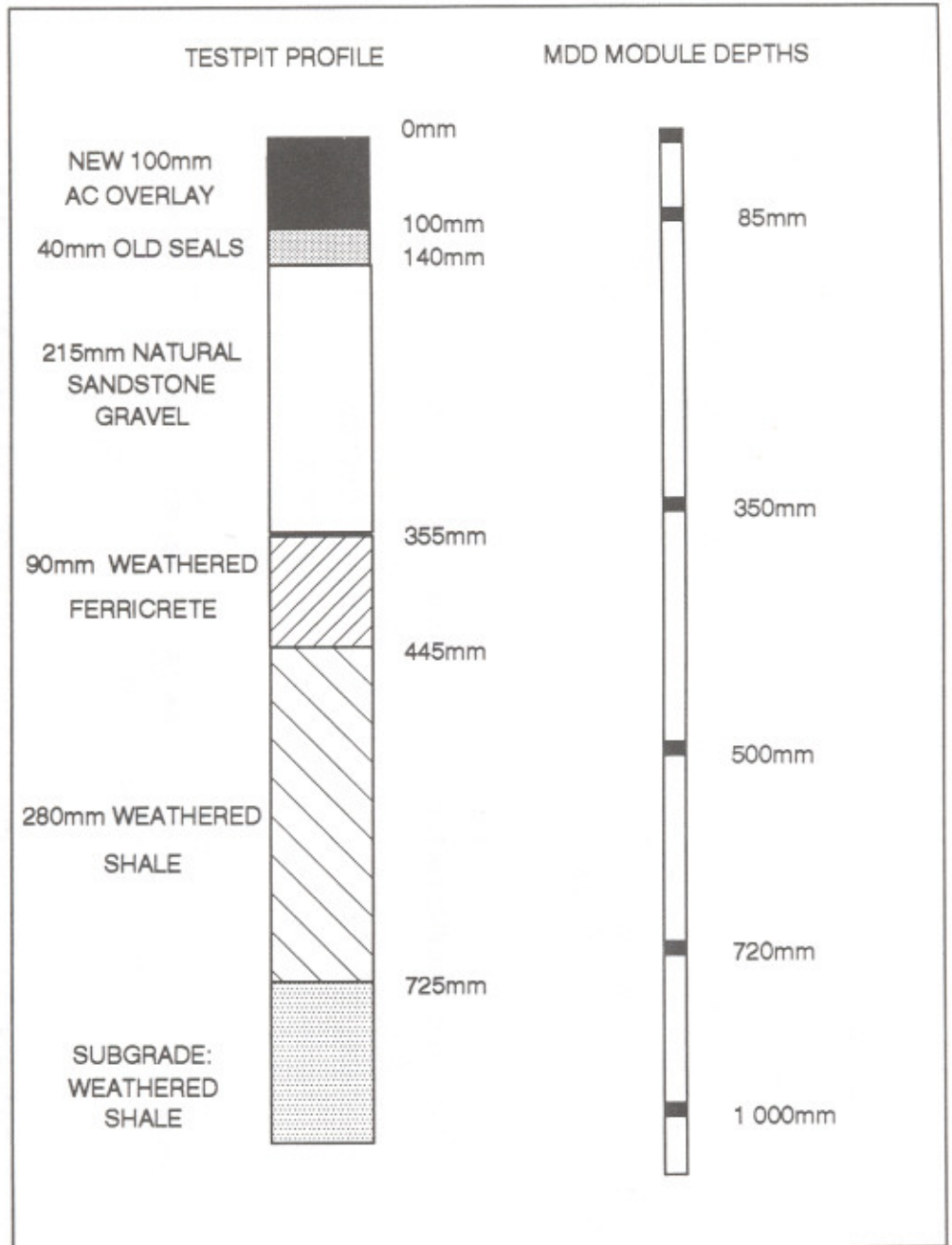


FIGURE 4.2 : PAVEMENT PROFILE WITH MDD MODULE DEPTHS FOR 100mm AC OVERLAY

THE WANDBERING TRAFFIC SECTION

FIGURE 4.3 : RUT PROFILE AFTER 164 000 REPETITIONS ON

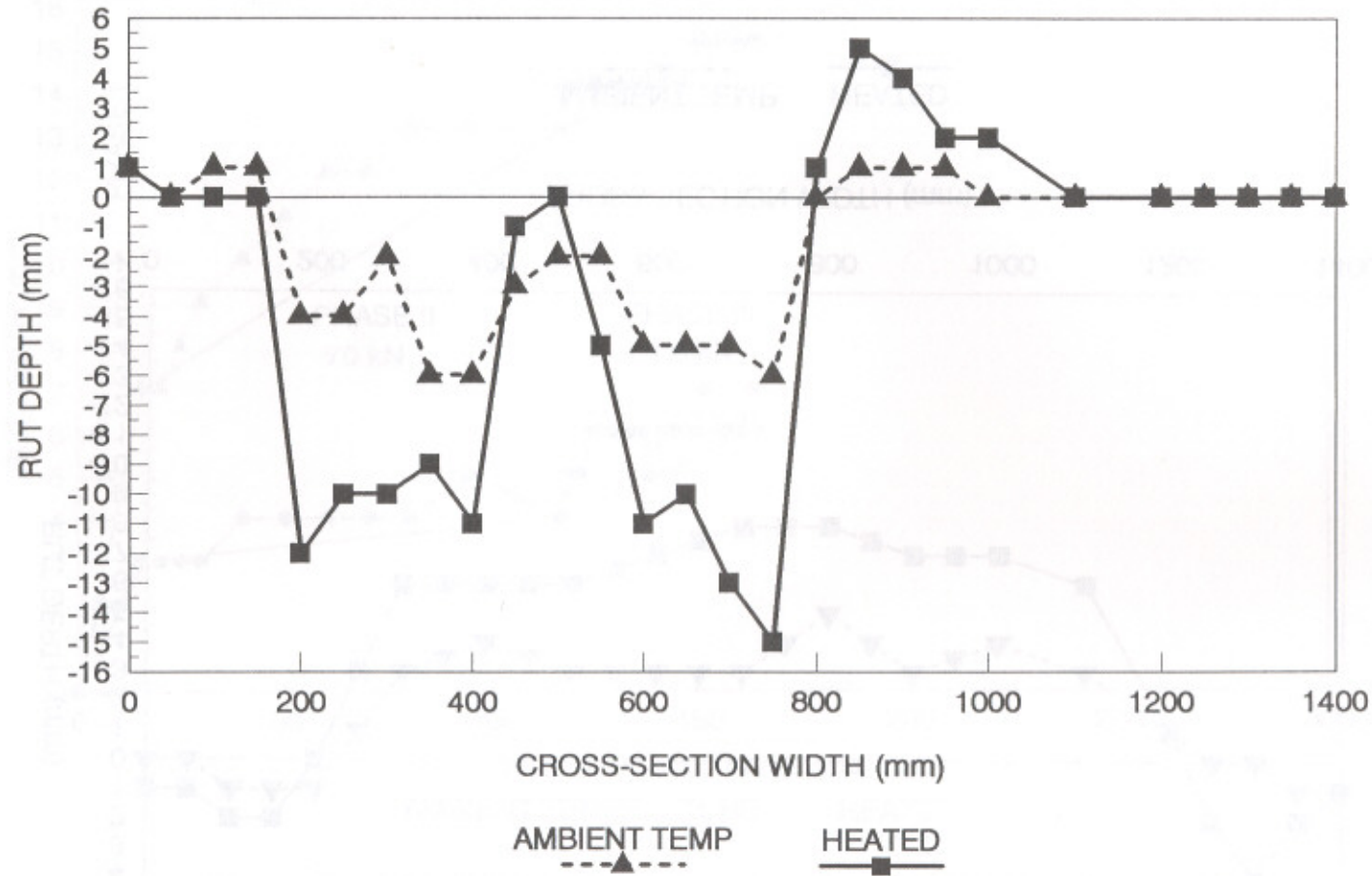


FIGURE 4.3 : RUT PROFILE AFTER 164 000 REPETITIONS ON THE CHANNELIZED TRAFFIC SECTION

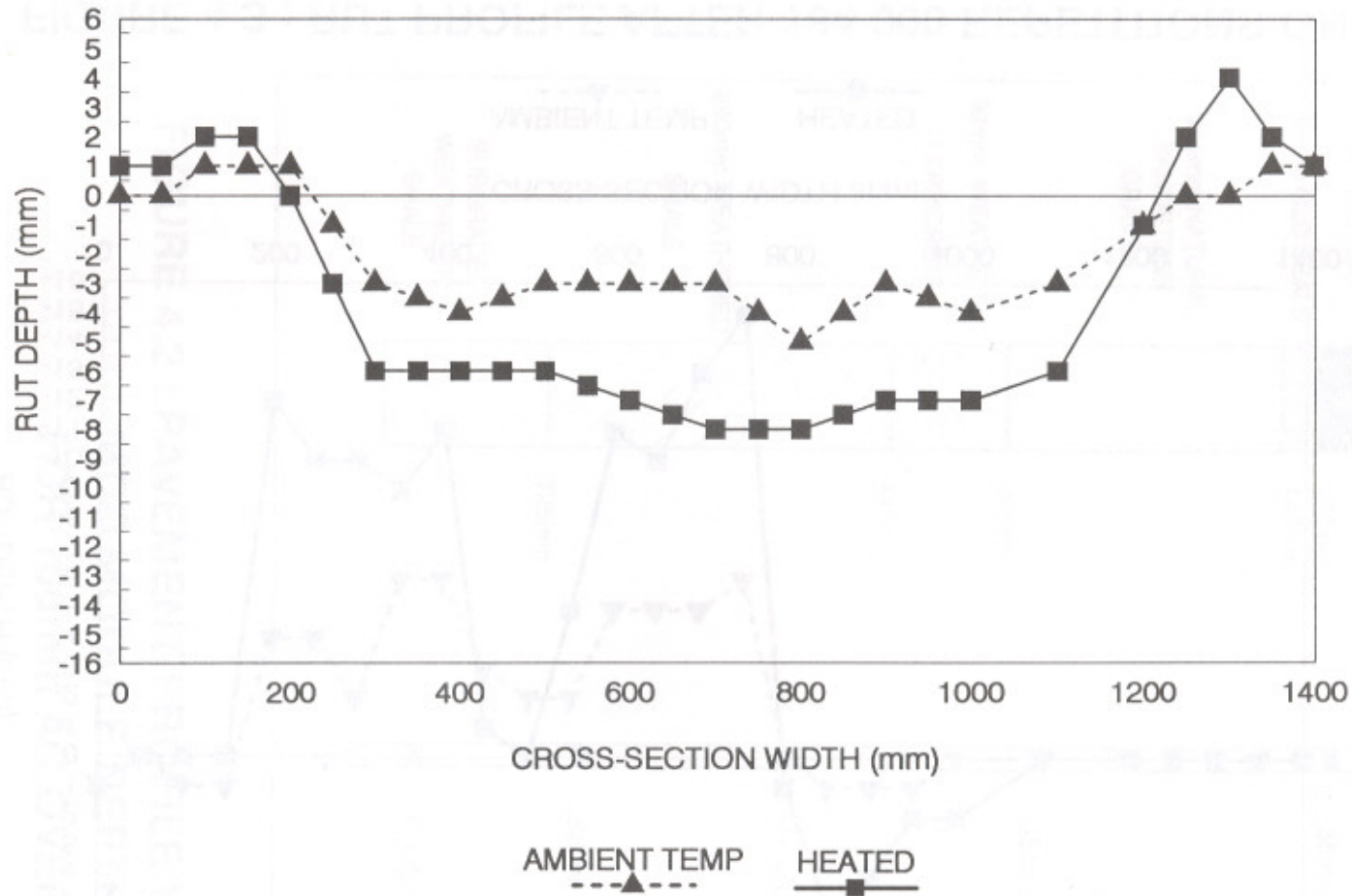


FIGURE 4.4 : RUT PROFILE AFTER 164 000 REPETITIONS ON THE WANDERING TRAFFIC SECTION

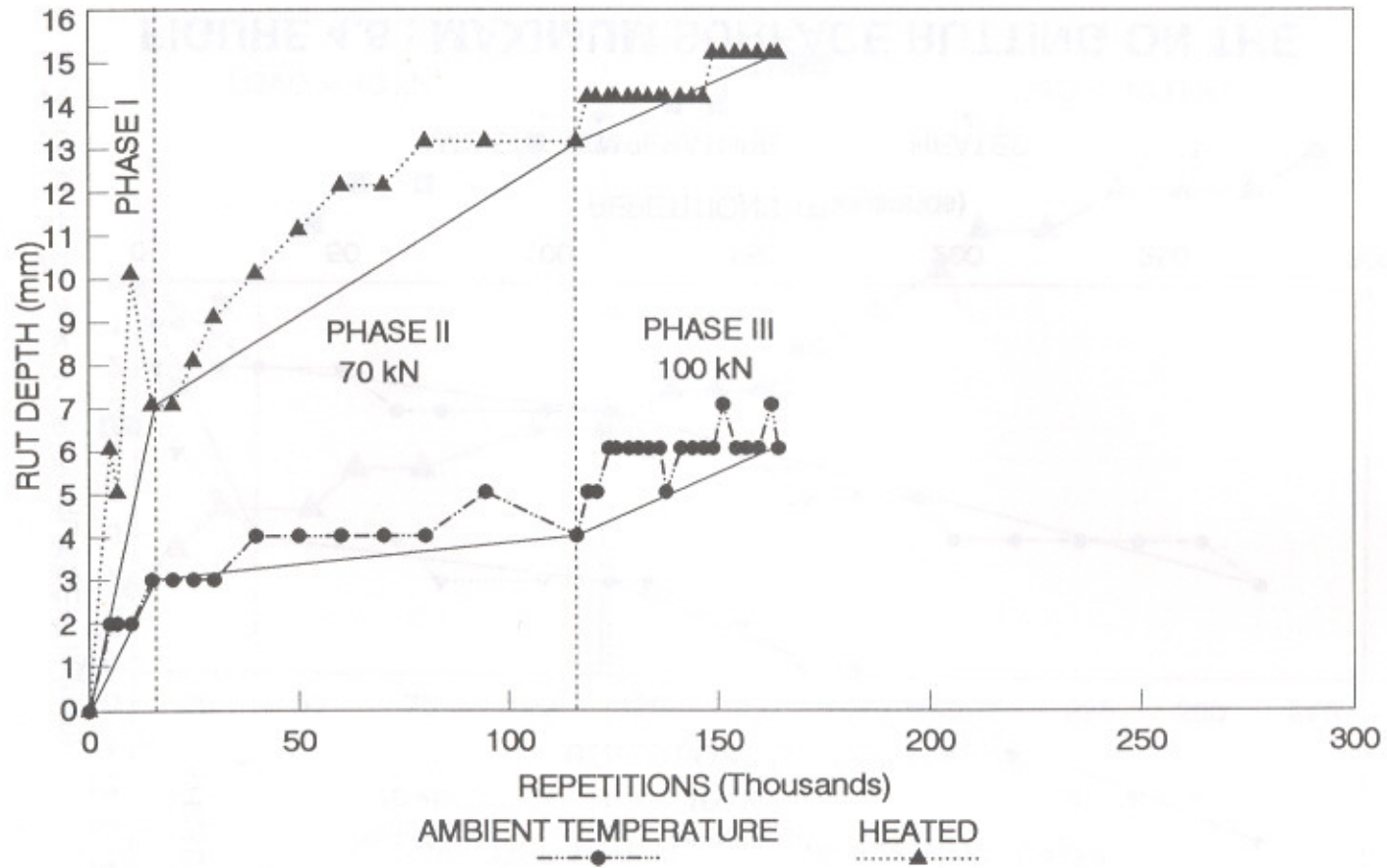


FIGURE 4.5 : MAXIMUM SURFACE RUTTING ON THE CHANNELIZED TRAFFIC SECTION

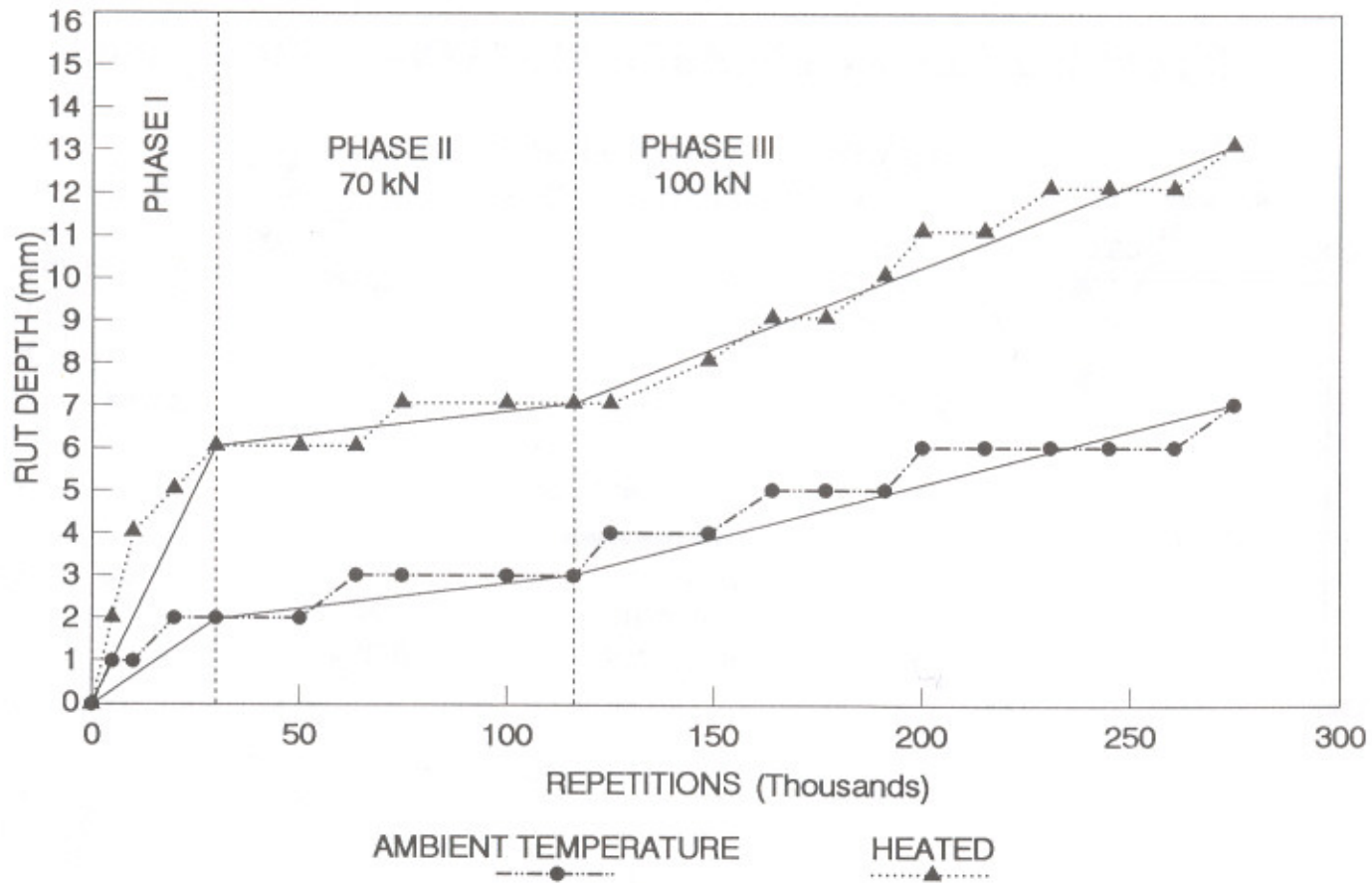


FIGURE 4.6 : MAXIMUM SURFACE RUTTING ON THE WANDERING TRAFFIC SECTION

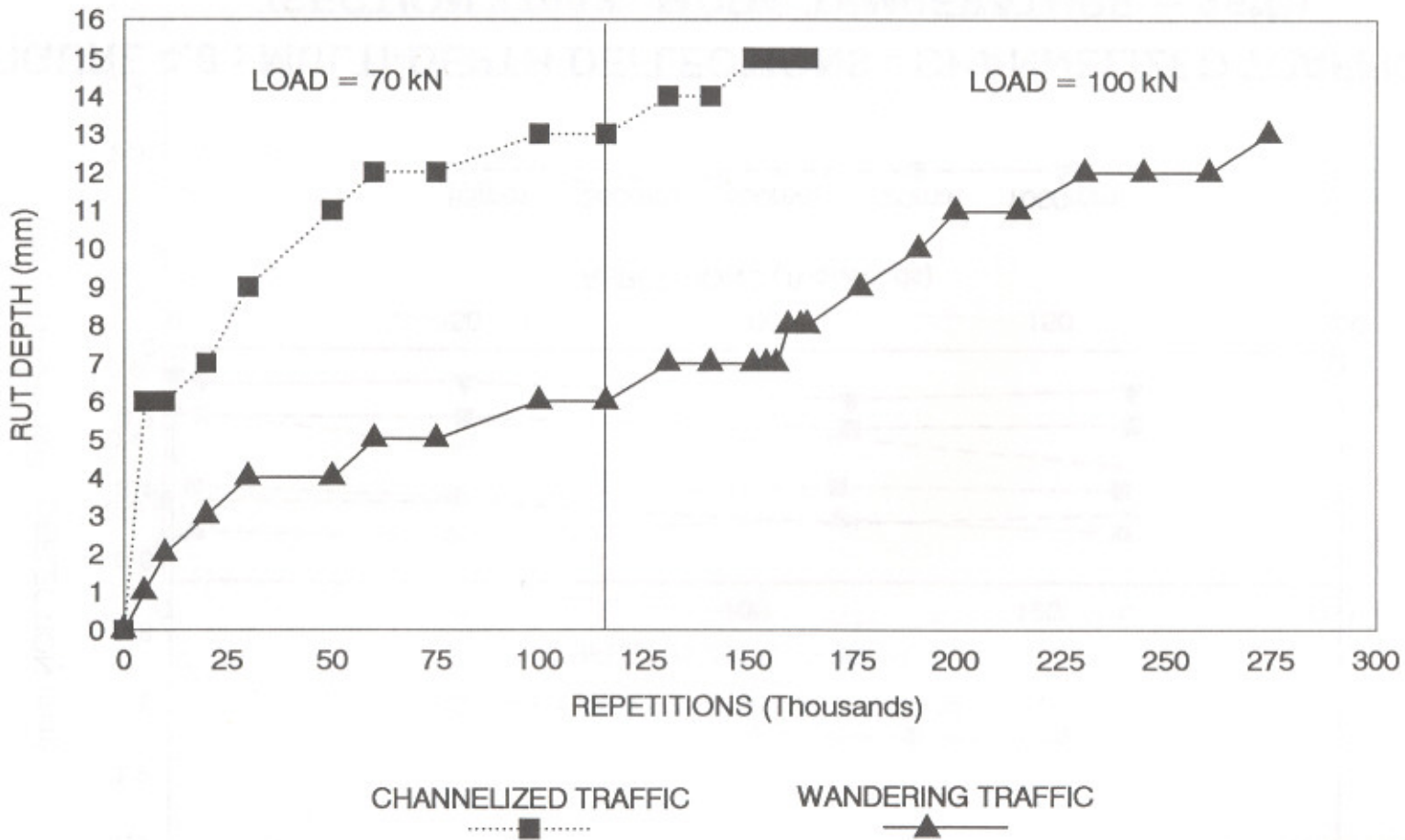
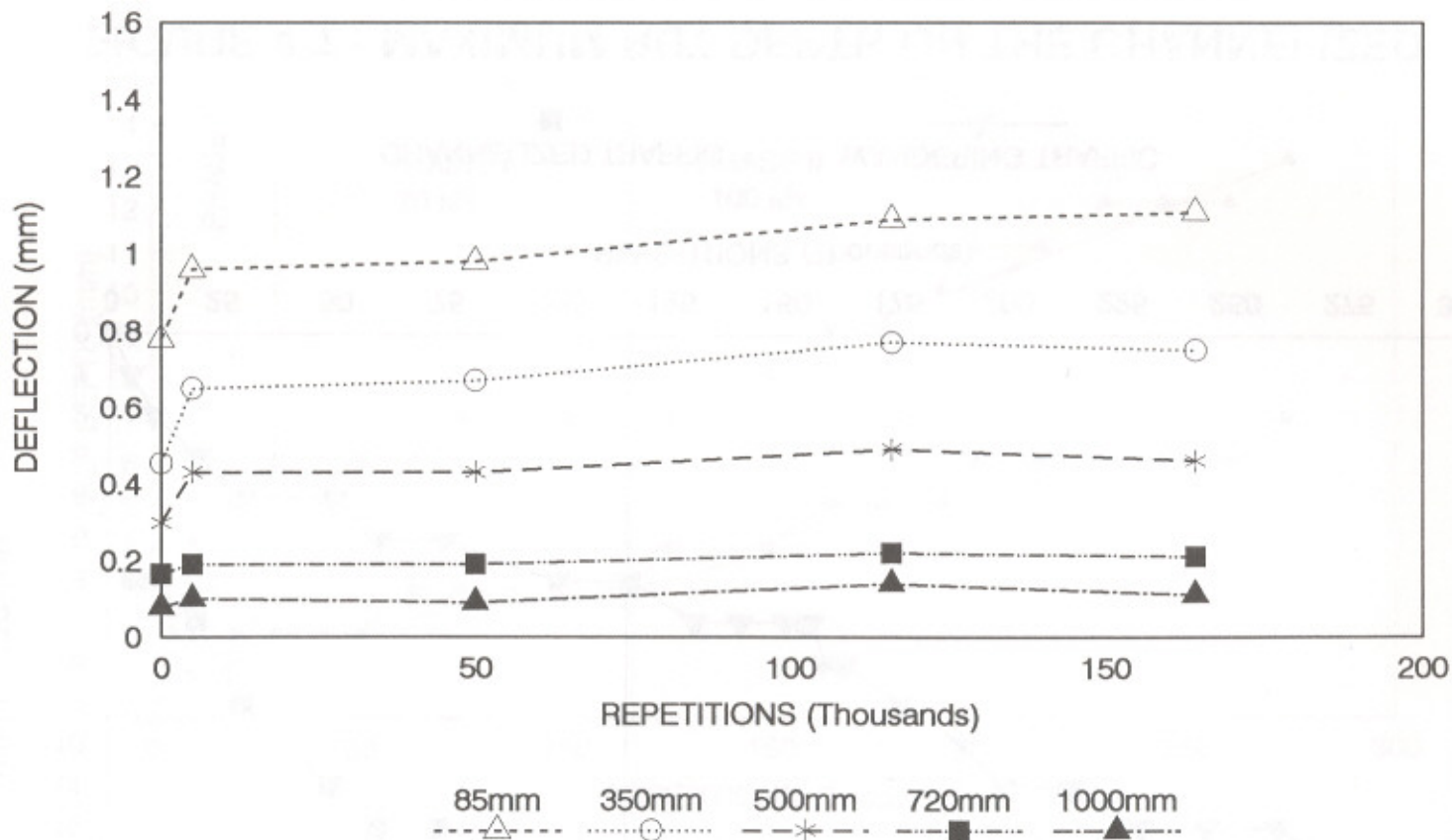
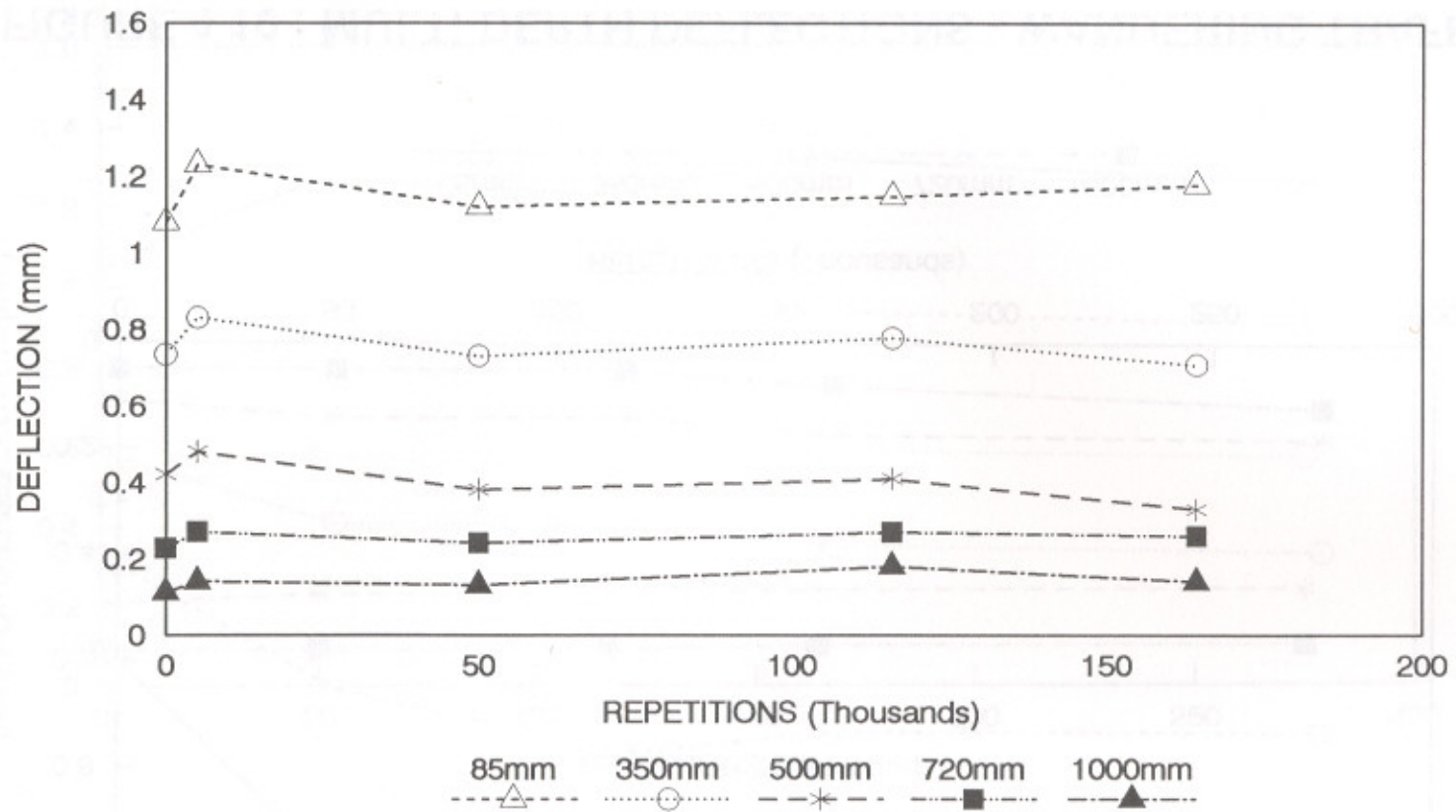


FIGURE 4.7 : MAXIMUM RUT DEPTH ON THE CHANNELIZED AND WANDERING TRAFFIC SECTIONS



**FIGURE 4.8 : MULTI-DEPTH DEFLECTIONS - CHANNELIZED TRAFFIC
(SECTION 379A3 - MDD4, TEMPERATURE = 25°C)**



**FIGURE 4.9 : MULTI-DEPTH DEFLECTIONS - CHANNELIZED TRAFFIC
(SECTION 379A3 - MDD12, TEMPERATURE = 40°C)**

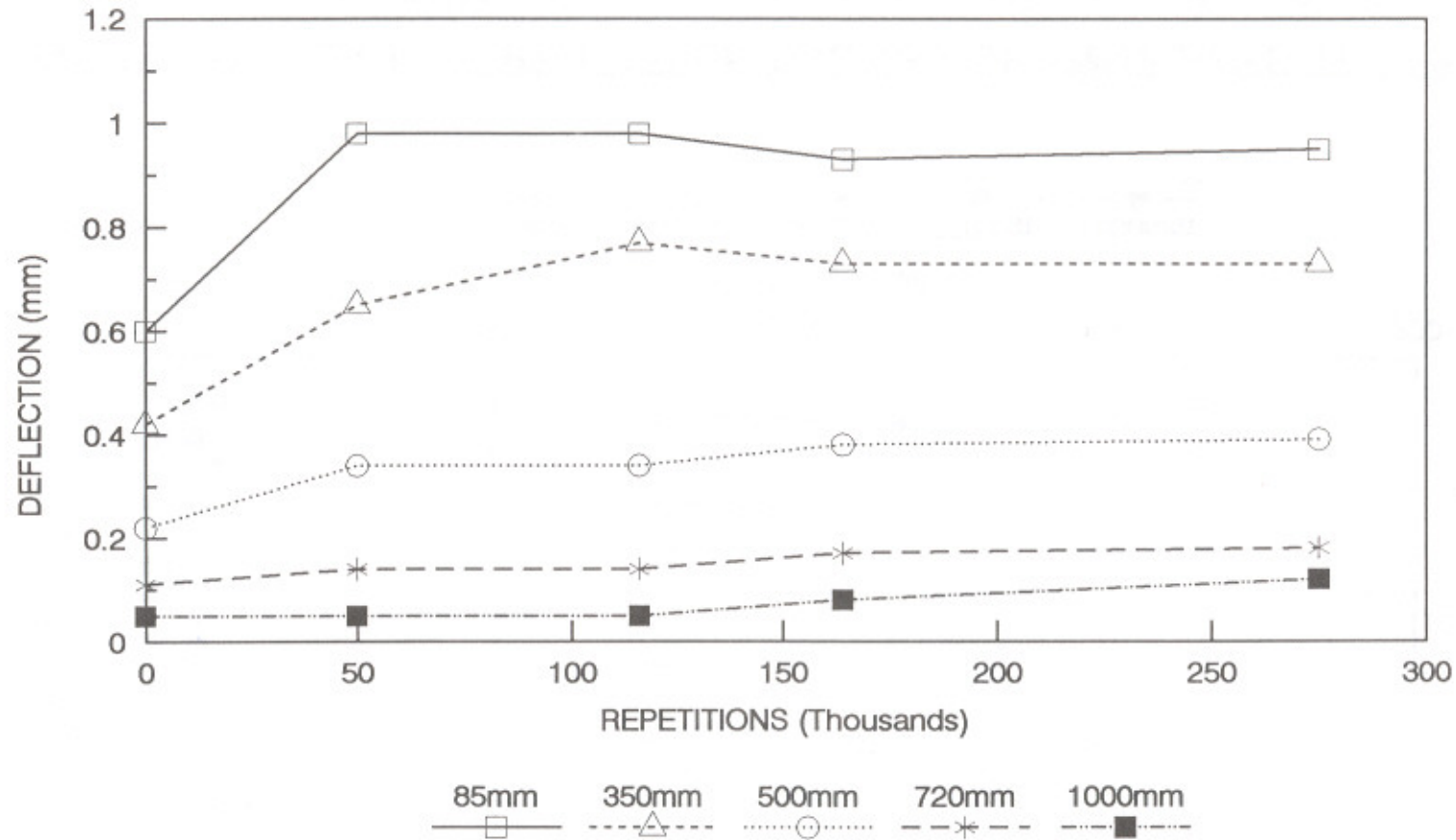


**FIGURE 4.10 : MULTI-DEPTH DEFLECTIONS - WANDERING TRAFFIC
(SECTION 380A3 - MDD4, TEMPERATURE = 25°C)**

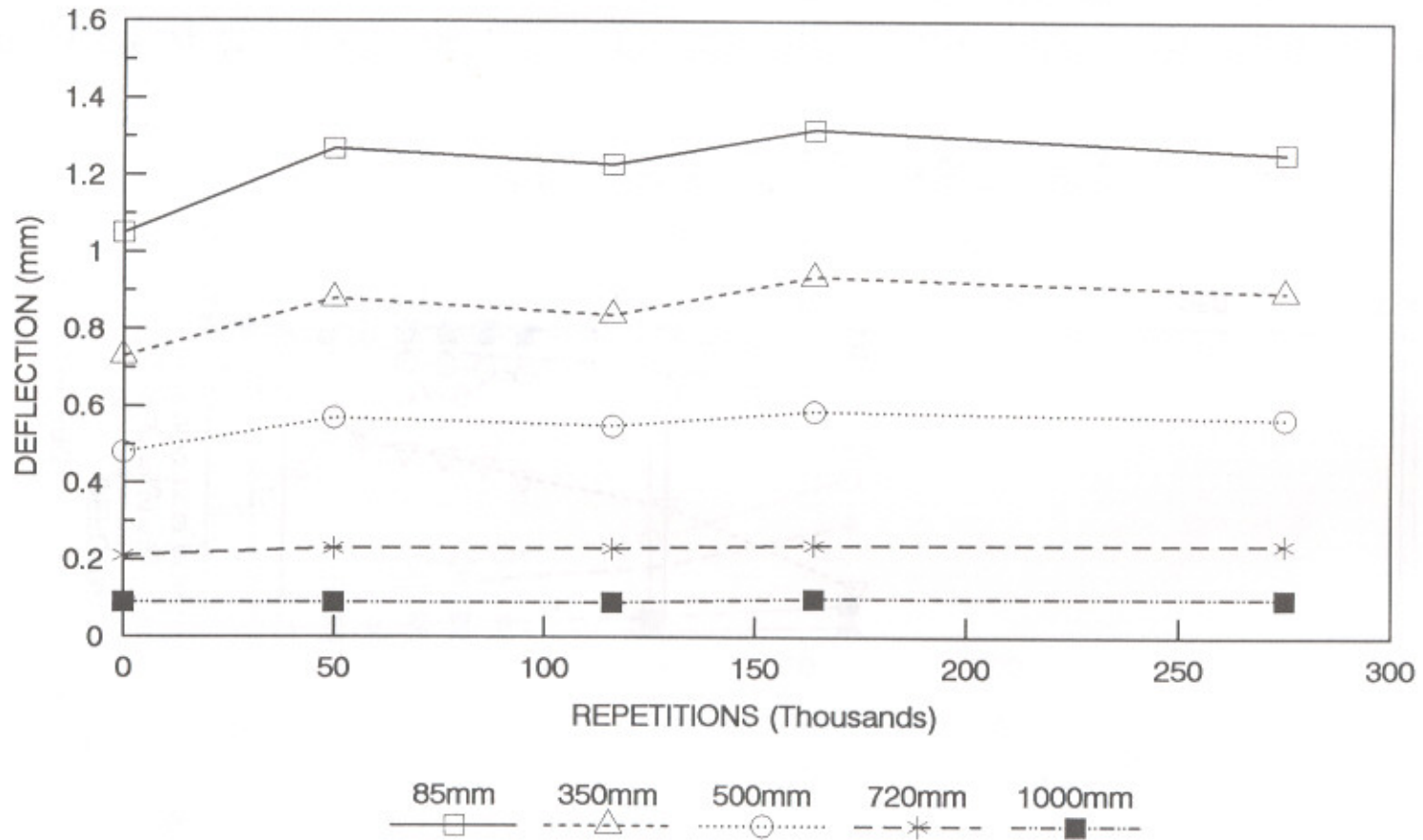


**FIGURE 4.11 : MULTI-DEPTH DEFLECTIONS - WANDERING TRAFFIC
(SECTION 380A3 - MDD12, TEMPERATURE = 40°C)**

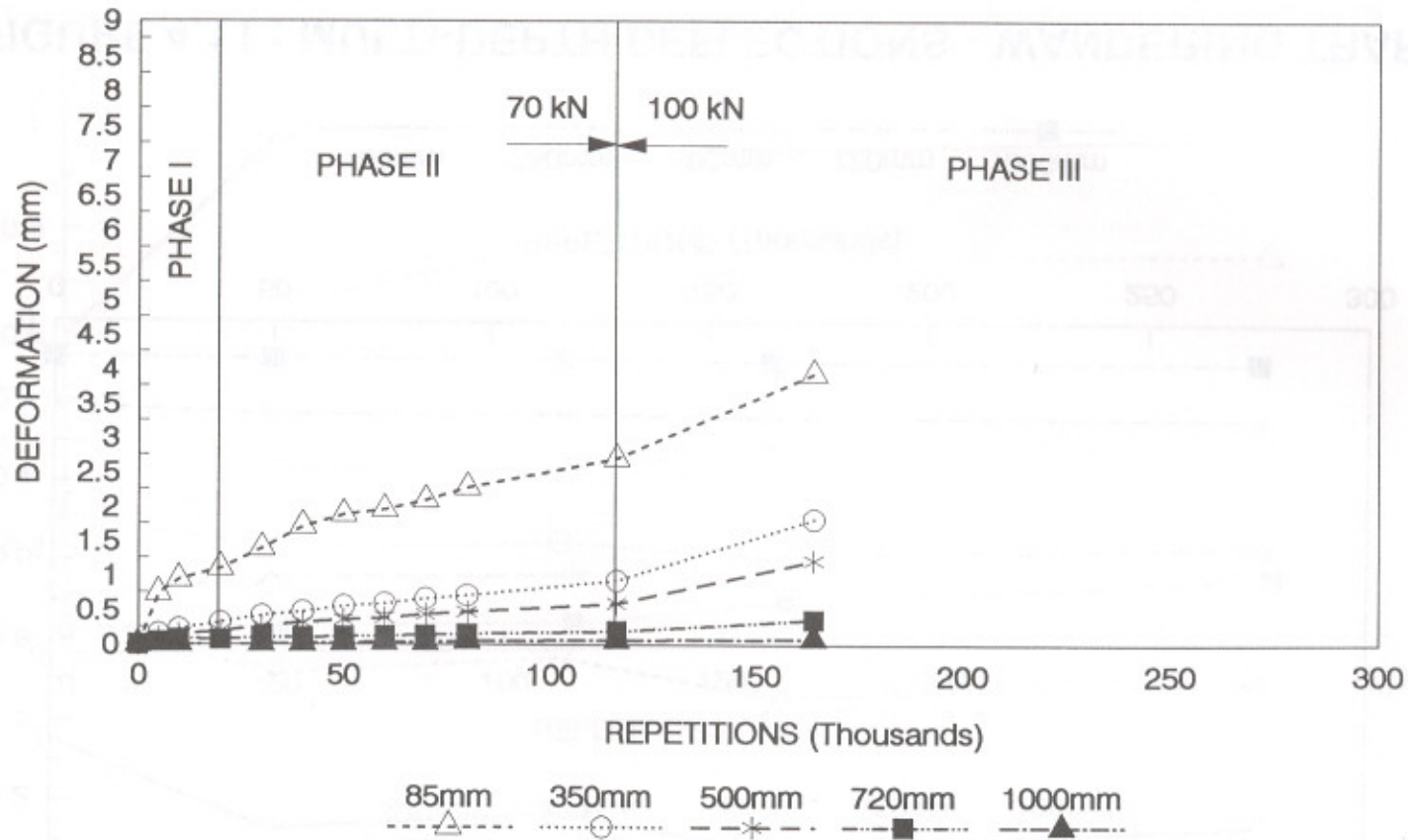


**FIGURE 4.12 : MULTI-DEPTH DEFORMATION - CHANNELIZED TRAFFIC
(SECTION 379A3 - MDD4, TEMPERATURE = 25°C)**

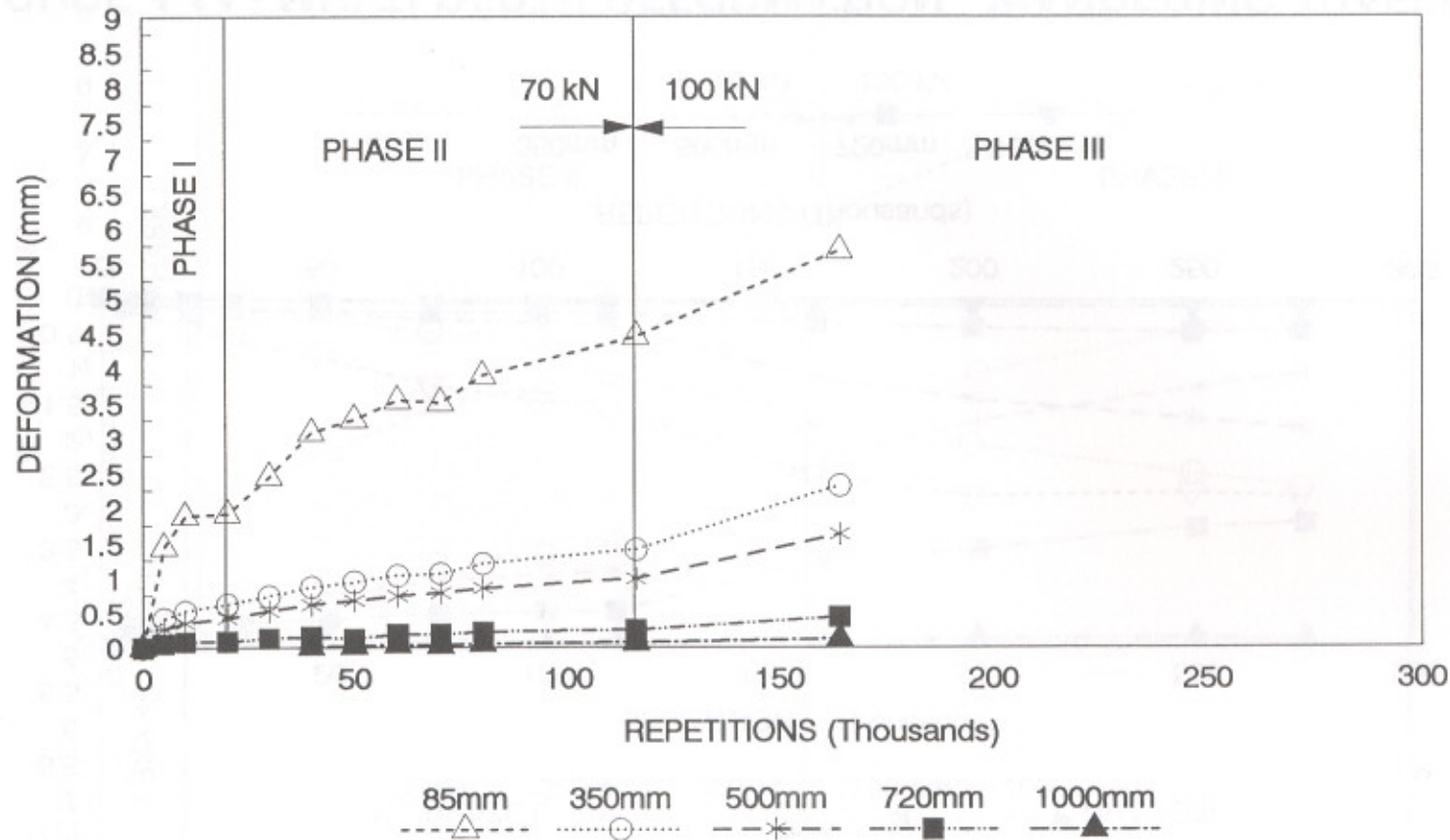


**FIGURE 4.13 : MULTI-DEPTH DEFORMATION - CHANNELIZED TRAFFIC
(SECTION 379A3 - MDD12, TEMPERATURE = 40°C)**

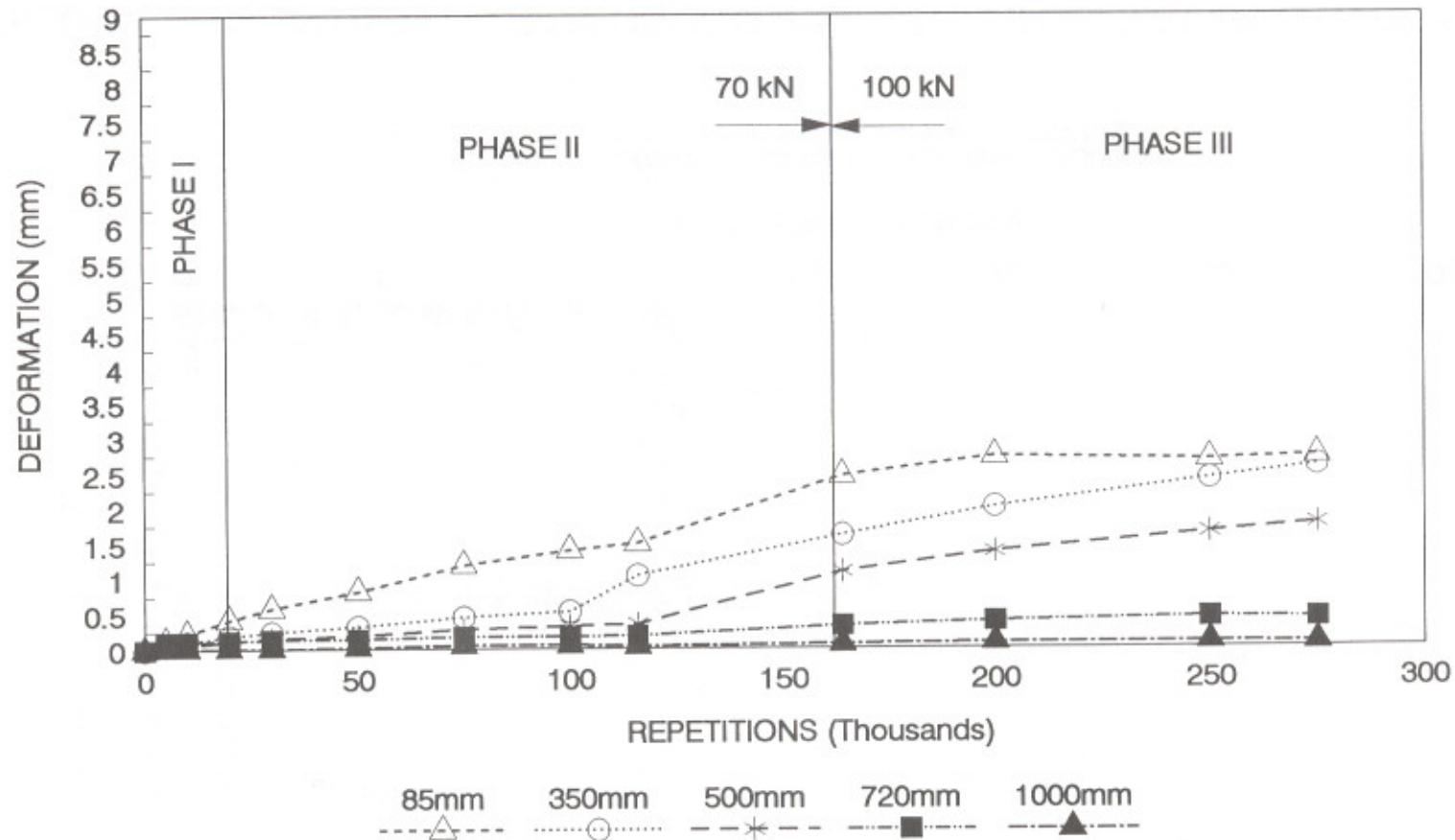


**FIGURE 4.14 : MULTI-DEPTH DEFORMATION - WANDERING TRAFFIC
(SECTION 380A3 - MDD4, TEMPERATURE = 25°C)**

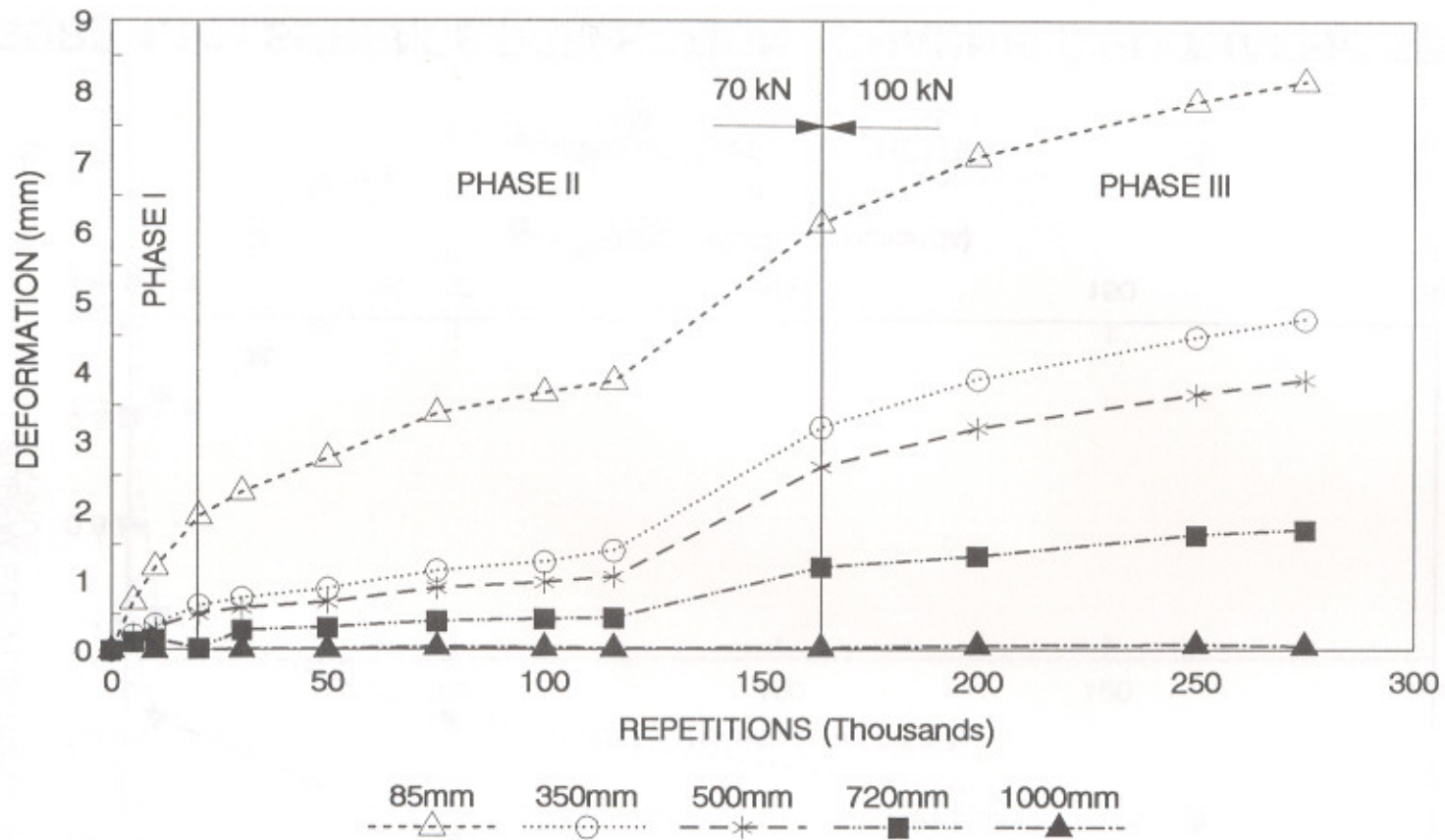


**FIGURE 4.15 : MULTI-DEPTH DEFORMATION - WANDERING TRAFFIC
(SECTION 380A3 - MDD12, TEMPERATURE = 40°C)**

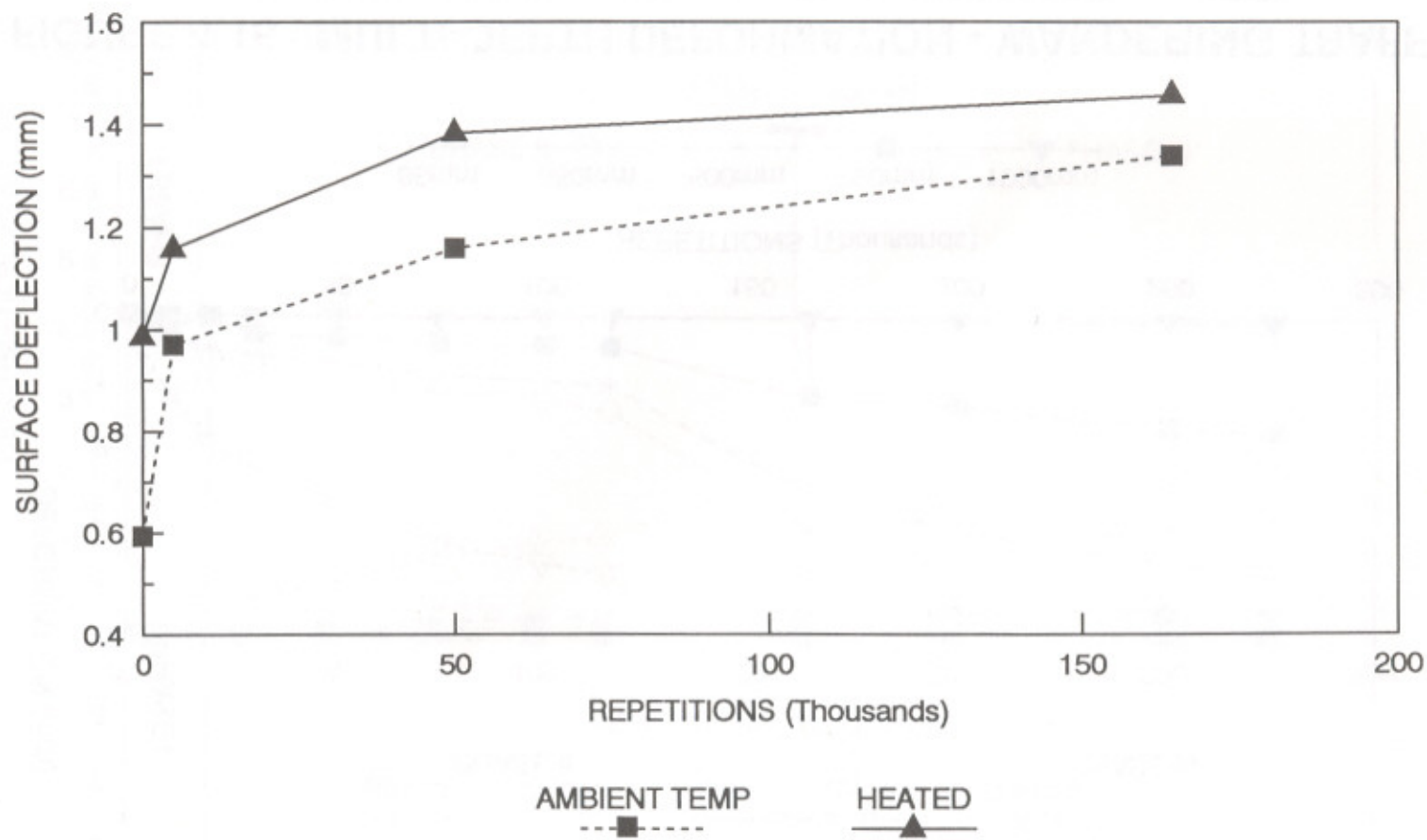


**FIGURE 4.16 : SURFACE DEFLECTION - CHANNELIZED TRAFFIC SECTION
(SECTION 379A3 - 40 kN TEST WHEEL LOAD)**

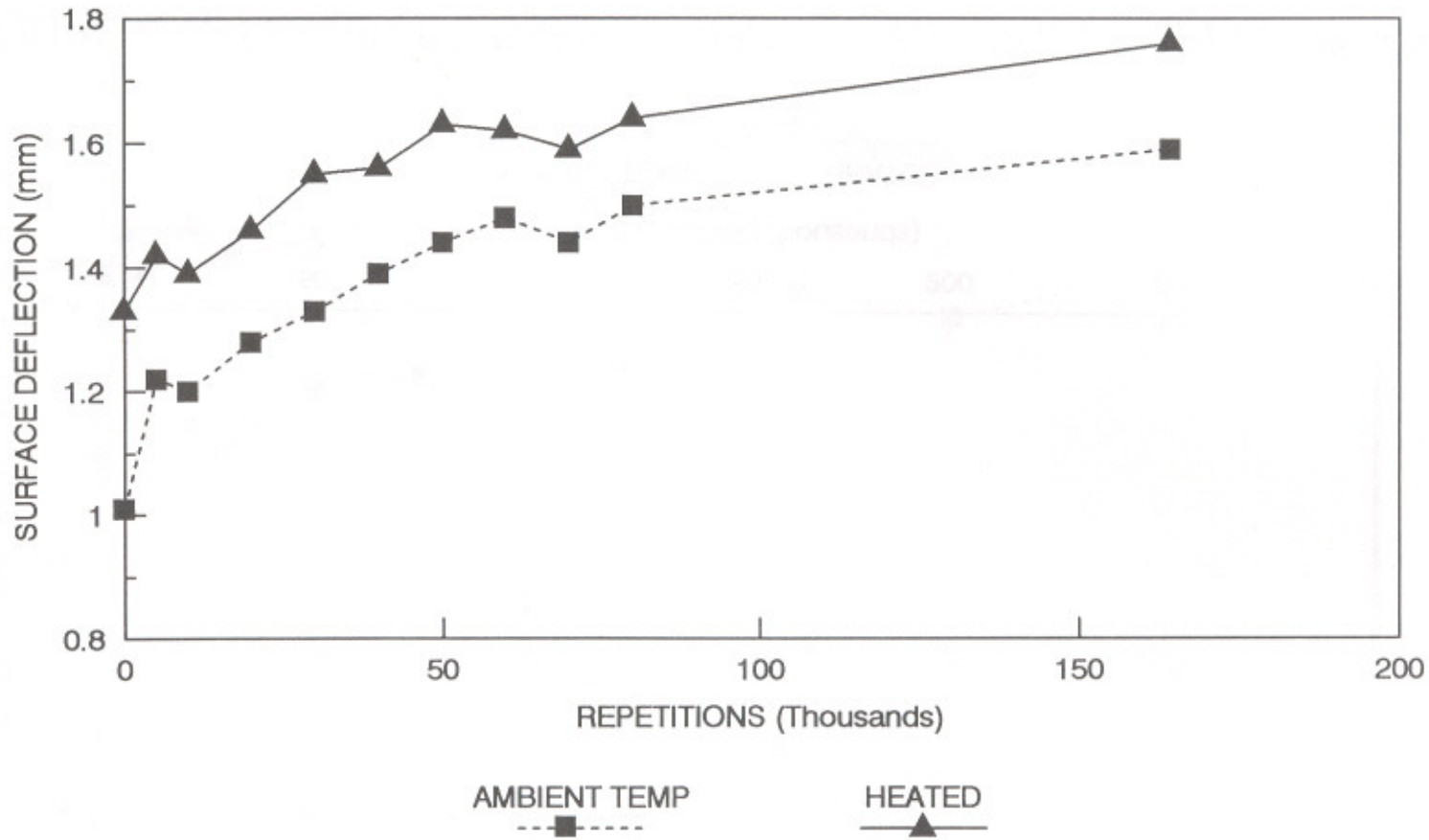


**FIGURE 4.17 : SURFACE DEFLECTION - CHANNELIZED TRAFFIC SECTION
(SECTION 379A3 - 70kN TEST WHEEL LOAD)**

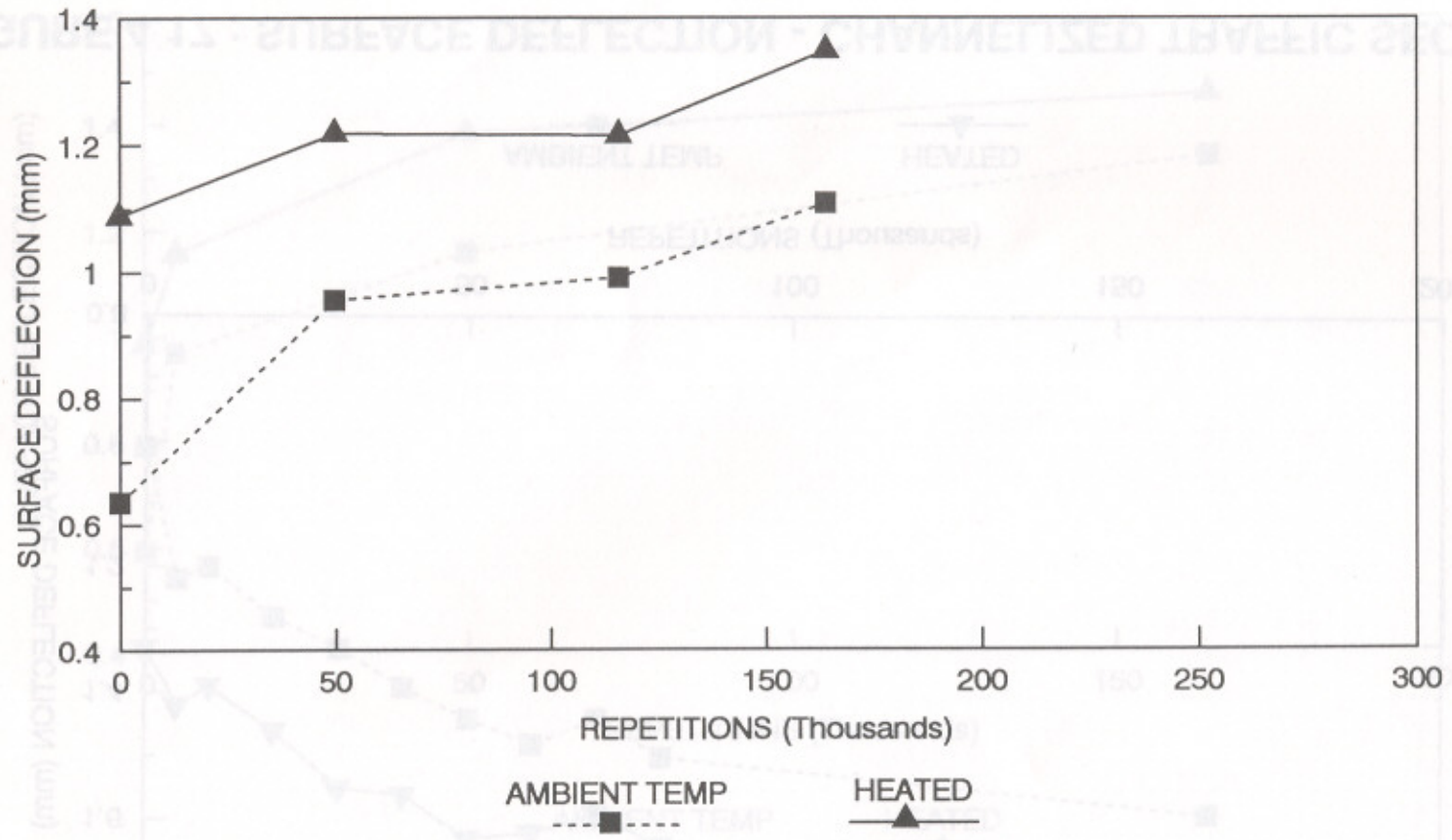


**FIGURE 4.18 : SURFACE DEFLECTION - WANDERING TRAFFIC SECTION
(SECTION 380A3 - 40kN TEST WHEEL LOAD)**

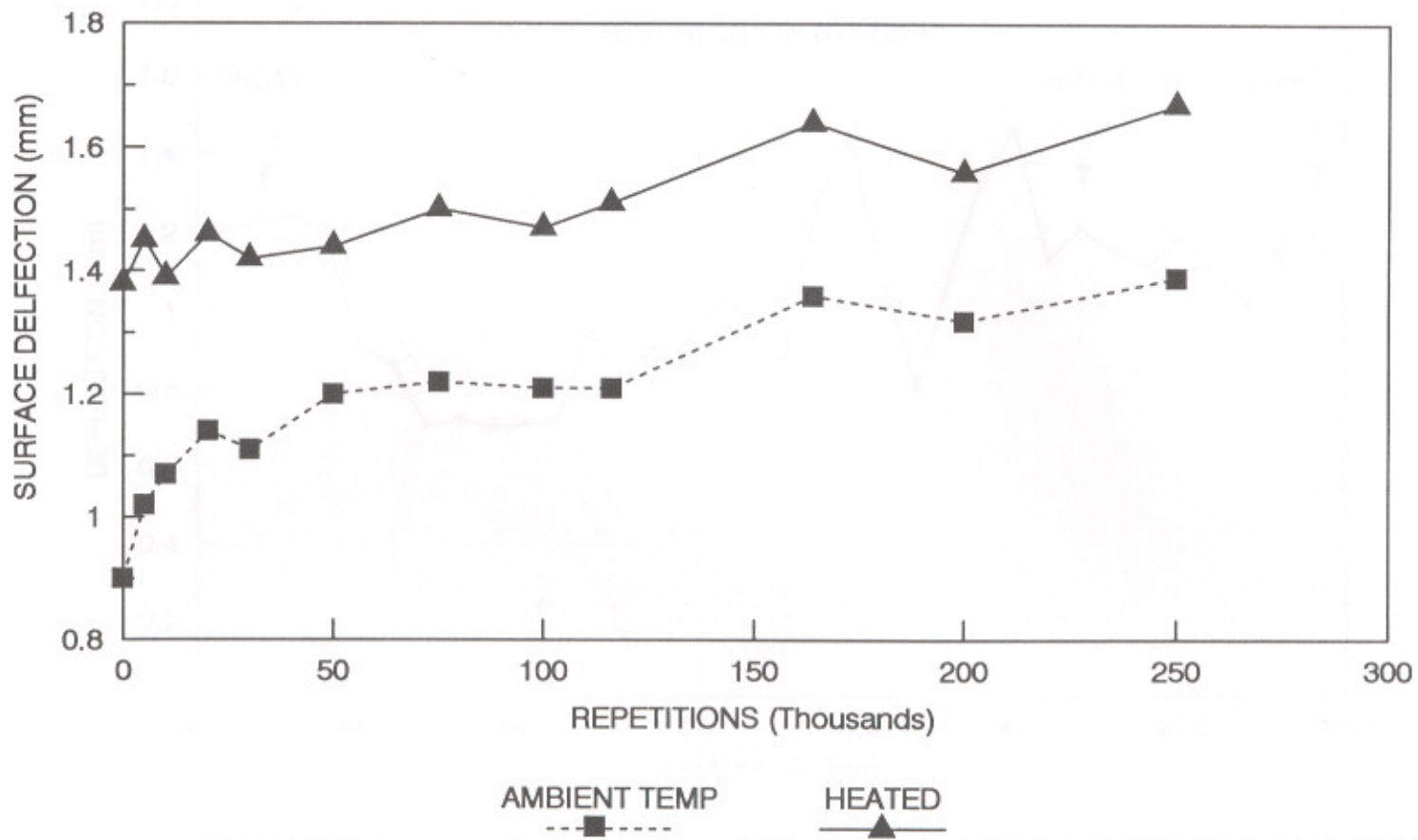


**FIGURE 4.19 : SURFACE DEFLECTION - WANDERING TRAFFIC SECTION
(SECTION 380A3 - 70kN TEST WHEEL LOAD)**

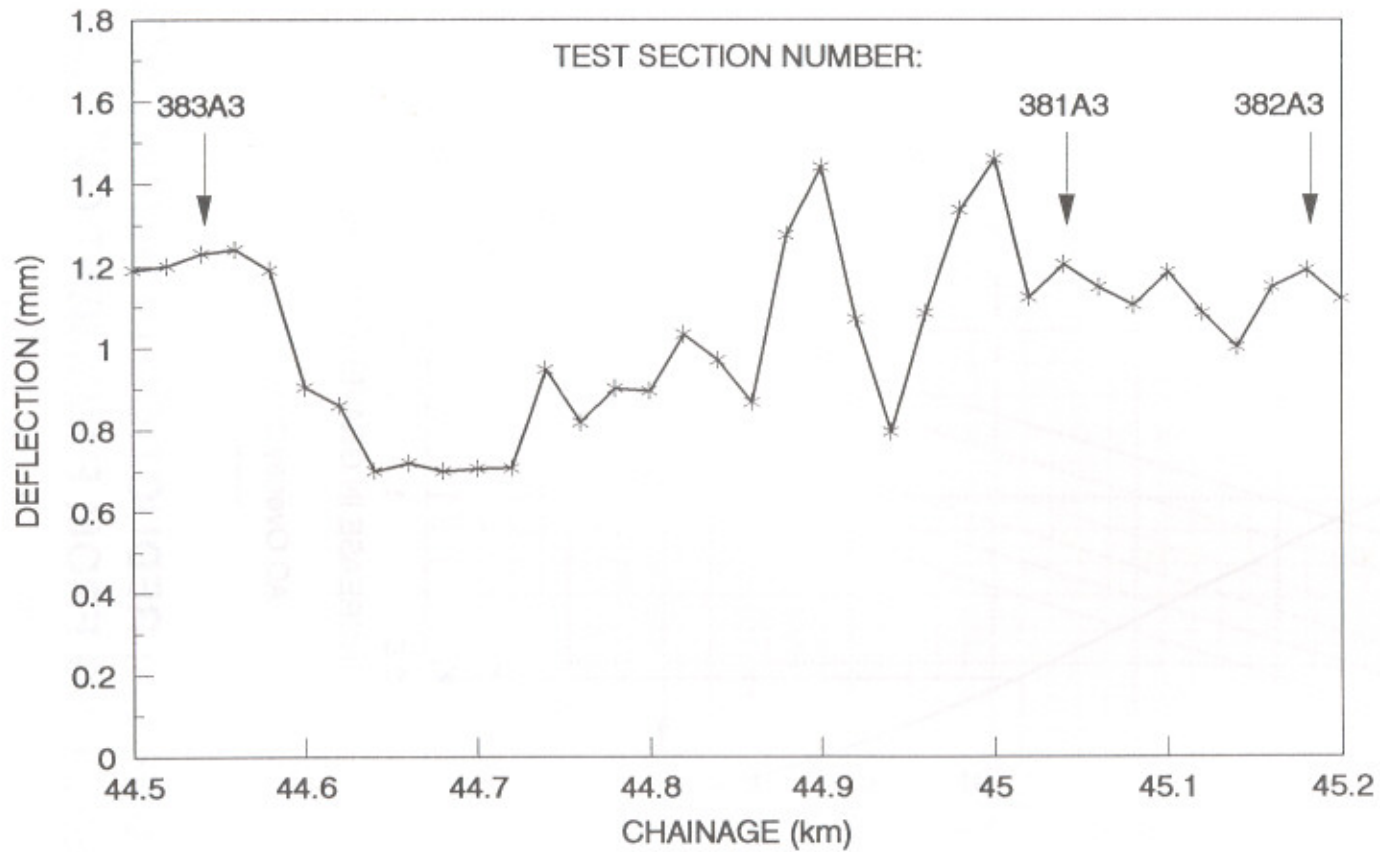


FIGURE 5.1 : RSD DEFLECTION MEASUREMENTS OF THE COLD TEMPERATURE TEST SECTIONS

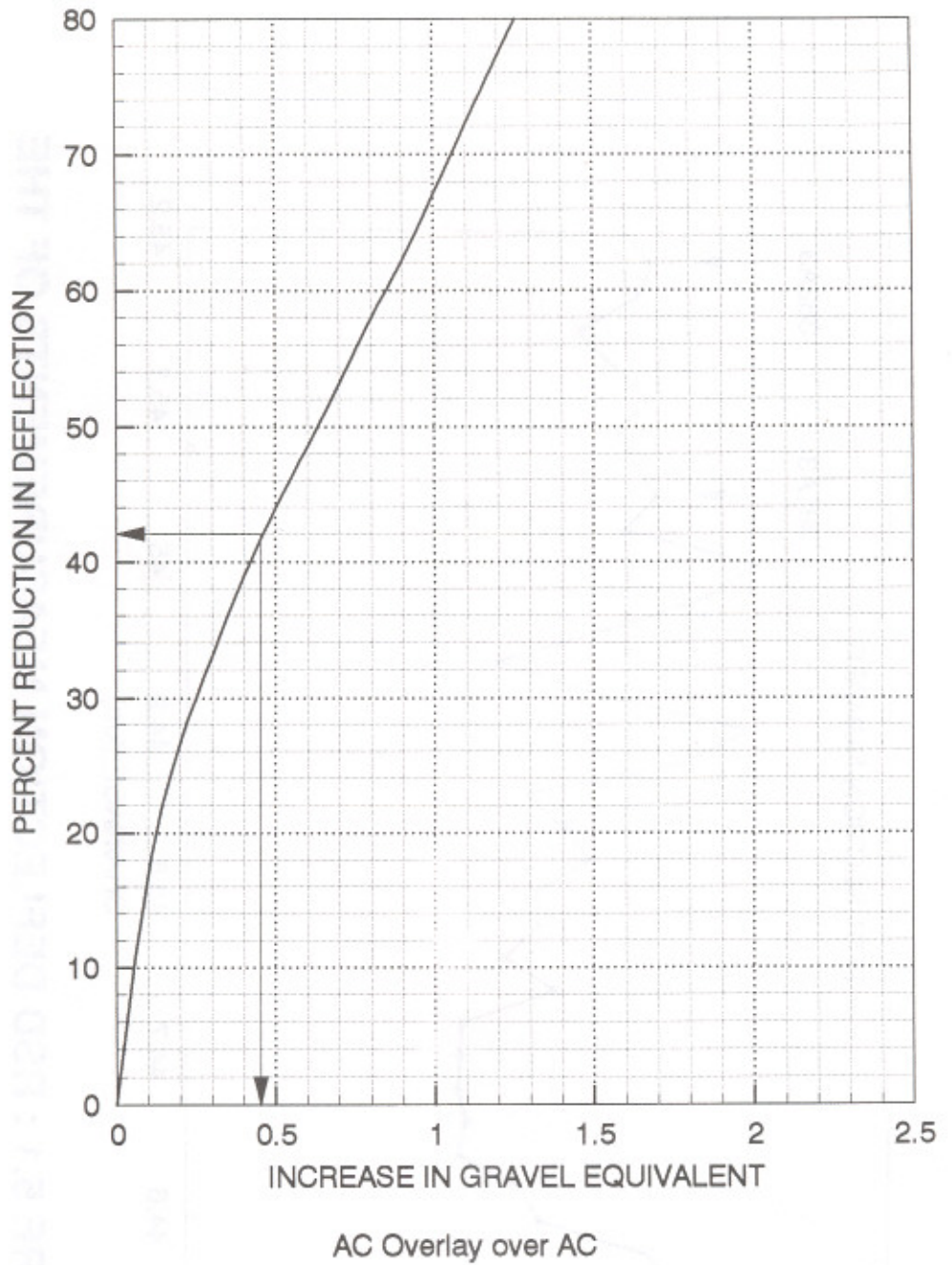


FIGURE 5.2: REDUCTION IN DEFLECTION RESULTING FROM PAVEMENT OVERLAYS

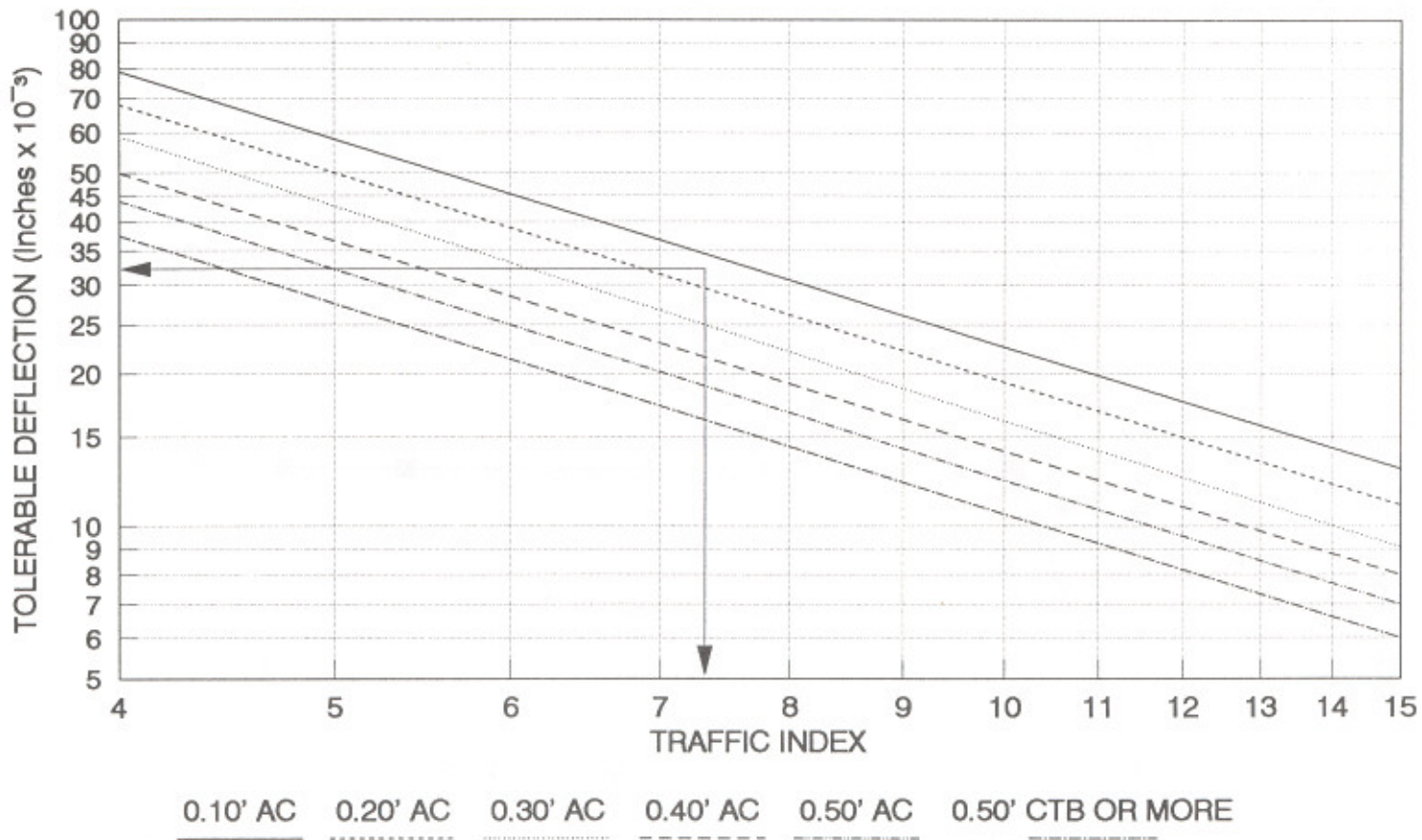
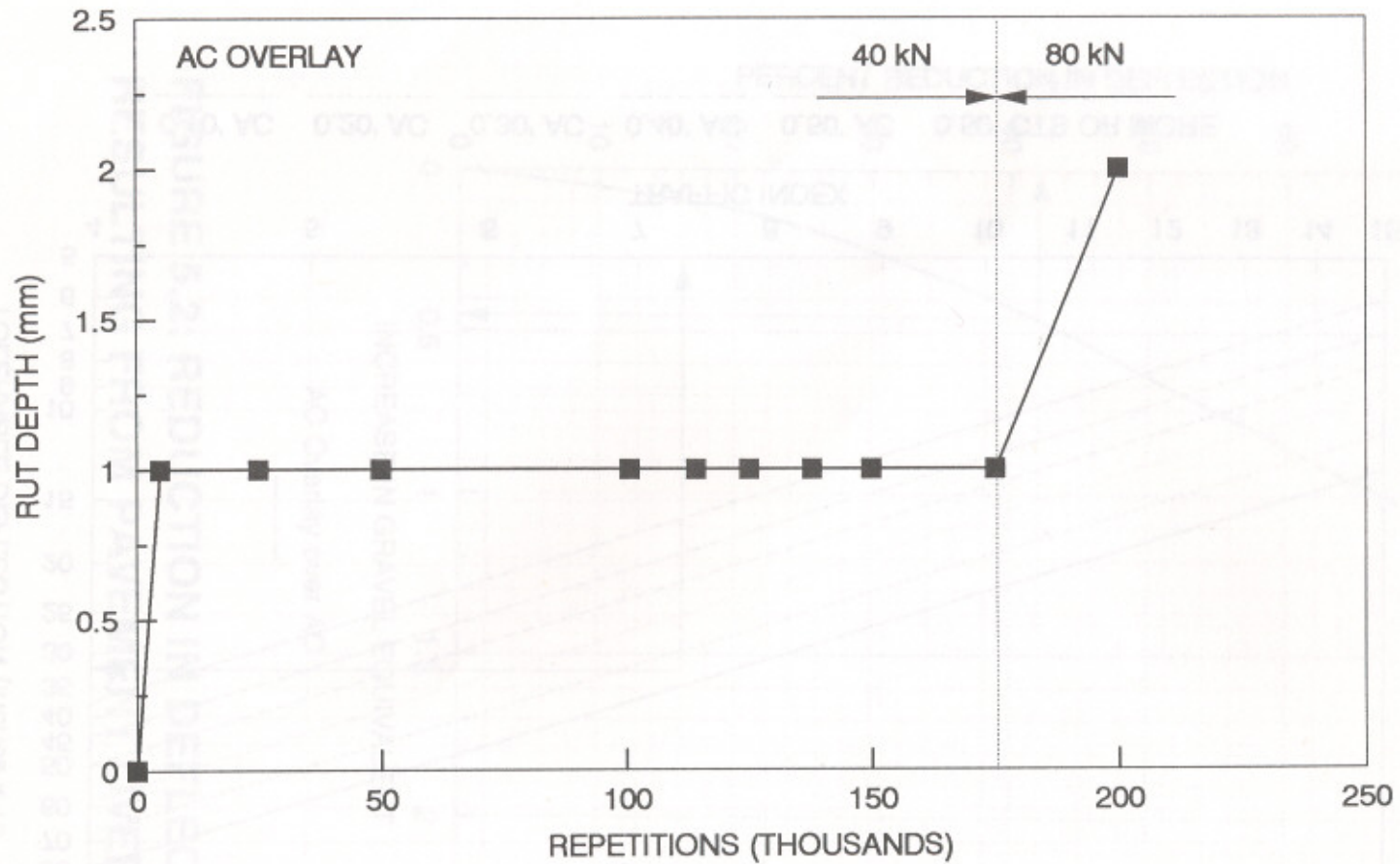
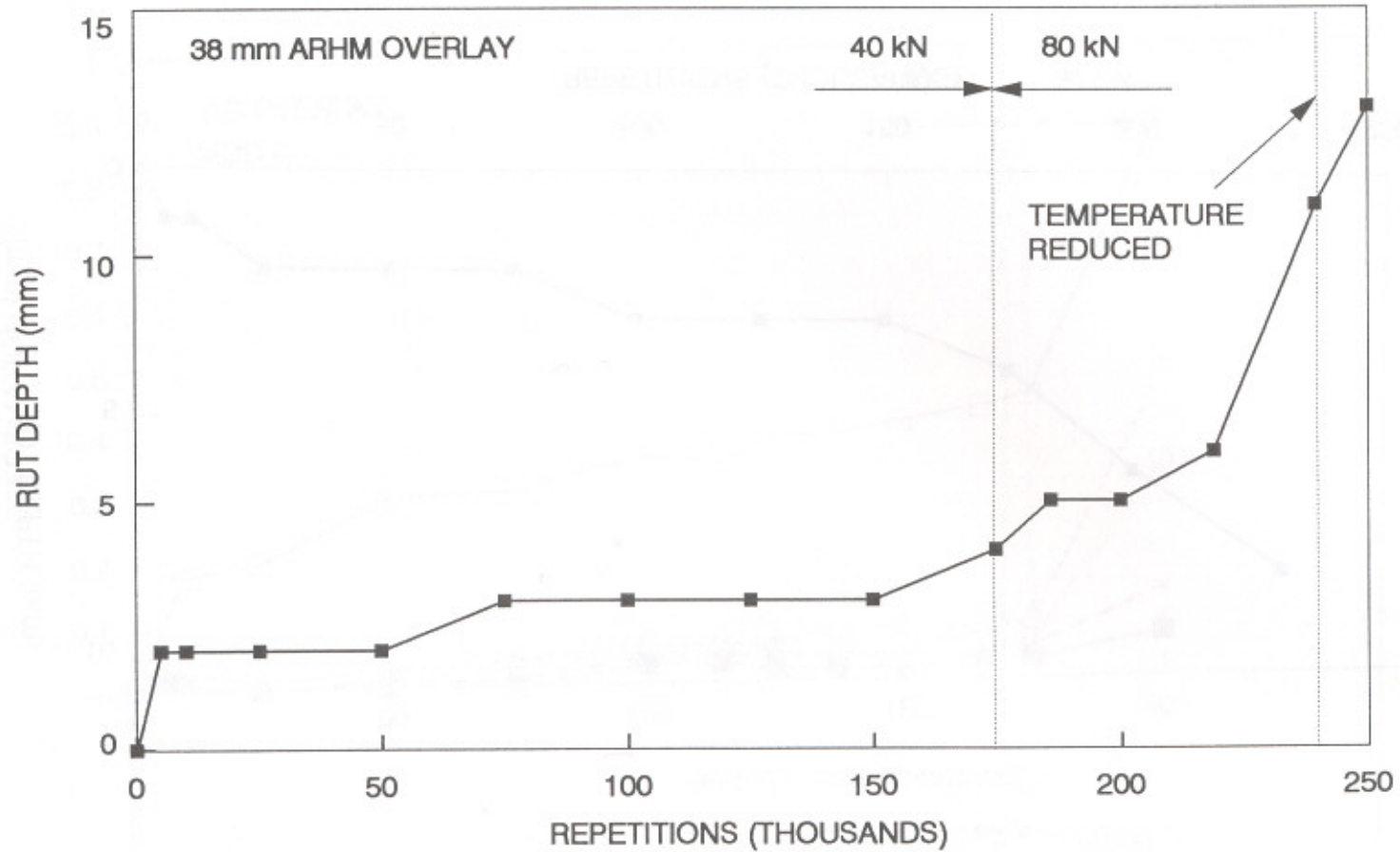


FIGURE 5.3: TOLERABLE DEFLECTION CHART



**FIGURE 5.4 : MAXIMUM SURFACE RUTTING ON SECTION 381A3
(75 mm AC OVERLAY)**



**FIGURE 5.5 : MAXIMUM SURFACE RUTTING ON SECTION 382A3
(38 mm ARHM OVERLAY)**

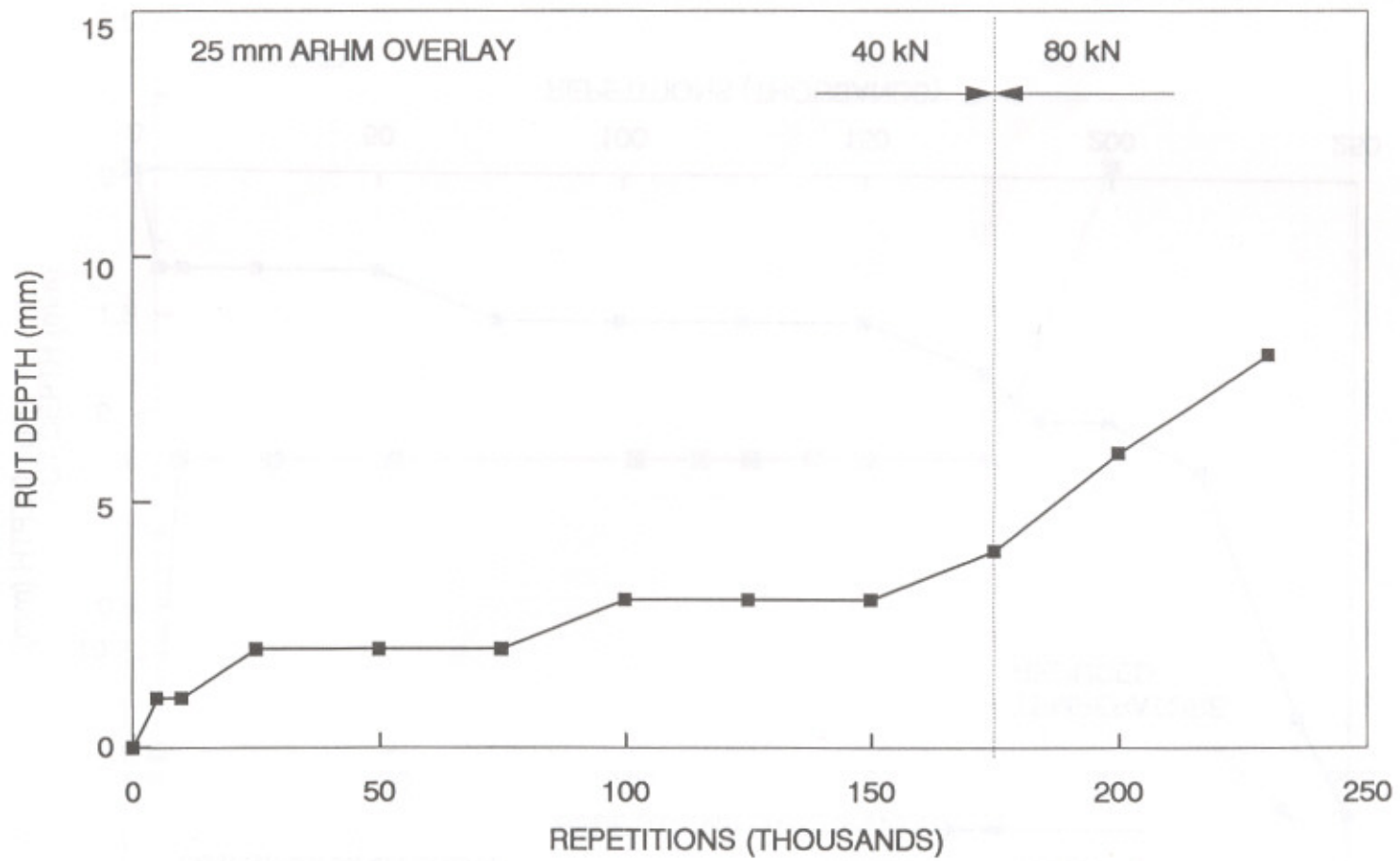


**FIGURE 5.6 : MAXIMUM SURFACE RUTTING ON SECTION 383A3
(25 mm ARHM OVERLAY)**

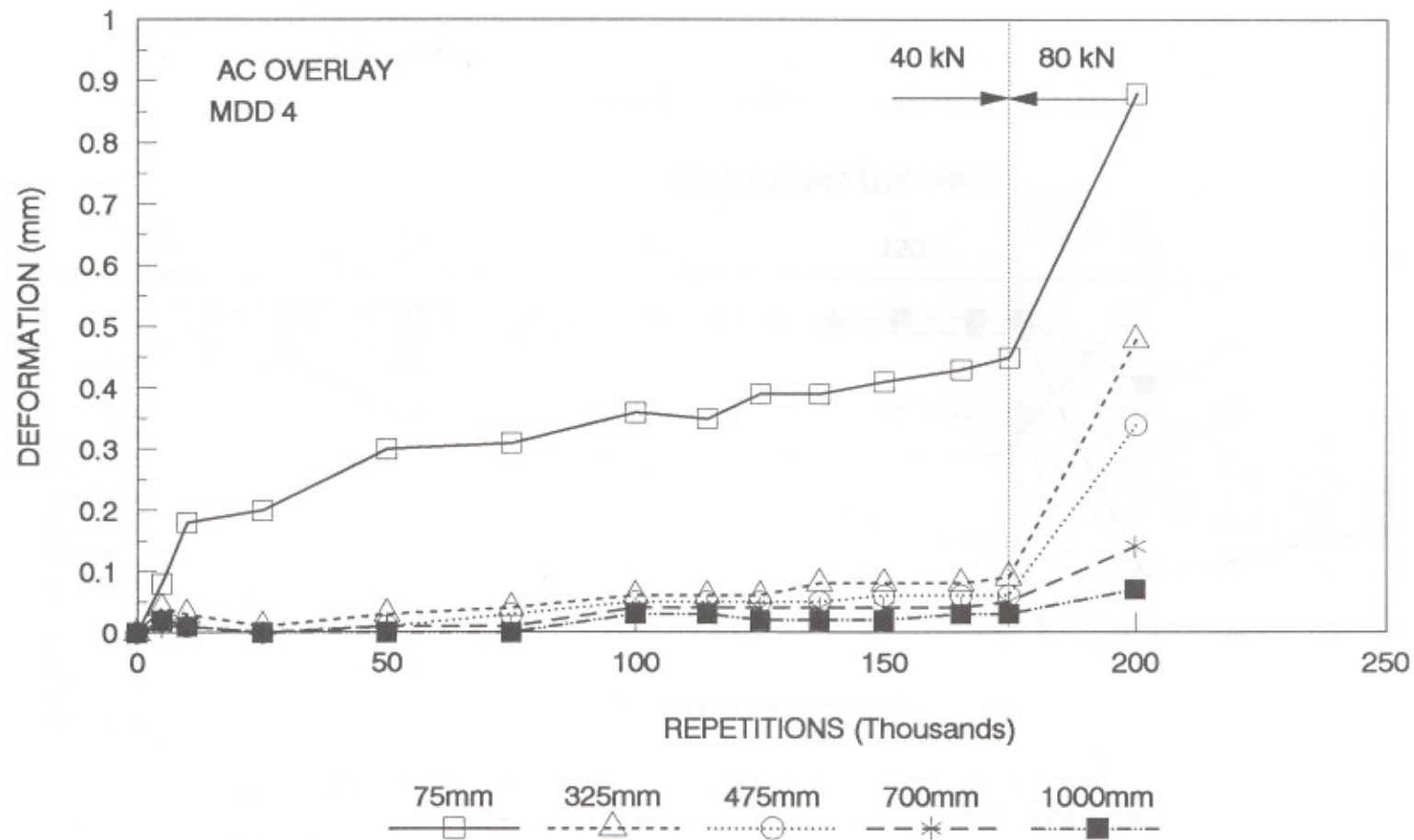


**FIGURE 5.7 : MULTI-DEPTH PERMANENT DEFORMATION, MDD 4
(SECTION 381A3, 75 mm AC OVERLAY)**

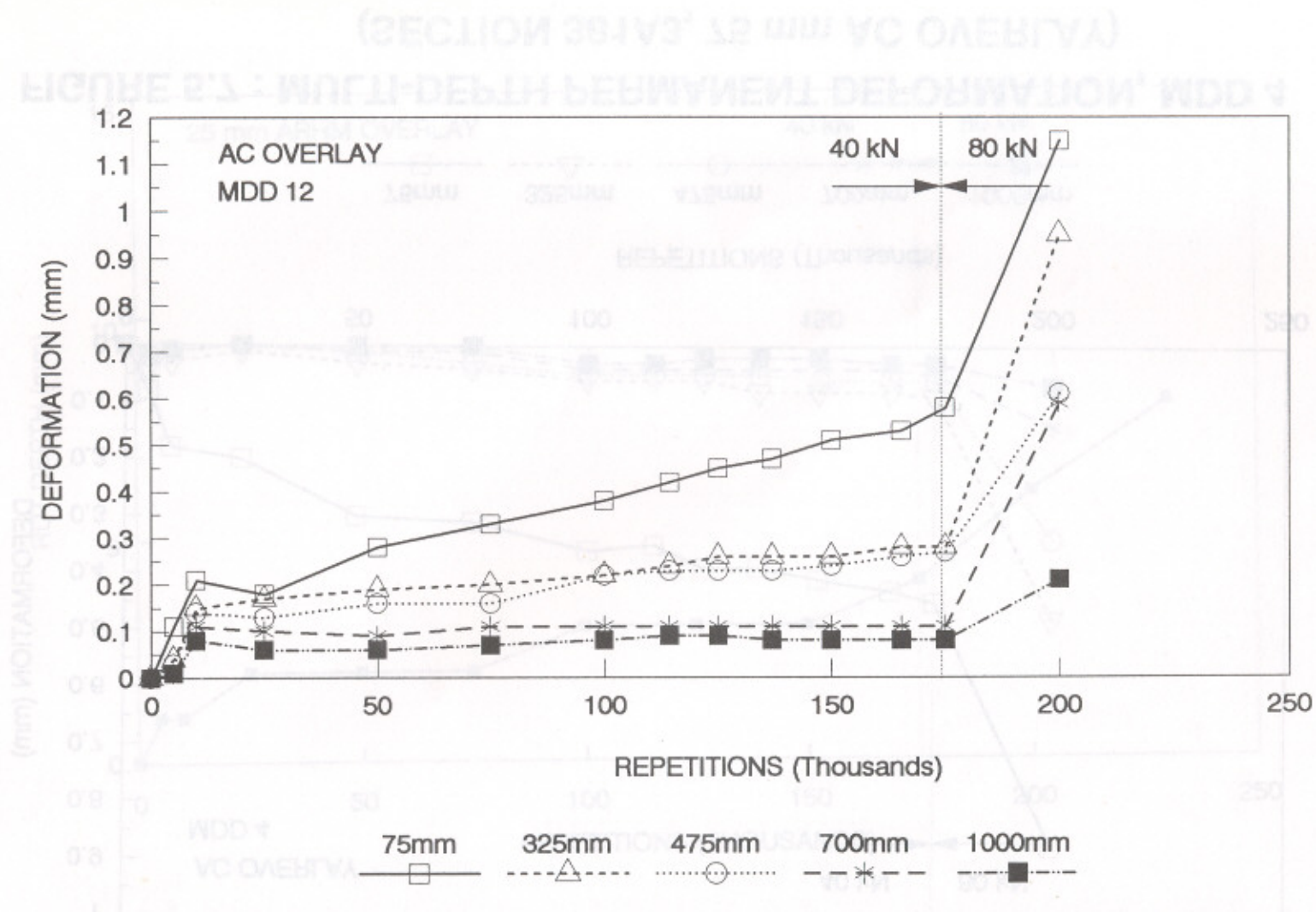


**FIGURE 5.8 : MULTI-DEPTH PERMANENT DEFORMATION, MDD 12
(SECTION 381A3, 75 mm AC OVERLAY)**

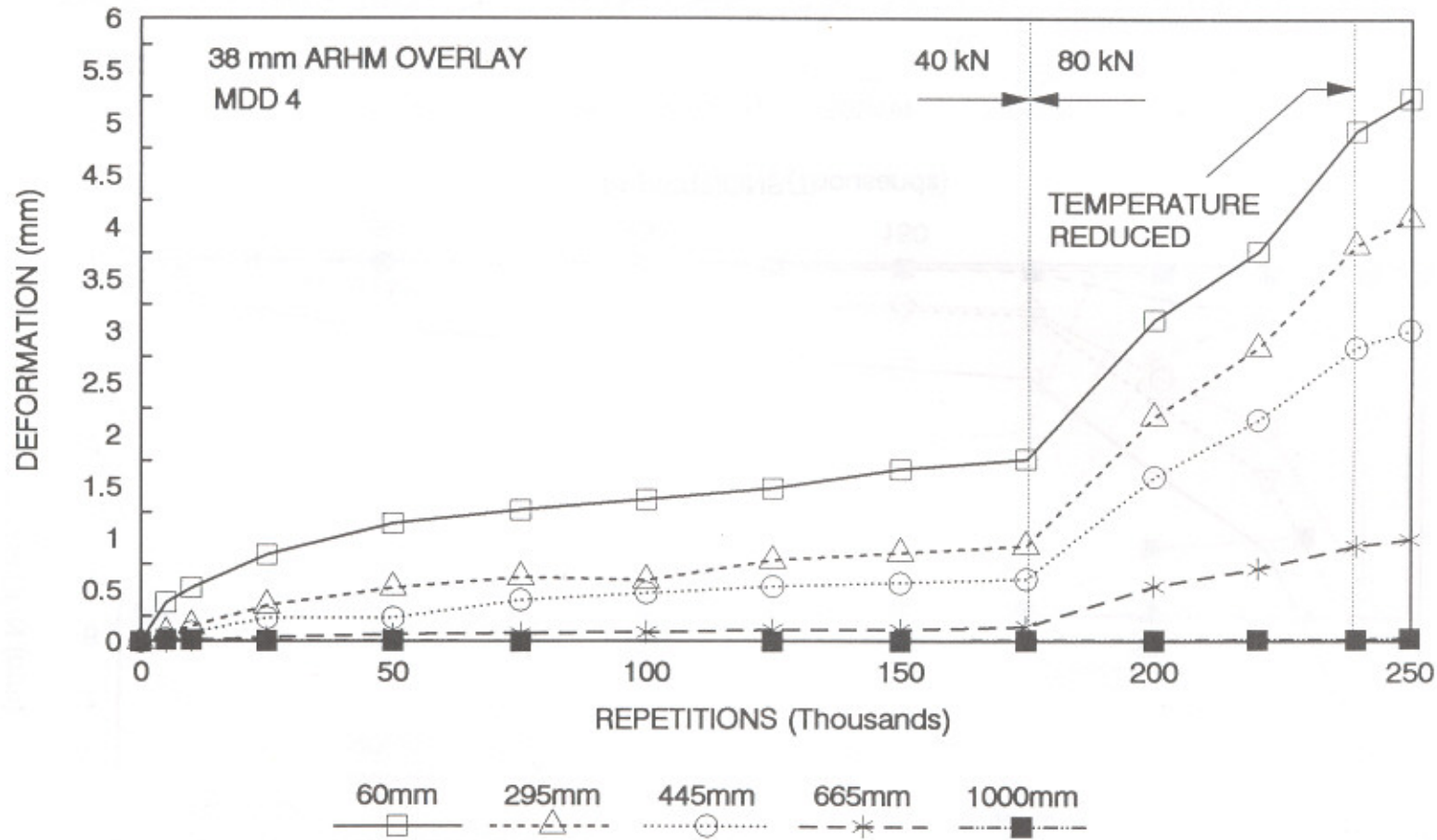


**FIGURE 5.9 : MULTI-DEPTH PERMANENT DEFORMATION, MDD4
(SECTION 382A3, 38 mm ARHM OVERLAY)**

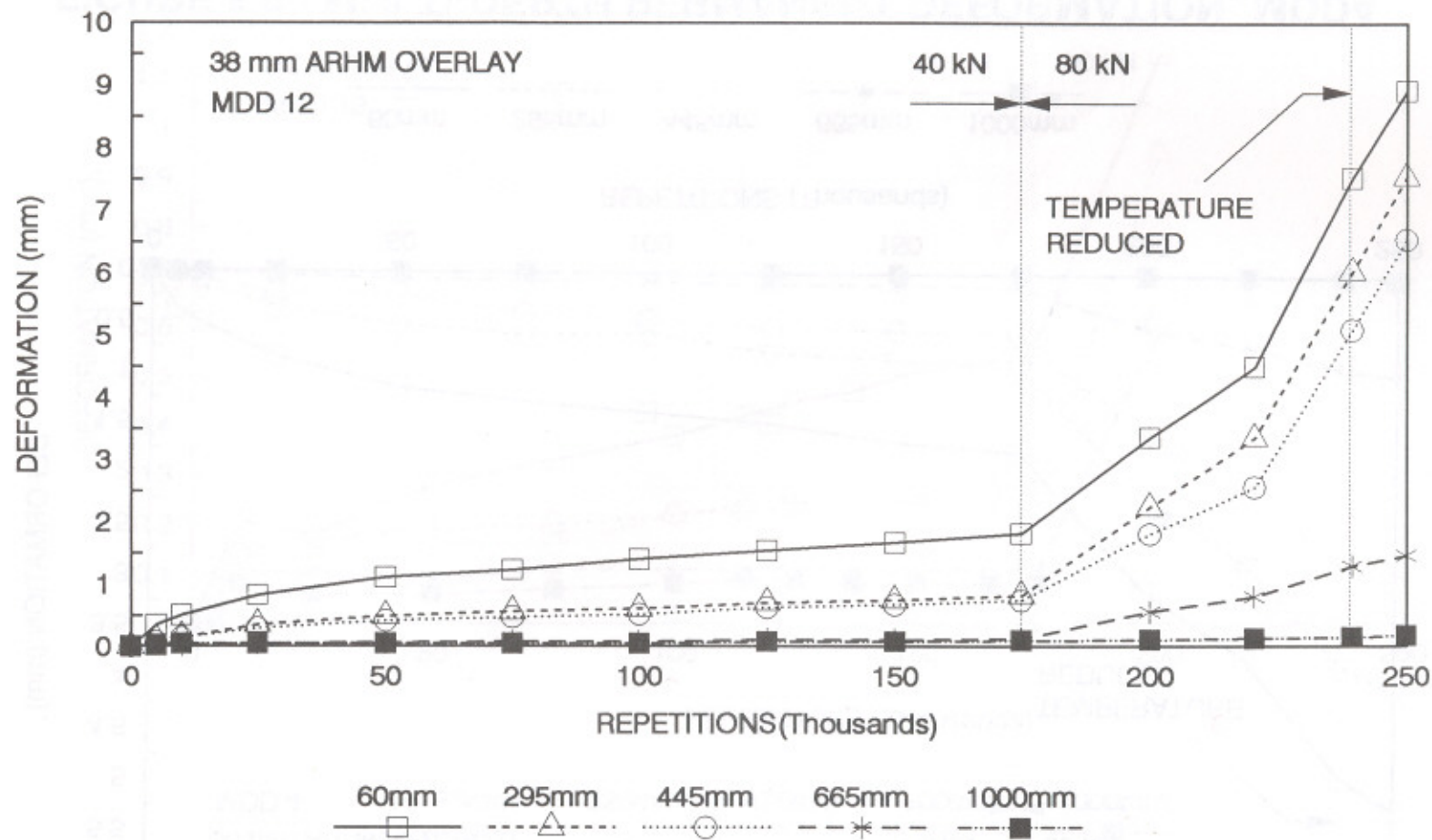


**FIGURE 5.10 : MULTI-DEPTH PERMANENT DEFORMATION, MDD 12
(SECTION 382A3, 38 mm ARHM OVERLAY)**

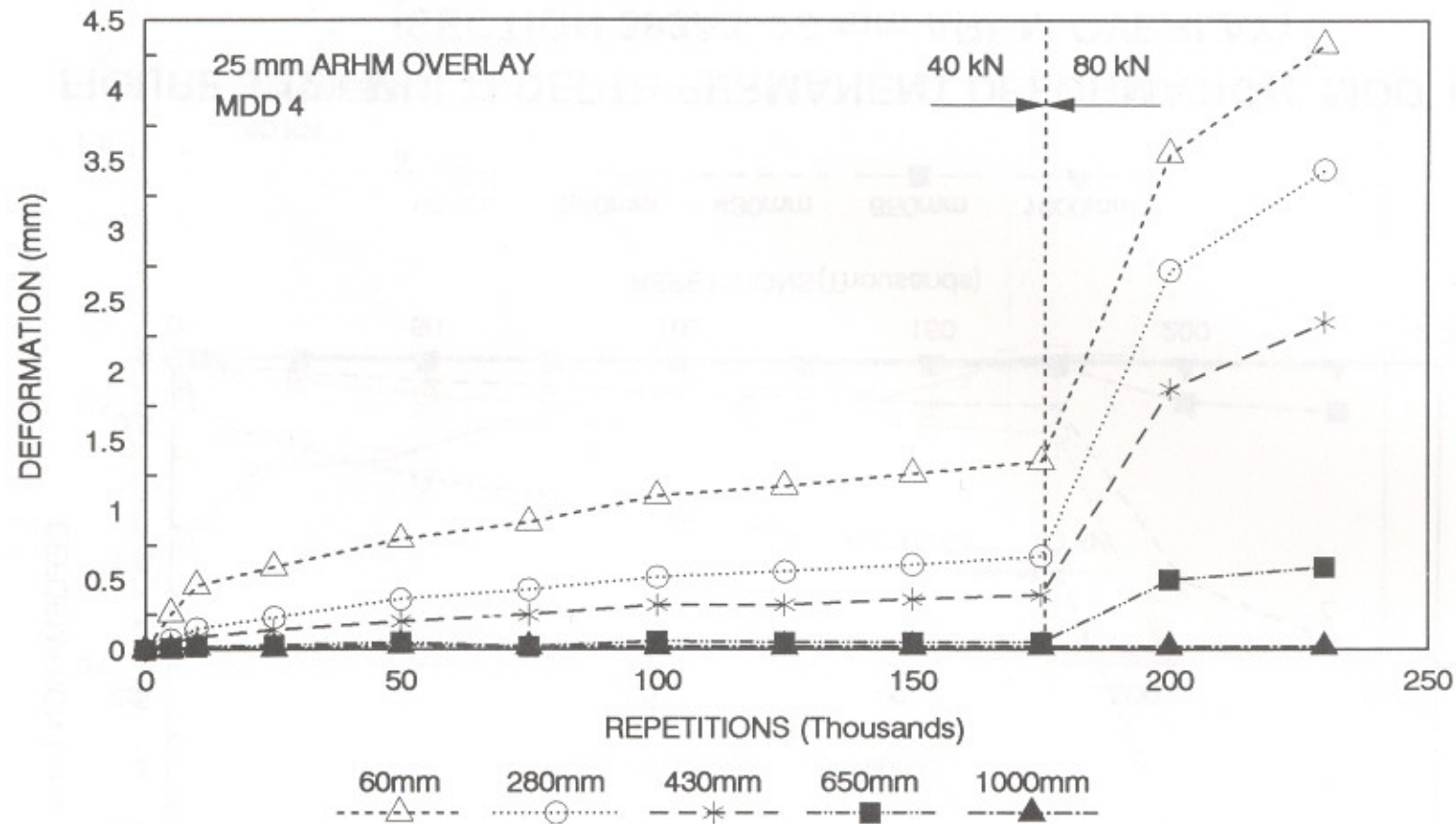


**FIGURE 5.11 : MULTI-DEPTH PERMANENT DEFORMATION, MDD 4
(SECTION 383A3, 25 mm ARHM OVERLAY)**

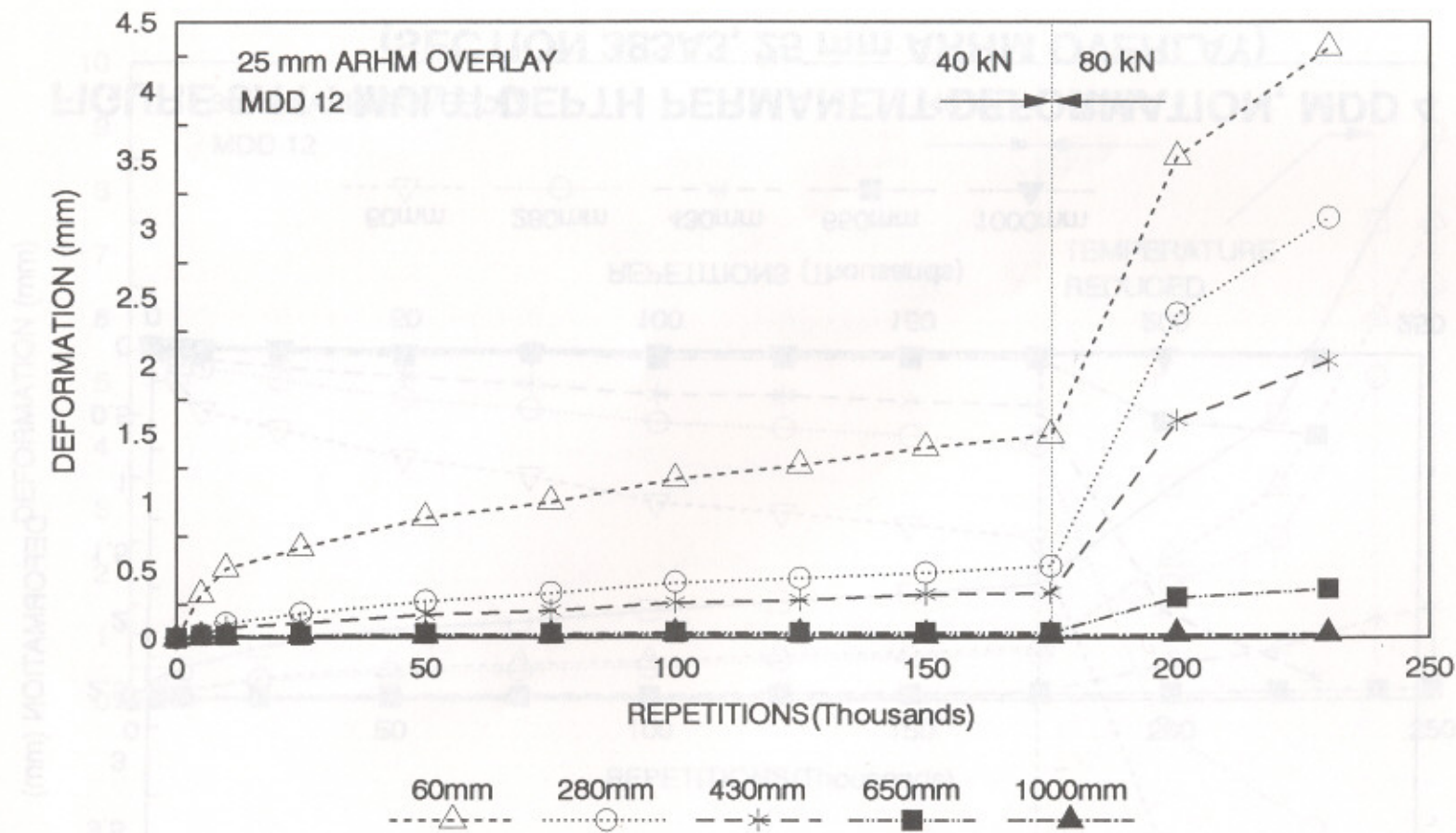


**FIGURE 5.12 : MULTI-DEPTH PERMANENT DEFORMATION, MDD 12
(SECTION 383A3, 25 mm ARHM OVERLAY)**

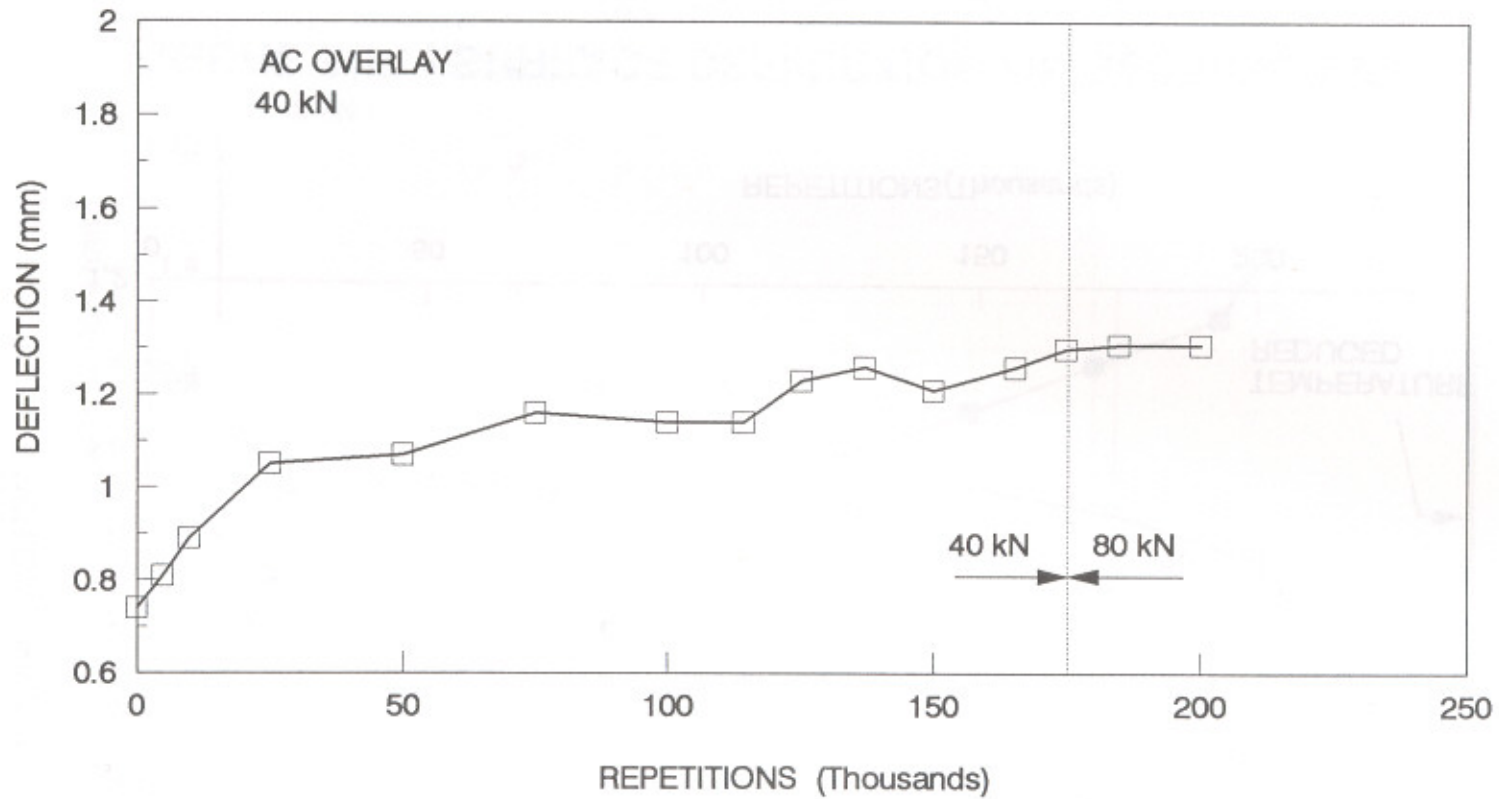


**FIGURE 5.13 : SURFACE DEFLECTION ON SECTION 381A3
(75 mm AC OVERLAY)**

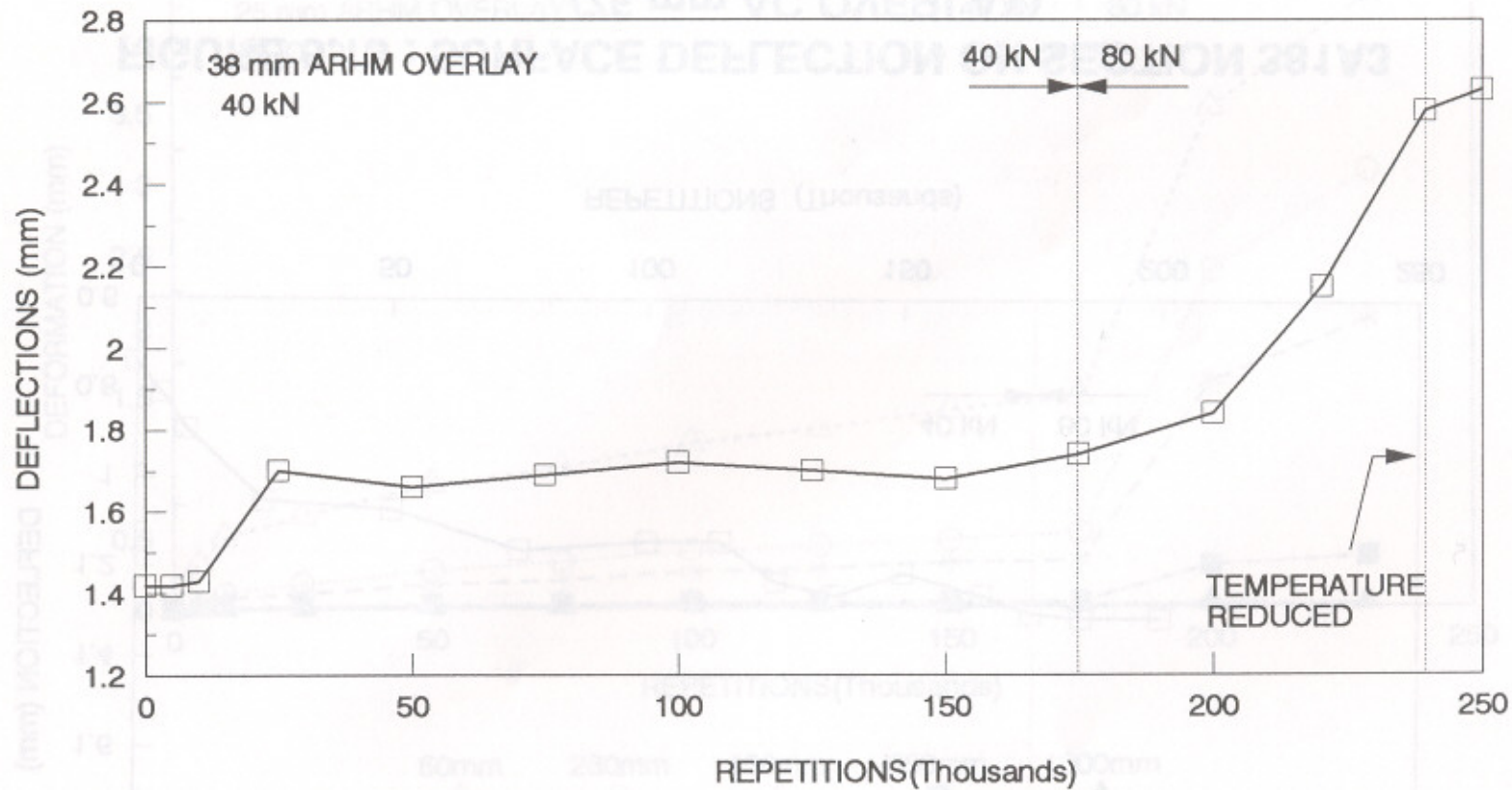


**FIGURE 5.14 : SURFACE DEFLECTION ON SECTION 382A3
(38 mm ARHM OVERLAY)**

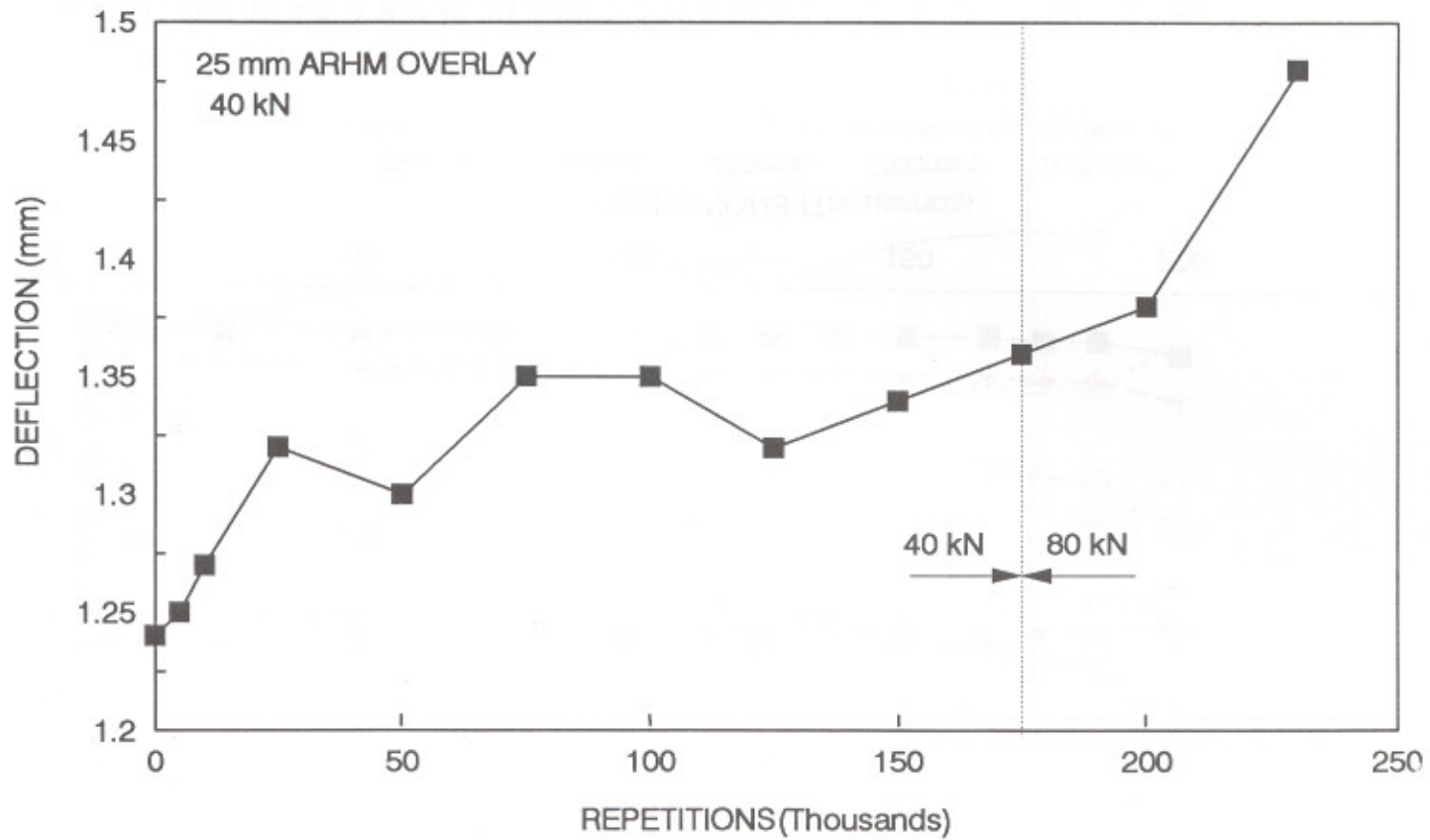


**FIGURE 5.15 : SURFACE DEFLECTION ON SECTION 383A3
(25 mm ARHM OVERLAY)**

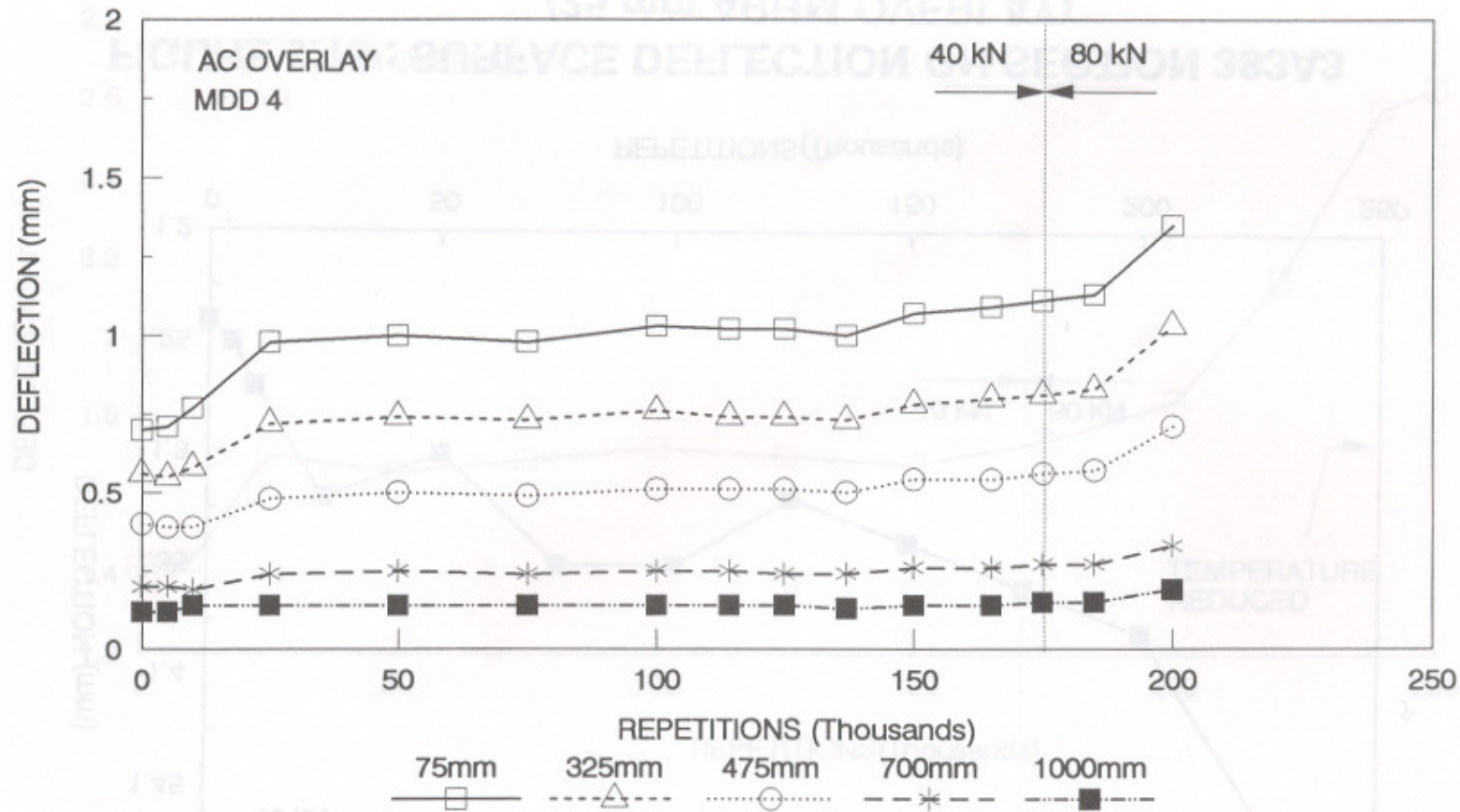


**FIGURE 5.16 : MULTI-DEPTH DEFLECTIONS, MDD 4
(SECTION 381A3, 75 mm AC OVERLAY)**

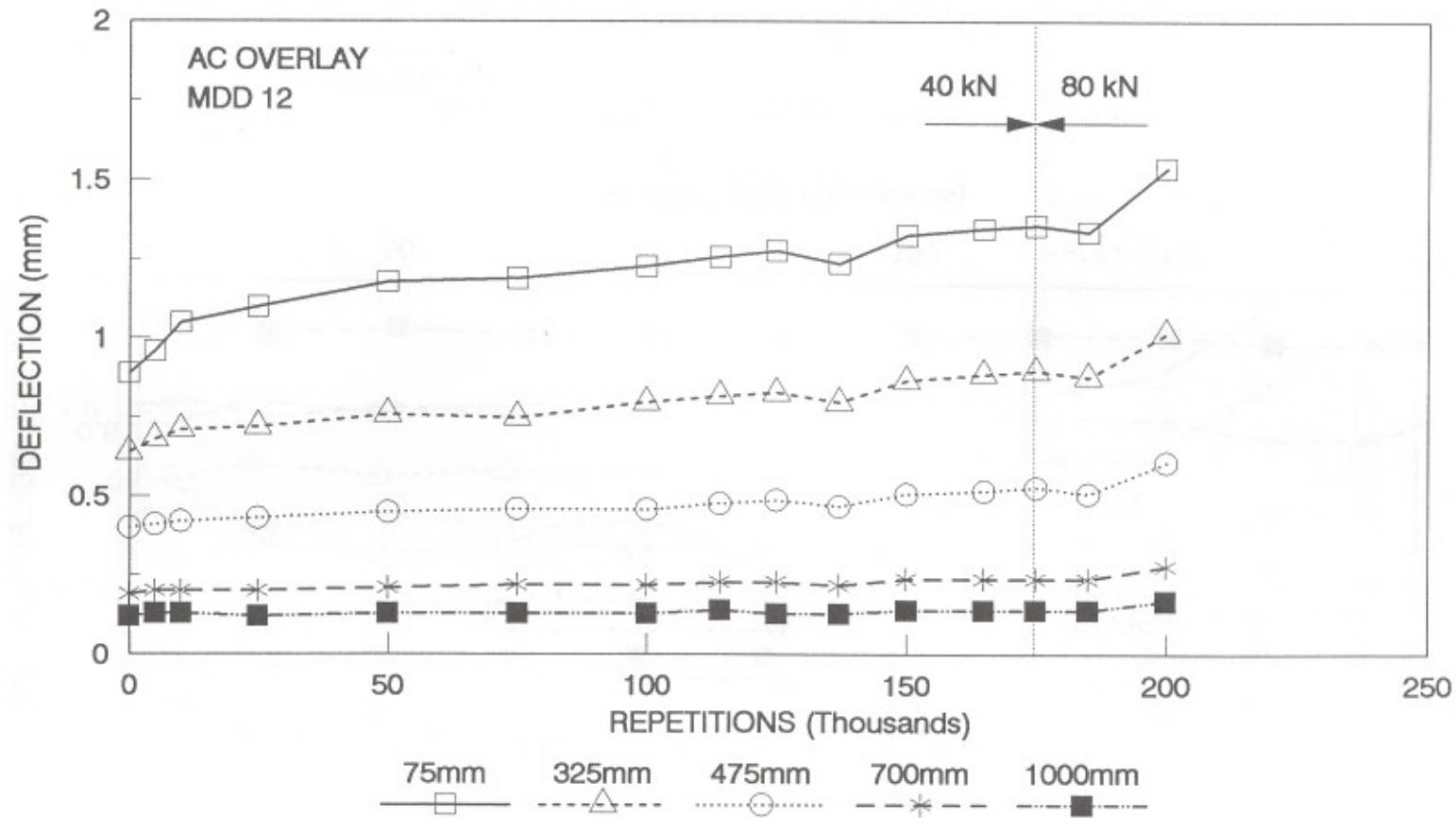


**FIGURE 5.17 : MULTI-DEPTH DEFLECTIONS, MDD 12
(SECTION 381A3, 75 mm AC OVERLAY)**

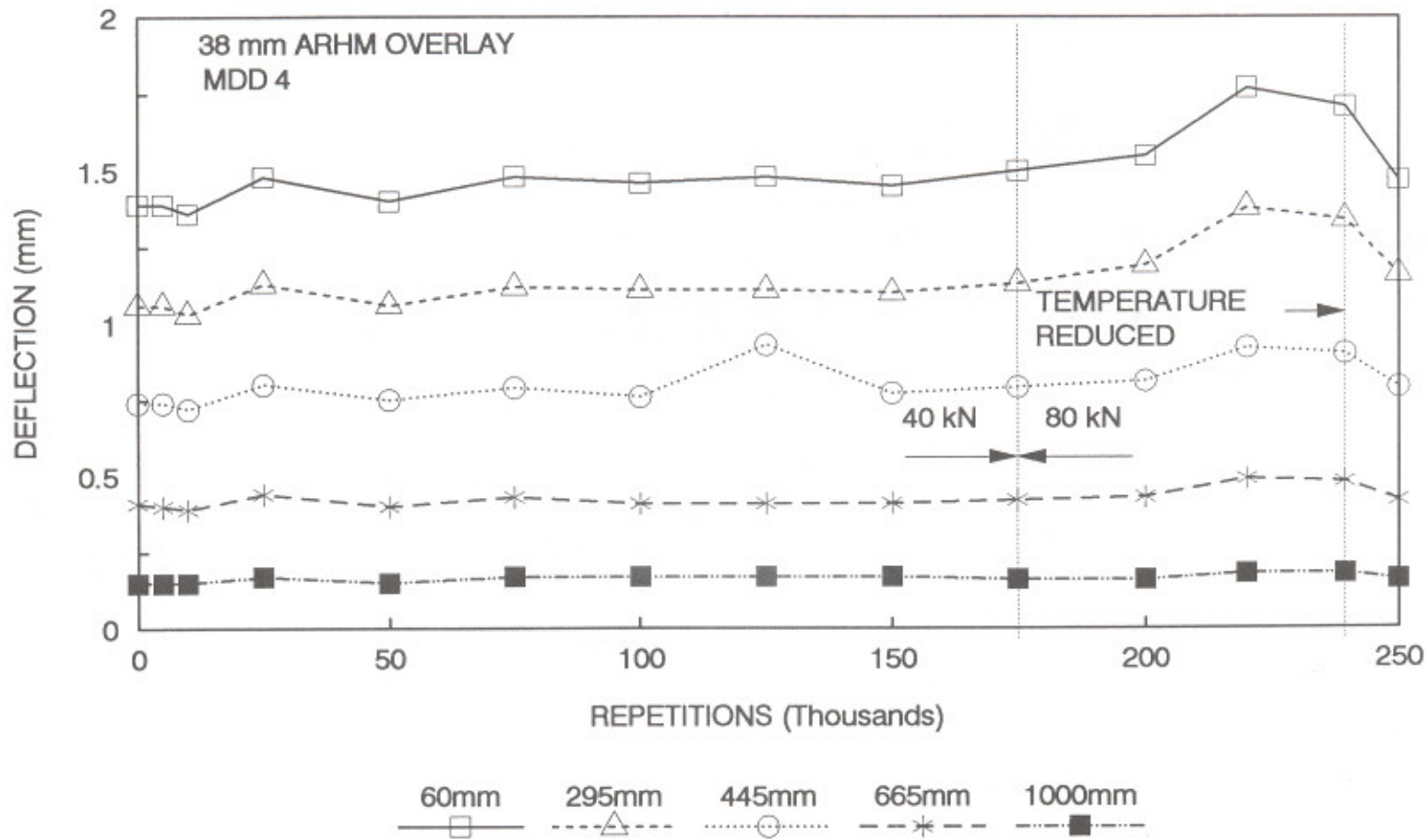


**FIGURE 5.18 : MULTI-DEPTH DEFLECTIONS, MDD 4
(SECTION 382A3, 38 mm ARHM OVERLAY)**

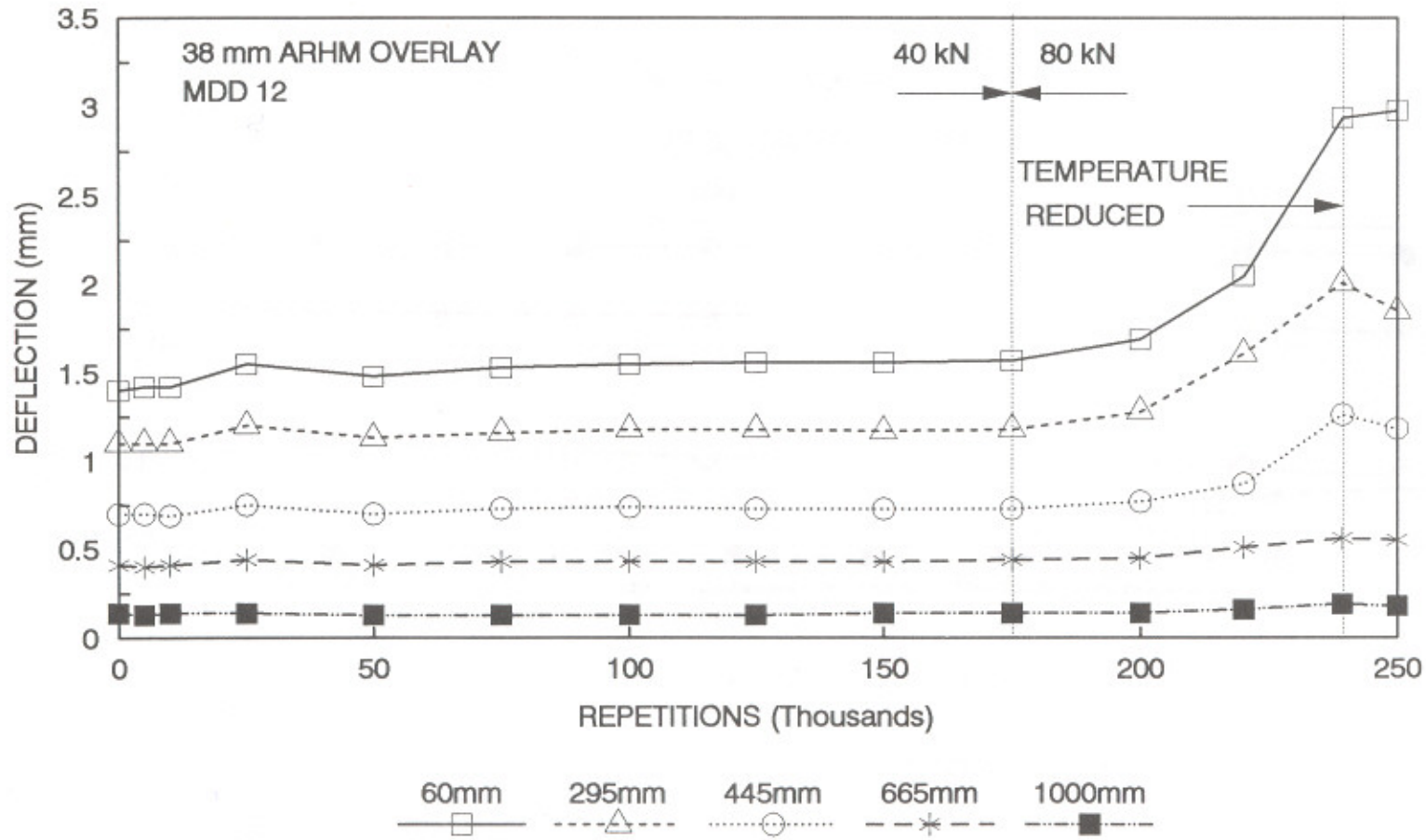


**FIGURE 5.19 : MULTI-DEPTH DEFLECTIONS, MDD 12
(SECTION 382A3, 38 mm ARHM OVERLAY)**

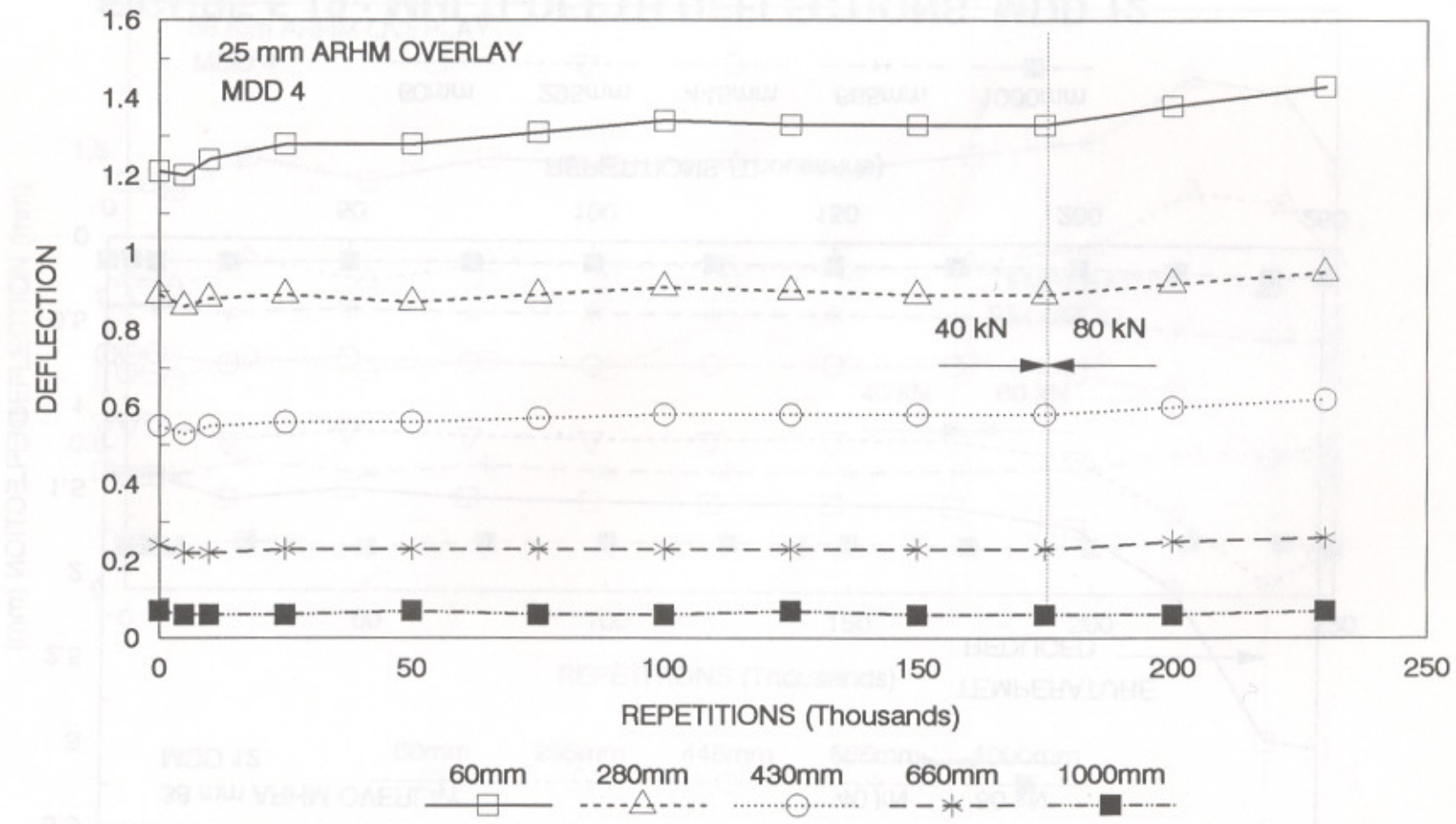


**FIGURE 5.20 : MULTI-DEPTH DEFLECTIONS, MDD 4
(SECTION 383A3, 25 mm ARHM OVERLAY)**

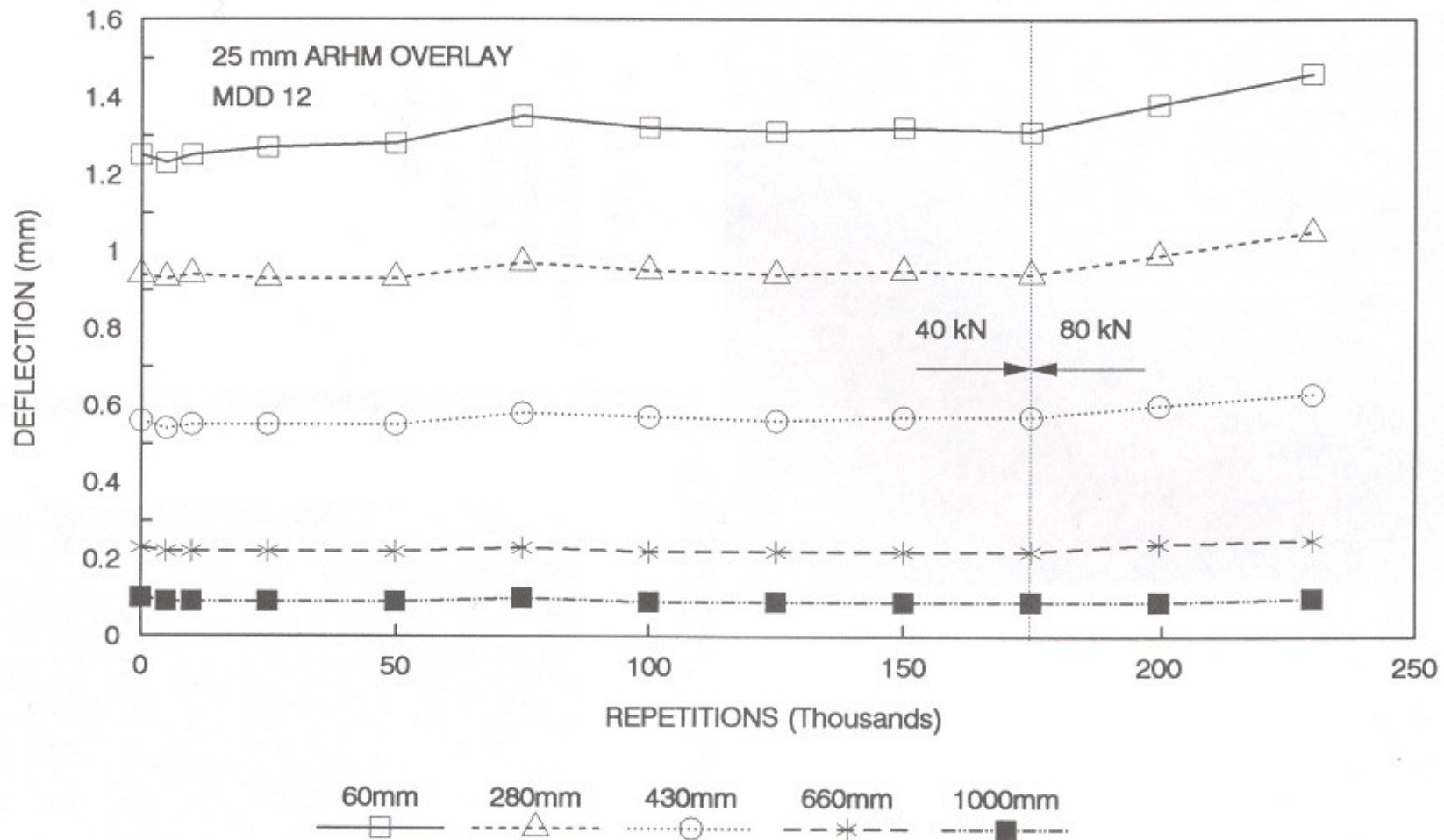


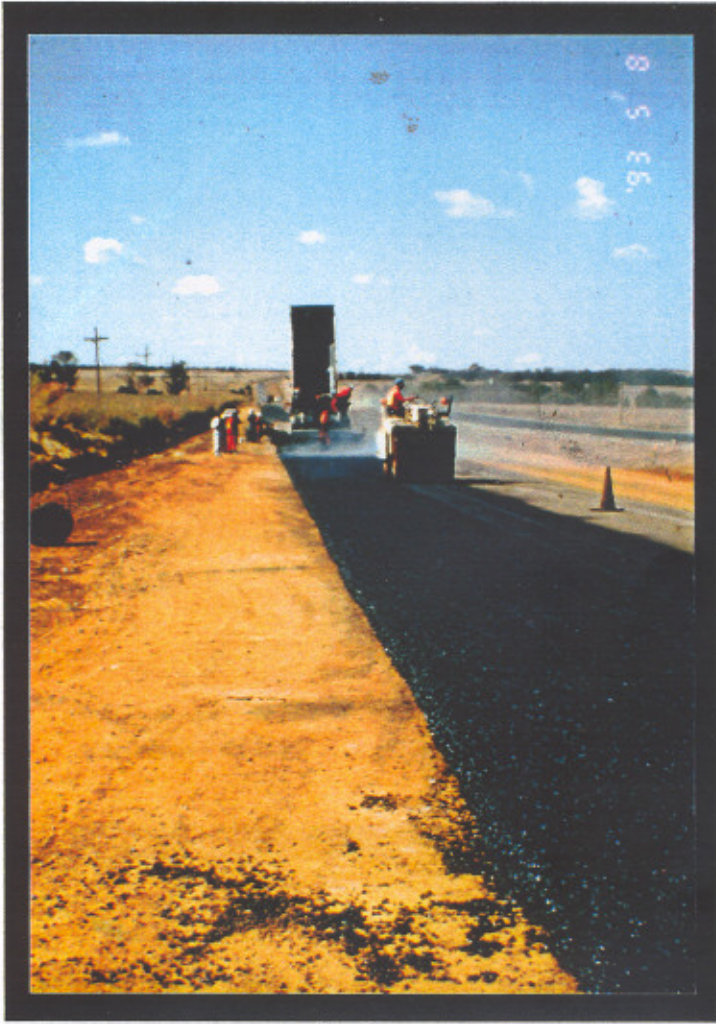
**FIGURE 5.21 : MULTI-DEPTH DEFLECTIONS, MDD 12
(SECTION 383A3, 25 mm ARHM OVERLAY)**



PHOTOGRAPH 1 :
The surface of P6/1,
Bapsfontein to Bronkhorspruit
currently showing extensive
cracking _

PHOTOGRAPH 2 :
Surface distress observed
during HVS testing of
P6/1 in 1979 HVS
test section 43A4
(after Maree⁵)





PHOTOGRAPH 3 :
Construction of the
CALTRANS trials



PHOTOGRAPH 4 : Heaters used to elevate the temperature in the asphalt mix



PHOTOGRAPH 5 : Rutting after channelized traffic



**PHOTOGRAPH 6 :
Rutting after
wandering traffic**



PHOTOGRAPH A.1 :
Prototype HVS
Commissioned in
October 1970



PHOTOGRAPH A.2 : One of the three, currently used, production type HVSs



PHOTOGRAPH A.3 : Long distance hauling of the HVS using a tractor



PHOTOGRAPH A.4 : The test carriage fitted with a dual truck wheel

PHOTOGRAPH A.5 : The Road Surface Deflectometer (RSD)



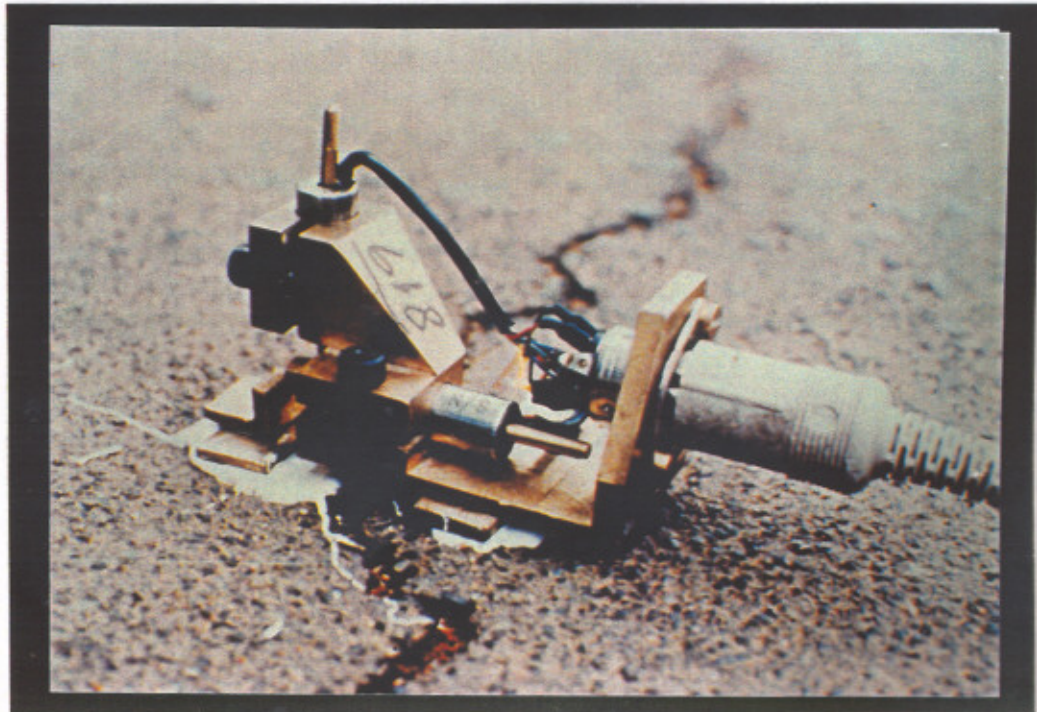
PHOTOGRAPH A.5 :
Electronic Profilometer



PHOTOGRAPH A.6 : The Road Surface Deflectometer (RSD)



PHOTOGRAPH A.7 :
The Multi-Depth
Deflectometer (MDD)



PHOTOGRAPH A.8 : The Crack-Activity Meter (CAM)

BRIEF DESCRIPTION OF THE HVS SYSTEM

A.1 THE HEAVY VEHICLE SIMULATOR

The development of the HVS has a long history, starting in the 1960s when the need for an accelerated trafficking device in South Africa was first identified¹. By 1966 a stationary system for applying wheel loads to a pavement had been constructed from Bailey Bridge sections. This led to the concept of the prototype HVS (see Photograph A.1) which was commissioned in October 1970. In 1972, the construction of three additional HVSs was undertaken. These machines incorporated a number of design improvements based on the experience gained from the prototype (see Photograph A.2). A line diagram of the HVS is shown in Figure A.1.

The HVS was designed to test pavement sections on in-service roads - even in remote parts of the road network. This meant that it had to be transported over long distances and be self-contained.

The HVS is fitted with a gooseneck at one end which enables it to be coupled to a tractor for long distance hauling (see Photograph A.3). The opposite end, the cabin of the machine, is fitted with sixteen wheels which distribute the weight of the machine sufficiently to avoid overloading the pavements. In this configuration the HVS can be towed at speeds of up to about 45 km/h, enabling long distances to be covered in a reasonable period.

For manoeuvring on a site or for travelling short distances, the HVS can be self-propelled. Two non-steerable dual wheel bogies are fitted at the tow end of the machine. One of the bogies is equipped with a hydraulic motor driven by the main engine of the HVS. This can propel the HVS at speeds of up to 25 km/h.

On arrival, the HVS is manoeuvred over the first section and stabilized by four hydraulically operated landing legs.

The HVS is powered by two air-cooled diesel engines. The main unit comprises a ten-cylinder 164 kW engine which drives a hydraulic pump supplying the power needed to propel the HVS and to drive the test wheels.

Loading is applied to the test section via either single or dual wheels mounted on a test carriage that runs on rails on the inside of the test beams (see Photograph A.4). The test carriage is rapidly drawn backwards and forwards over the test section by means of a chain driven by a reversible hydraulic motor. Loads of up to 200 kN are applied to the test wheels by means of hydraulic rams pressurised by an electrically operated power pack mounted on the test carriage. A nitrogen accumulator is provided in the hydraulic circuit so that surface irregularities in the pavement do not affect the magnitude of the applied wheel load significantly.

The test beam can be moved laterally across the pavement test section during testing by means of hydraulic sideshift rams. Thus the loading applied to the pavement can be

automatically distributed over the test section up to a width of 1,5 m. Usually a normal distribution of traffic is used, but the wheel can also be constrained to run in a single wheel path simulating channelized traffic.

The fleet of three HVSs has been used extensively over the last 20 years to evaluate both trial sections as well as in-service pavements. The approximately 4 Gbyte of information generated during this period is contained in a database on a main frame computer. The development of an improved user interface with this database is currently underway.

A.2 HVS INSTRUMENTATION

During HVS testing various pavement condition measurements are taken to characterise the performance of the pavement with increased trafficking. Instrumentation includes the following:

- The Electronic Profilometer (EP), which is used to measure the permanent deformation on the surface of the pavement (see Photograph A.5).
- The Road Surface Deflectometer (RSD), which is essentially a Benkelman Beam instrumented with an Linear Variable Differential Transducer (LVDT) and is used to measure the road surface deflection basin (see Photograph A.6).
- The Multidepth Deflectometer (MDD)², which consists of a number of LVDTs positioned at the layer interfaces in the pavement and is used to measure both the elastic deflection basins at depth as well as the permanent deformation at various depths (see Photograph A.7).
- The Crack-Activity Meter (CAM)³, which is used to measure the horizontal and vertical movement of a crack as a wheel passes over it (see Photograph A.8).
- Thermocouples used to measure pavement temperature at various depths.

Figure A.2 shows a typical 8,0 m long by 1,0 m wide HVS test section. The 8,0 m length is divided into 16 measuring points each 0,5 m apart.

In addition to the above, other field measurements such as Dynamic Cone Penetrometer (DCP) testing is often conducted to complement the findings of HVS testing. Test pits are always dug after testing to observe pavement behaviour visually. The HVS test results are usually also supported by a full set of laboratory tests on the materials contained in the pavement.

A.3 REFERENCES

- 1 Richards, R.G. Paterson, W.D.O. Loesch, M.D. 1977. *The NITRR Heavy Vehicle Simulator: Description and operational logistics*. NITRR Technical Report RP/9/77, Pretoria: DRTT, CSIR.
- 2 De Beer, M. Horak, E. Visser, A.T. 1988. The Multi-Depth Deflectometer (MDD) System for determining the Effective Elastic Moduli of Pavement Layers. ASTM Special Technical Publication, STP 1026. *Papers presented at the First International Symposium on Non-destructive Testing of Pavements and Backcalculation of Moduli*, Baltimore, USA, 1988.
- 3 Rust, F.C. 1984. *Description and use of the Crack-activity Meter (CAM)*. NITRR Technical Note TP/132/84. Pretoria: DRTT, CSIR. 1984

LINE DIAGRAM OF THE HEAVY VEHICLE SIMULATOR (HVS)

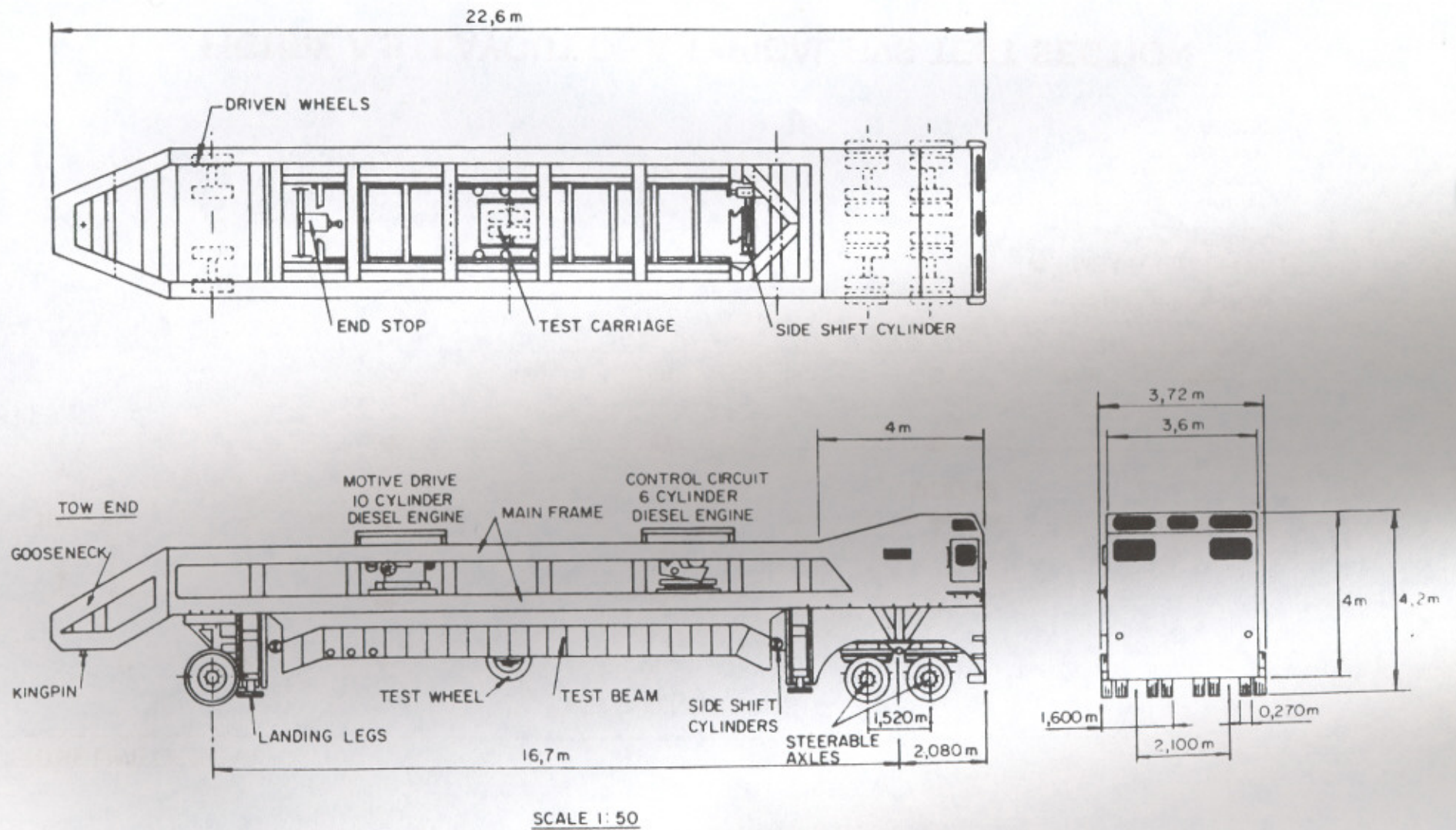


FIGURE A.1 : LINE DIAGRAM OF THE HEAVY VEHICLE SIMULATOR (HVS)

FIGURE A.1 : THE PROBLEM OF THE RSD AS THE TEST SECTION FOR A BRIDGE

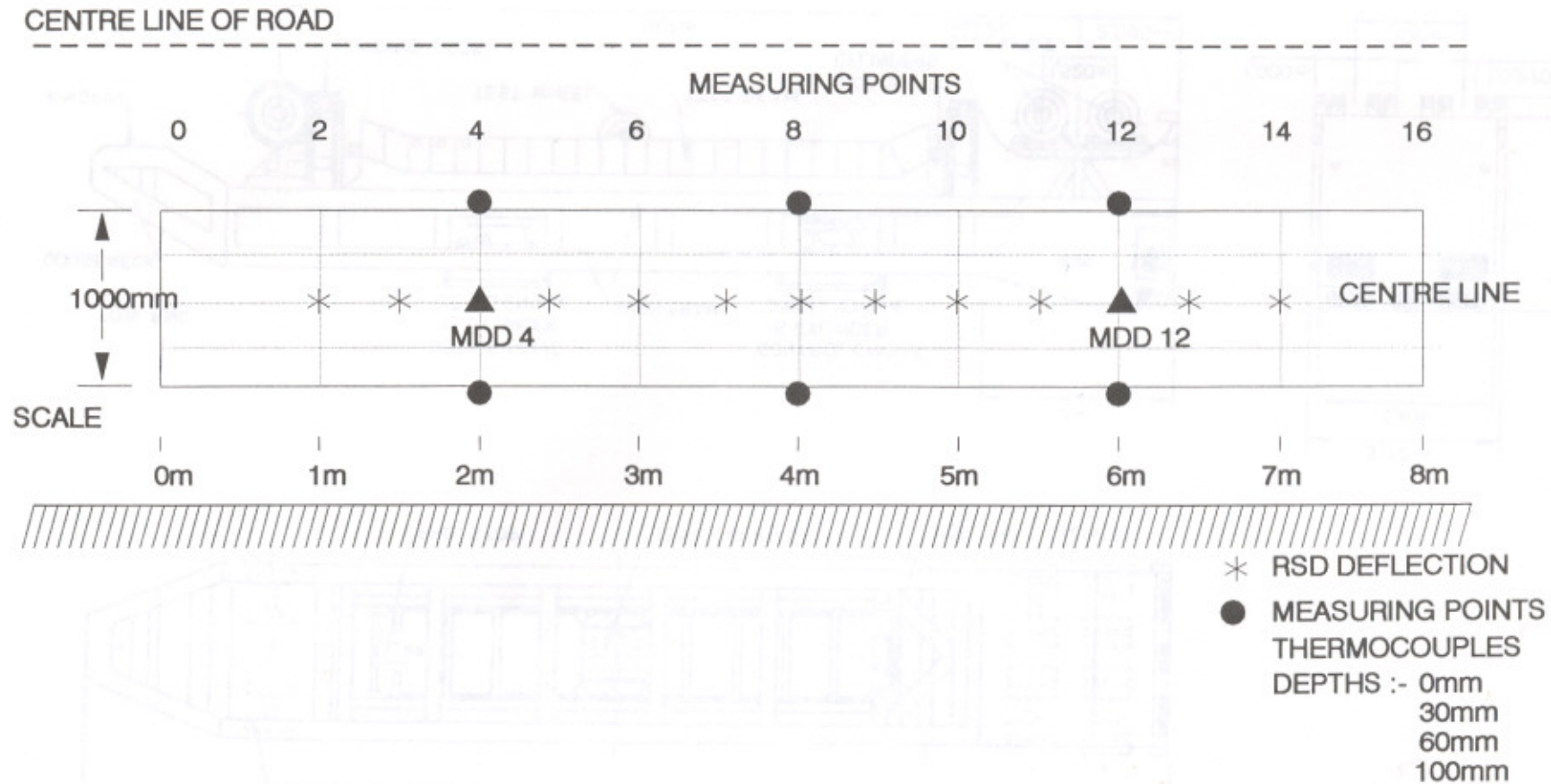


FIGURE A.2 : LAYOUT OF A TYPICAL HVS TEST SECTION